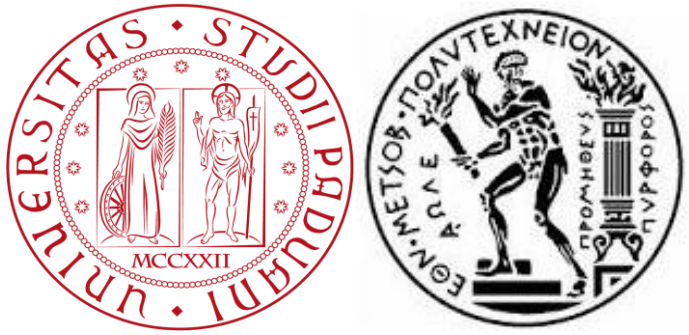

UNIVERSITA' DEGLI STUDI DI PADOVA

NATIONAL TECHNICAL UNIVERSITY OF ATHENS

DIPARTIMENTO DI INGEGNERIA INDUSTRIALE
CORSO DI LAUREA MAGISTRALE IN INGEGNERIA ENERGETICA

TESI DI LAUREA

DESIGN AND PERFORMANCE EVALUATION OF AN ORC SYSTEM EXPLOITING THE WASTE HEAT OF THE MAIN ENGINE OF A TANKER

Relatori: Proff. CHRISTOS A. FRANGOPOULOS, ANDREA LAZZARETTO
Correlatore: Ing. GIOVANNI MANENTE

Laureando: STEFANO MANCINI
Matr.n. 1020442

Anno accademico 2012/2013

Δεν υπάρχει εξορία μόνο μια καινούργια πατρίδα

Contents

Nomenclature

Abbreviations

DPP	Dynamic payback period
ECO	Economizer
EGB	Exhaust gas boiler
EVA	Evaporator
FW	Fresh Water
FWG	Fresh water generator
HFO	Heavy Fuel Oil
IRR	Internal rate of return
HCC	Hot composite curve
CCC	Cold composite curve
JWC	Jacket water cooler
L.O.	Lubrication oil
M/E	Main engine
MDO	Marine Diesel oil
NPV	Net Present value
ORC	Organic Rankine cycle
ORCs	Organic Rankine cycle system
PP	Payback period
SH	Super heater
SW	Sea water

Symbols

A	Exchange Surface (m^2)
C	cost
c_p	Isobaric specific heat (kJ/kg K)
Δh_{fg}	Enthalpy of vaporization (kJ/kg)
Δh_{is}	Isentropic enthalpy change in turbine (kJ/kg)
Δs	Entropy different (kJ/kgK)
E	Annual energy savings (kWh)
n	0.375-0.38
f	Optimization function
h	Specific enthalpy (kJ/kg)
H_u	Lower calorific Value
HT	High temperature
k	$\frac{\dot{Q}_j}{\sum_{i=1}^{n} \dot{Q}_i}$

k^*	$\frac{k_L}{K_{100}}$
LT	Low temperature
$\dot{m}$	Mass flow rate (kg/s)
p	Pressure (bar)
$\dot{Q}$	Thermal power [kW]
SP	Turbine Size parameter
s	Specific entropy (kJ/kgK)
T	Temperature (K)
UA	Total heat transfer capacity (kW/K)
v	Specific volume (m^3/kg)
$\dot{V}$	turbine exit volume flow rate
$\dot{W}$	Mechanical power [kW]

Greek symbols

ϕ	Recovery efficiency
ζ	Inverse of the slope of saturated vapor curve
η	efficiency
η_1	Cycle thermal efficiency (%)
η_2	Second law efficiency (%)
$\tau_{r,ev}$	Reduced evaporation temperature

Subscript

a	air
at	After turbine
av	available
bt	Before turbine
c	Critical
ca	Air cooler
con	Condenser
ev	Evaporator
g	Exhaust gas
in	input
is	isoentropic
jw	Jacket water
h	hour
hl	High loop
r	reduced
tot	Total
ll	Low loop
L	load
lo	Lubrication oil
net	Electric power
out	output

R	regenerator
r	radiation
R	Rankine
s	steam
T	Total heat recovey
TH	Rankine efficiency
y	year

List of Figures

List of Tables

Acknowledgement

I would like to thank all the people who supported me in developing this thesis, in particular:
Christos A. Frangopoulos at the School of Naval Architecture and Marine Engineering of NTUA Athens. Nikolaos Kakalis, George Dimopoulos, DET NORSKE VERITAS (DNV). Andrea Lazzaretto, Giovanni Manente, Marco Soffiato and Sergio Rech, University of Padova.
Raymond Genesse and Alberto Schiavon, Zeno Rama, Claudia Marino for my English writing.

I desire to thank my family who supported me in all these years of study from all points of view.

Abstract

The vast majority of the world's trade is conducted across water. Ships remain one of the best means of transport. Cleaner technologies are inevitable in this field as well. Solutions for this new request are developing by some shipping companies. One solution is the reduction of the fuel consumption keeping the equivalent performance of the ship without fuel reduction. An ORC may be an answer of this problem. In this work an ORC system applied to cooling system of the Main Engine of a Tanker is investigated. The energy balance is calculated for the main operating loads. Three main operating loads are taken into consideration for the ORC system (80%, 70%, 55%). Four working fluids R134a, R245fa, R236fa, R227ea have been considered. At first the best match between the choice of working fluid and ORC configuration is carried out at design point (80% engine load). Then, using the ORC system at design point, the maximum electric power is evaluated in the three main loads. After that, the annual energy saving is calculated using the output power and the duration for each operating load. An economic analysis is carried out through three parameters: net present value (NPV), dynamic payback period (DPP), internal rate of the return (IRR).

Introduction

Energy conservation and environmental protection have become more important with the rapid development of global industrialization and urbanization. The industrialization has risen to a level never reached before, releasing in the same process large quantities of CO_2 into the atmosphere. Current concerns over climate change call for measures to reduce greenhouse gases. Some modification could be a decrease in the energy intensity of buildings and industry, use clean power generation by renewable energies, a shift from fossil fuels for transportation and heating. Organic Rankine cycle (ORC) technology can play a non-negligible role in these proposed solutions. It can have a beneficial effect on the energy intensity of industrial processes mainly recovering waste heat for electricity production or it can be used to convert renewable heat sources (as geothermal, biomass and solar sources) into electricity.

Environmental pollution of the ocean has become increasingly serious owing to shipping. Total CO_2 emissions generated in the domestic and overseas shipping industries reached a record of about 1 billion tons in 2007, constituting 3.3% of global CO_2 emissions. The MEPC (Marine Environmental Protection Committee) of the IMO (International Maritime Organization) under the umbrella of the UN (United Nations) has modified its marine pollution prevention convention, i.e. the MARPOL (International Convention for the Prevention of Pollution From Ships) Annex VI, in order to lower the CO_2 emitted from newly built ships and existing ships [Choi and Kim (2013)].

The amount of CO_2 emitted from a ship is directly related to the amount of fuel consumed by the internal combustion engine propelling the ship. Therefore a power generation system that makes use of the waste heat from its main engine (a waste heat recovery system) could be a principal technology to reduce CO_2 emissions on boat. There are several waste heat recovery power generation systems: a power turbine scheme, in which the kinetic energy of the gas is utilized to directly drive the turbines, a steam turbine scheme, or a combination of both these schemes. If the ship needs vapor for internal utility, an exhaust gas boiler (system to produce steam by exhaust gas) could be installed. New studies proved the advantages of ORC technology against steam technology. It is possible to substitute the steam turbine with an ORC. Conceptually the ORC is similar to a steam Rankine Cycle. The ORC involves some components as a conventional steam power plant (a boiler, a work-producing expansion device, a condenser and a pump). However the working fluid is an organic compound characterized by a lower boiling temperature than water and allowing power generation from low temperature heat sources. Another advantage is that ORC requires less space than the steam technology given the same conditions.

When designing an ORC, special attention must be paid to the choice of the appropriate working fluid based on heat source temperature. Chen et al (2011) considered 35 pure working fluids. They analyzed the working fluids selection criteria for ORC such the types of working fluids, density, specific heat, latent heat critical point, thermal conductivity. Lakew and Bolland (2010) concluded that R227ea produces the highest power for heat source temperature range considered (80-160°C), while R245fa gives higher power for heat source temperature higher than 160°C.

Many researches have also investigated ORC system design and parametric optimization. Roy et al (2010) conducted a parametric optimization and performance analysis of a waste heat recovery system based on an organic Rankine cycle using R12, R123, R134a as the working fluid for power generation. Schuster et al. (2010) presented a simulation study of an ORC when using supercritical parameters and various working fluids. Vaja and Gambarotta (2010) described a specific thermodynamic analysis in order to efficiently match an ORC to an internal combustion engine.

In the present study, it was investigated a heat recovery power generation system applied to the cooling system of the main engine of a Tanker ship that is actually in operation. At the beginning the literature on working fluids and ORC system was reviewed. The energy balance was then evaluated using a combination of various source: documentation available, and engine software available on the website of the manufacture. Air cooler, lubricating oil and jacket water heat are available for ORC cycle. Waste heat from exhaust gas is already recovered by the exhaust gas boiler. The three main operating condition are 80%, 70%, 55% of the engine load. Operation at 80% engine load is chosen as design point of ORCs Four organic fluids, R134a, R245fa, R227ea and R236fa have been considered as working fluids for the ORCs after the literature review in Chapter 1. Several configurations are studied to find the one that gives the maximal power. After that the dual stage system and the R236fa are selected as the best mach. They lead to the higher net power output. An approximate evaluation is carried out (without using a detailed off-design model) to evaluate the power output at 70% and 55% of the engine load. Using the output power and the duration for each operating load, the annual energy saving was calculated. In conclusion an economic analysis is made by three parameters: net present value (NPV), payback period (PP) and internal rate return (IRR).

1. Review of the Literature on ORC Working fluid

1.1. Introduction

The literature on ORC presents extensive analyses and comparisons among different thermodynamic cycles and working fluids. However, most of the comparisons were conducted under certain predefined temperature conditions and used only a few working fluids. The claims for best working fluids and the cycle with highest efficiencies may not hold true under other operating conditions and with other working fluids. In this chapter, the pertinent properties of the fluids are first described and then the criteria and the procedure for selecting appropriate fluids for a particular application are presented.

1.2. Working Fluid Properties

The thermodynamic and physical properties, stability, environmental impacts, safety and compatibility with the materials and size of heat exchangers and turbine, are among the important properties that have to be considered when selecting a working fluid for an ORC system.

The properties of organic fluids are different from those of water [Stine et al. (1985)]. The slope of the vapor-side saturation curve of a working fluid in a T–s diagram can be positive (e.g. isopentane), negative (e.g. R22) or vertical (e.g. R142b), and the fluid is accordingly called ‘‘wet’’, ‘‘dry’’ or ‘‘isentropic’’. Wet fluids like water usually need to be superheated, while many organic fluids, which may be dry or isentropic, do not need superheating. Another advantage of organic working fluids is that ORCs typically require only a single-stage expander, resulting in a simpler, more economical system in terms of capital costs and maintenance [Andersen et al. (2005)].

There is no best fluid that meets all the criteria discussed for heat sources with different temperatures. Compromise must be made when selecting the fluids. Among all the criteria and concerns, the critical temperature and the ζ value (see Eq. (1.1)) are important parameters that suggest which type of cycle a fluid may serve and the applicable operating temperature of the fluid. The ζ parameter is in fact the aforementioned slope of the vapor-side saturation curve of a fluid and it is defined by the equation

$$\zeta = \frac{ds}{dT} = \frac{c_p}{T_{ev}} - \frac{\left(\frac{n\tau_{r,ev}}{1-\tau_{r,ev}}\right)+1}{T_{ev}^2}\Delta h_{fg} \tag{1.1}$$

The type of working fluid can be classified by the value of ζ: if ζ>0 it is a dry fluid (e.g. pentane), if ζ=0 it is an isentropic fluid (e.g. R143a), and if ζ < 0 it is a wet fluid (e.g. water). $\tau_{r,ev}$ (=T_H/T_C) denotes the reduced evaporation temperature.

Isentropic or dry fluids were suggested for organic Rankine cycles to avoid liquid droplet impingent on the turbine blades during the expansion. However, if the fluid is ''too dry,'' the expanded vapor will leave the turbine with substantial ''superheat'', which is a waste and adds to the cooling load in the condenser. The cycle efficiency can be increased using this superheat to preheat the liquid after it leaves the feed pump and before it enters the boiler. There is still a great need to find proper working fluids for supercritical Rankine cycles. Anyway dry fluids may serve better than wet fluids in supercritical states, because the dry fluid can still leave the turbine at superheated state, without decreasing the performance of turbine; moreover the heating process of a supercritical Rankine cycle, resulting in a better thermal match in the boiler, with less irreversibility. As a working fluid for supercritical Rankine cycle, carbon dioxide has desirable qualities such as moderate critical point, stability, little environmental impact and low cost. However, the low critical temperature of carbon dioxide, 31.1 °C, might be a disadvantage for the condensation process; carbon dioxide has to be cooled below the critical point (31.1 °C), preferably to around 20 °C in order to condense, which is quite a challenge for the design of a cooling system for many cases.

1.2.1. Effectiveness of superheating

Superheating contributes negatively to the cycle efficiency for dry fluids, and is not recommended. For wet fluids, superheating is mostly necessary for turbine expansion safety and improvement of the cycle efficiency.

Propyne, HC-270, R-152a, R-22 and R-1270 are wet fluids and superheating is usually needed for this group of fluids. They might be applied in supercritical Rankine cycles if the temperature profile of the heat source meets the requirements. However, propyne, HC-270 (cyclopropane) and R-1270 (propene) are not normally used in their supercritical state due to the stability concerns. Propyne, HC-270 and R-1270 have relatively low molecular weight. Applying these fluids implies a larger system size compared to those fluids with higher molecular weight.

Among these fluids, R-141b, R-142b (isentropic fluids), R-123, R-245ca, R-245fa (dry fluids) and R21 (wet fluid) have critical temperature above 400 K, making them more likely to be used in organic Rankine cycle than in supercritical cycle for low temperature heat sources. Fluids R-601, R-600, R-600a, FC-4-1-12, R-C318, R-3-1-10 are considered dry fluids, they may be used in supercritical Rankine cycles and organic Rankine cycles. Since superheat has a negative effect on the cycle efficiency when dry fluids are used in organic Rankine cycle, superheating is not recommended.

1.2.2.Critical points of the working fluids

Condensation is a necessary process in the organic Rankine cycle. The design condensation temperature is normally above 300 K in order to reject heat to the ambient; therefore, fluids like methane with critical temperatures far below 300 K are out of consideration because of the difficulty in condensing. On the other hand, the critical point of a fluid considered as the working fluid of a supercritical Rankine cycle should not be too high to overpass. The critical point of a working fluid, being the peak point of the fluid saturation line in a T–s diagram, suggests the proper operating temperature range for the working fluid of liquid and vapor forms, and the critical temperature is an important data for fluid selection. Another important thermodynamic property is the freezing point of the fluid, which must be below the lowest operating temperature in the cycle. The fluid must also work in an acceptable pressure range. Very high pressure or high vacuum has a tendency to impact the reliability of the cycle or increase the cost.

Fluids R-170, R-744, R-41, R- 23, R-116, R-32, R-125 and R-143a are wet fluids with low critical temperatures and reasonable critical pressures; which are desirable characteristics for supercritical Rankine cycles. Among these fluids, R-170, R-744, R-41, R-23 and R-116 have critical temperatures below 320 K, which require low condensing temperatures, not achievable under many circumstances. The critical temperatures of R-32, R-125 and R-143a are above 320 K, so the design of condensers for these fluids is not a big concern. Provided other aspects are satisfied, R-32, R-125 and R-143a could be promising working fluids for supercritical Rankine cycles.

Table 1-1 Critical points of working fluids

Working Fluids	T_c [K]	P_c [bar]	Properties	
R170	305.33	48.7	Critical temperature below 320 K	Complicated design condenser
R744	304.13	73.8		
R41	317.28	59		
R23	299.29	48.3		
R116	293.03	30.5		
R32	351.26	57.8	Critical temperature above 320 K	Promising working fluids for supercritical
R125	339.17	36.2		
R143a	374.21	37.6		

1.2.3.Stability of the fluid and compatibility with materials in contact

Unlike water, organic fluids usually suffer chemical deterioration and decomposition at high temperatures. The maximum operating temperature is thus limited by the chemical stability of the working fluid. Additionally, the working fluid should be noncorrosive and compatible with engine materials and lubricating oil. Calderazziet al (1997) studied the thermal stability of R-134a, R-141b, R-13I1, R-7146 and R-125 associated with stainless steel as the container material. Ammonia as a deep wet fluid, needs superheating when used in an organic Rankine cycles. Ammonia is not recommended in supercritical Rankine cycles, since the critical pressure (11.33 MPa) is relatively high. Meanwhile ammonia is highly hydrophilic and ammonia-water solution is corrosive, limiting the materials that may be used [Huijuan (2010)]. For example it is not possible to use ammonia with copper.

1.2.4. Environmental aspects

As to the environmental aspects, the main concerns include:

ODP: the ozone depletion potential
GWP: global warming potential
ALT: atmospheric lifetime.

The ODP of a chemical compound is the relative amount of degradation to the “ozone layer” it can cause, with trichlorofluoromethane (R-11 or CFC-11) being fixed at an ODP of 1.0. Chlorodifluoromethane (R-22), for example, has an ODP of 0.055. CFC 11, or R-11 has the maximum potential amongst chlorocarbons because of the presence of three chlorine atoms in the molecule.

The GWP is a relative measure of how much heat a greenhouse gas traps in the atmosphere. It compares the amount of heat trapped by a certain mass of the gas in question to the amount of heat trapped by a similar mass of carbon dioxide. A GWP is calculated over a specific time interval, commonly 20, 100 or 500 years. GWP is expressed as a factor of carbon dioxide (whose GWP is standardized to 1).

The ODP and GWP represent substance’s potential to contribute to ozone degradation and global warming. Due to environmental concerns, some working fluids have been phased out, such as R-11, R-12, R-113, R-114, and R-115, while some others will be phased out in 2020 (such as R-21, R-22, R-123, R-124, R-141b and R-142b). Those phased-out substances are not included in the following discussion of potential working fluids. Alternative fluids are being found and applied. The alternatives are expected to retain the attractive properties and avoid their adverse environmental impact. The most promising candidates are still found among fluids containing fluorine and carbon atoms.

The inclusion of one or more hydrogen atoms in the molecule, results in it being largely destroyed in the lower atmosphere by naturally occurring hydroxyl radical, ensuring that little of the fluid survives to enter the stratosphere.

The refrigerants that are considered “mainline” for use in marine applications for refrigerant cargo air conditioning and provision Room refrigeration system are the following: R-134a, R-744 (CO_2), R-407a, R-407c, R717, R290, R600, R600a, R123, R245fa, R141b, R227a [MARPOL].

Table 1-2 Mainline refrigerants for use in Marine applications.

Category and name	ASHRAE number	Tc [°C]	Pc [bar]
Hydrocarbons (HCs)			
propane	R290	96	41.8
N-butane	R600	152	37.9
Isopentane	R601a	187	33.7
Hydroflurocarbons (HFCs)			
1,1,1,2-Tetrafluoroethane	R134a	101	40.6
1,1,1,3,3 Pentafluoropropane	R245fa	153	36.1
1,1,1,2,3,3,3 Heptafluoropropane	R227ea	101	28.7
Hydrochlorofluorocarbons (HCFCs)			
1,1-Dichloro-1-fluoroethane	R141b	204	42.1
1,1-Dichloro-2,2,2-trifluoroethane	R123	183	36.6
Inorganic			
Ammonia	R717	132	113.3
Carbon dioxide	R744	31	73.8
Blends			
Blend of 32/125/134a	R407a	82.8	45.4
Blend of R-32/125/134a	R407c	86.8	46.2

1.2.5.Safety

The ASHRAE refrigerant safety classification is a good indicator of the fluid’s level of danger. Generally, characteristics like noncorrosive, non-flammable, and non-toxic are expected. But they are not always practically satisfiable or critically necessary. Many substances, like R-601, are considered flammable but this is not a problem if there is no ignition source around. However, auto ignition is a problem, in particular for longer alkanes at temperatures above 200°C. The maximum allowable concentration and the explosion limit should also be under consideration. Instead R12 having a little odor and colorless gas or liquid, non-flammable, non-corrosive of ordinary metals and stable is a

CFC refrigerant Roy (2010). The ASHRAE refrigerant safety classification is a good indicator of the fluid's level of danger. Generally, characteristics like non-corrosive, non-flammable, and non-toxic are expected, but the most essential requirement is chemical stability.

A refrigeration system is expected to operate many years, and all other properties would be useless if the refrigerant decomposed or reacted to form something else.

The next most important criterion relates to health and safety; the ideal refrigerant would have low toxicity and be nonflammable.

ASHRAE classifies refrigerants according to their toxicity (with "A" being a "lower degree of toxicity" as indicated by a "permissible exposure limit" of 400 ppm or greater, while "B" refrigerants have a "higher degree of toxicity" and flammability (ranging from "1" for nonflammable fluids to "3" for highly flammable fluids, such as the hydrocarbons). Flammability class "2" has a further subclass ("2L") for refrigerants of very low flammability, as defined by a burning velocity of less than 10 cm/s. Thus, an ideal refrigerant would be class "A1," and such refrigerants can be used with minimal health and safety restrictions. Other classes are restricted, such as maximum limits on the system charge or restriction to use in dedicated machine rooms.

Manente (2011) describe some examples: alkanes that are non-toxic but flammable are class A3. They require safety devices. R152a is classified A2 (lower flammability and non-toxic). R134a is of class A1 (non-flammable and non-toxic). R123 is B1 (non-flammable but toxic). Ammonia classified B2 (toxic and lower flammability) could be used in an open space with lesser precaution compared with alkanes. Shengjun (2011) provides the ASHRAE coefficient of several fluids. R227ea and R236fa are of class A1 and R245fa is of class B1.

1.2.6.Size of the system

There are two indicators to describe the ORC size: one of those is the total area of heat exchangers and the other one is the turbine size.

The evaporator contributes more area to the total area required for two reasons; more heat is exchanged in the evaporator than in the condenser and air side heat transfer coefficient is the dominant. It is known that air or exhaust gas have lower heat transfer coefficient than water (which is the heat sink in this case).

He et al. (2011) attempted to compute a turbine size factor instead of making a detailed design of the turbine. The turbine size factor is defined in terms of the turbine exit volume flow rate and enthalpy drop in the turbine and it is an indicator of turbine size:

$$SP = \frac{\sqrt{\dot{V}}}{\sqrt[4]{\Delta h_{is}}} \tag{1.2}$$

The size parameter is proportional to actual turbine size.

In the work by He et al (2012) described in Section 1.3, they discovered that working fluids R717, methanol, R600a, R142b, R114, R600, R245fa, R123, R601a, n-pentane, R11, R141b and R113 have the lower size factor; instead, Lakew et al. (2010) from a selection of working fluids concluded that R134a has the lowest turbine size factor.

1.3. Fluid Selection and Parametric Optimization for Basic Rankine Cycle

Lakew et al. (2010) presented the performance of different working fluids to recover low temperature heat source. Working fluid considered are R-134a R-123, R-227ea, R-245fa, R-290 N-pentane. A simple Rankine cycle with subcritical configuration is considered, which consists of a pump, evaporator, turbine and condenser. The working fluid is saturated liquid at the exit of the condenser, then it gains heat from the heat source, later at the exit of the evaporator, the fluid is saturated vapor. Pump and turbine efficiency is 80%, and generator efficiency is 90%, the condensation temperature is fixed at 20°C, minimum approach temperature of 10°C in the evaporator and 5°C in condenser.

The result shows the efficiency increases with pressure. At higher pressure the working fluid takes less heat and produces less power but higher thermal efficiency (the thermal efficiency is the ratio between the power output and the input thermal power, it is described in Eq. (2.1)). For heat source at 80°C maximum power is produced with R-227ea at 8 bar, also at 120°C the maximum is given by the R-227ea with 16 bar R-134a at 22 bar gives the second highest power; when the heat source temperature is 200°C, R245fa at 21 bar produced the highest power. R290 has the lowest power output for all heat sources. The maximum power output is showed for different heat sources in Table 1-3. In conclusion, R227ea gives highest power for heat source temperature ranging from 80–160°C and R245fa produces the highest power for heat source ranging from 160–200°C.

Table 1-3 Maximum power output of Lakew's works.

Maximum Power		**Heat source temperature [°C]**			
Parameter	**Units**	80	120	160	200
Working fluids	**-**	R227ea	R227ea	R227ea	R245fa
Evaporator pressure	**bar**	8	16	28	21
Power	**kW**	160	577	1269	2255

About the heat exchanger area, for heat source of 80°C the n-pentane requests the lowest area (728 m^2) with 1.6 bar, for the same temperature R124 requests 772 m^2 at 14

bar, but the turbine size factor of n-pentane is around 3 times that of R134a. For 120°C R123 and n-pentane require comparably minimum area (1171 m^2-1172 m^2) but R134a requires 1249 m^2). Also at this temperature, the turbine size factor is more than two times that of R134a, the highest power is produced by R227ea (160kW) and the maximum power output of all fluids is practically the same: it is in the range of 155-160 kW. The tables Table 1-4 and Table 1-5 showed the results of these evaluations.

Unfortunately, there is no working fluid (among those studied in this paper) which requires both minimum heat exchange area and smallest turbine size factor.

Table 1-4 Minimum heat exchange area of Lakew's works.

Minimum heat exchange area		**Heat source temperature [°C]**			
Parameter	**Units**	80	120	160	200
Working fluids	**-**	N-pentane	R123/ N-pentane	R123/ N-pentane	R245fa/ N-pentane
Evaporator pressure	**bar**	1.6	3.9/2.8	6.9/5	14/6
Area	**m^2**	728	1171/1172	1250/1250	1900/1900

Table 1-5 Minimum Turbine size factor of Lakew's work.

Turbine size factor		**Heat source temperature [°C]**			
Parameter	**Units**	80	120	160	200
Working fluids	**-**	R134a	R134a	R134a	R134a
Evaporator pressure	**bar**	20	24	24	24
Sp	**m**	0.08	0.08	0.08	0.08

Wang, et al. (2011) presented a working fluid selection and parametric optimization using a multi-objective optimization model, the screening criteria considered included heat exchanger area per unit power output (A/W_{net}) in order to improve the power produced by per unit of heat exchange area and in order to reduce the capital cost, (80%-90% of the system capital cost was assigned on the heat exchangers) and heat recovery efficiency. The independent parameters are the evaporation and condensation pressures, working fluid and cooling water velocities in tubes. This work considered a basic components of a subcritical ORC system and the pinch point was chosen at about 15°C.

In addition, in the above paper, the capital cost of each heat exchanger is determined the following way: 80%-90% of the price was assigned to the heat exchangers.

In order to improve the power produced per unit of heat exchange area, the ratio of the total heat exchange area to net power output is selected as the first objective function:

$$\min f_1(x) = \frac{A_e + A_c}{\dot{W}_{net}} \quad (1.3)$$

On the other hand, higher heat recovery efficiency means more energy recovered from wasted heat and more net power. Therefore, the second objective function is the heat recovery efficiency

$$\min f_2(x) = \frac{1}{\eta_1} \quad (1.4)$$

The evaluation function for the optimization is expressed by:

$$F(x) = w_1 f_1(x) + w_2 f_2(x) \quad (1.5)$$

The authors suggest the values: $w_1 = 0.6$ and $w_2 = 0.4$.

With this model Eq.(1.5) and with a comparison of optimized results for 13 working fluids the following results are obtained:

a) The evaporating pressure in the cycle increases with the decrease of the boiling temperature of working fluids.
b) The value of objective function of R-123 is the lowest for the temperature ranges from 100°C to 180°C, and R141b is the optimal working fluid when the temperature higher than 180°C.
c) When the heat source temperature is 140°C, the payback period for R-123 is 3.68 years. Compared to R123 the payback period of R134a increases by 59.8%, when the temperature is higher than 180°C, R-141b is the best, when the temperature is 120°C the payback period of R-123 is 5.25 years.
d) The optimal pinch point for ORC system is about 15°C.
e) When the heat source temperature is lower than 100°C, the ORC technology is inappropriate and the payback rises to 9.35 years with the R123, too long for the ORC system.

He et al. (2011) proposed a subcritical simple ORC where it compared 22 different working fluids and the maximum net power output, suitable working pressure, total heat transfer (UA_{tot}) capacity and expander SP are considered as the criteria to screen the working fluids of subcritical ORC. A simple configuration is considered, the hypotheses are as follows: the system has reached the steady state, there is no pressure drop in the evaporator, pipes and condenser. The heat losses in the components are negligible, and isentropic efficiencies of the pump and the expander are given (75%, 80%). The working

fluid at the expander inlet and condenser outlet is saturated vapor and saturated liquid, respectively. The waste heat source temperature is 150°C and the mass source flow rate is 1 kg/s, the pinch temperature difference in the evaporator is 5 K and the pinch point temperature difference in condenser is 5 K.

Table 1-6 Results obtain by He et al (2011).

Working fluids	Power output [kW]	Pressure [kPa]	UA_{tot} [kW/K]	SP [m]
R114	9.61	1206	6.2-7.5	0.03
R142b	9.58	1835	8-12	0.03
R600a	9.54	1714	8-12	0.03
R245fa	9.52	1040	6.2-7.5	0.03
R600	9.43	1307	6.2-7.5	0.03

The results from this paper show that the maximal net power output values vary with the different working fluids like R600a, R142b, R114, R600, R245fa; there is highest net power of ORC when R114 is adopted, and the smallest with R245fa between the fluid shown before. The lowest net power outputs of ORC is with methanol and toluene.

In this work it can be deduced that the larger net power output will be produced when the critical temperature of working fluid approaches the temperature of the waste heat source.

The working pressure at the maximal net power output are shown in Table 1-6, for some working fluids like toluene, n-heptane and n-octane the pressure could be much lower than atmospheric pressure and it means the system need a perfect sealing and extra cost.

For working fluids like R600a, R142b the total heat transfer capacity could change from 8 kW/K to 12 kW/K, for working fluids R141b, R600, R144, R245fa, R113, R123, R600a, toluene the heat transfer capacity is between 6,2 kW/K-7,5 kW/K. For the remaining fluids like n-heptane, n-octane, the total heat transfer capacity is less than 6 kW/K. Usually higher total heat transfer capacity means more costs of the heat exchanger, but for the last two fluids, the power output and working pressure are not ideal for these working fluids.

As regards the turbine size, for working fluids R600a, R142b, R114, R600, R245fa, R123, R600a the expander SP is smaller than 0.03 m.

At the end the authors suggest working fluids such a R114, R245fa, R123, R600a,n-pentane, R141b and R113 are better ones under the given conditions in their paper.

Roy (2010) presented an analysis of an ORC using R12, R123, R134a. The assumptions are Ideal Rankine cycle, isentropic expansion in the turbine, and the pump work is neglected during the optimization study. The heat source is exhaust gas with temperature of 140°C and the mass flow rate of 312 kg/s. A parametric optimization of turbine inlet pressure was performed to obtain the maximum system efficiency, at each inlet pressure during TIT (turbine inlet temperature) optimization W,η_2 , η_1 were calculated and the improvements in performance on superheating were investigated up to the available waste heat temperature under this study.

The results show that for R12 the optimum work of 16.84 kJ/kg with an efficiency value of 12.09%, the superheating is required at moderate pressure to keep the turbine outlet vapor quality within acceptable limit.

R123 as the working fluid appears to be a better choice, a turbine inlet pressure value at 1.945 MPa with 55.56 kJ/kg and 25.30% efficiency. The superheating for this fluid is not suggested.

For R134a the optimum work of 28.03 kJ/kg with an efficiency of 15.53% is obtained at the pressure 3.533 MPa, with a turbine outlet vapor quality of 0.866. If the pressure is increased, the outlet vapor quality is further reduced to value 0.7872 then the superheating is not at all beneficial.

Table 1-7 Results obtained by Roy (2010).

Parameters/output	**R12**	**R123**	**R134a**
Turbine inlet pressure (MPa)	3.332	1.945	3.533
Optimum work (kJ/kg)	16.84	55.56	28.03
η_1 **First law efficiency (%)**	12.09	25.30	15.53
η_2 **Second low efficiency (%)**	30.01	64.40	37.80

Vaja et al. (2010) describe in their paper three different working fluids (R134a, R11 and Benzene) in three different cycles (ORC simple cycle thermally powered by engine exhaust gases, ORC simple cycle thermally powered by engine refrigerant water and a Regenerated ORC thermally powered by engine exhaust gases.

The exhaust gas temperature is around 470°C and engine jacket water is around 79/90°C. Around 1700 kW_t is available by cooling the exhaust gases down to 120°C and about 1000 kW_t is available from the engine cooling water. In the result it can be noted that the benzene is the fluid with the highest power output value and it has the smallest variations from the optimal power. In the Table 1-7 it is showed the optimum pressure and the maximal power of the ORC simple cycle.

Table 1-8 Results obtained for simple ORC by Vaja et al. (2010).

Working fluids	Power output [kW]	Pressure [kPa]	η_1	v_{at}/v_{bt}
R134a	147	3723	0.085	5
R11	290	3835	0.165	32
Benzene	376	4470	0.215	374

The parameter v_{at}/v_{bt} (the ratio between specific volume after and before the turbine) is particularly significant as it shows how much the fluid volume increases through the expansion, and the benzene has the highest value. Considerations regarding the power curve for benzene suggest that a lower evaporating pressure would allow a reduction of turbine outlet/inlet volume flow ratios; for this reason a new optimal value of evaporating pressure for benzene is selected at 2000 kPa.

Table 1-9 Benzene properties on simple ORC.

Working fluids	Power output [kW]	Pressure [kPa]	η_1	v_{at}/v_{bt}
Benzene	349.3	2000	0.198	107

By exploiting the heat discharged from the cooling circle of the engine the power output increase significantly when the fluids R11 or R134a are used but still the power output remains lower than the power obtained with benzene.

Table 1-10 Results obtained by Vaja et al. (2010) for the ORC using heat from cooling water.

Working fluids	Power output [kW]	Power Increase
R134a	199.5	0.348
R11	332.5	0.145
Benzene	386	0.099

For the fluids considered in this cycle only, benzene is suitable for direct regeneration, (the cycle is described in the section 2.6). The net power output is increased by 12.4% with respect to the simple cycle and with this configuration the power

is 392.6 kW with a cycle efficiency of 22.3%. But the benzene is not recommended for installation on board because it is flammable.

Wang et al. (2012) propose a novel system combining a gasoline engine with a dual loop ORC (the description of the cycle in 2.5, R245fa is selected as the working fluid for the HT (high temperature 353.15-404.59 K) and R134a is selected for the LT (low temperature 304.15-348.15 K) loop. R245fa was chosen because of its good safety and environmental properties, and R134a was selected because it is environmental friendly refrigerant widely used in automotive air conditioners.

Borsukiewicz-Gozdur (2010) proposed hybrid power plant to increase the utilization of geothermal resource supposed available at 80–120 °C, i.e. to reduce the temperature of the returned geothermal water. The author proposed two solutions, a dual-fluid hybrid power plant and an hybrid power plant. The proposed dual-fluid power plant consists of an upper Hirn cycle, in which water is vapourized in a biomass boiler and is then condensed in a condenser–vapourizer exchanger, which is the thermal link between the upper and lower cycles. The lower cycle is an ORC where the organic liquid is preheated by the geothermal resource. Thus, in this dual-fluid power plant, the low-pressure part of the classical steam–water power plant (i.e. condenser) is replaced by a ORC. The geothermal water could also be used for preheating of the working fluid (water or another substance) in a single cycle power plant. Borsukiewicz-Gozdur (2010)called this cycle simply hybrid plant, and chose a biomass boiler for the upper part of the cycle, while the working fluid selected is cyclohexane. In the calculation, Borsukiewicz-Gozdur (2010) supposed to reject the geothermal water down to a very low temperature, i.e. 35 °C. The author found out that, with the scope to use the least share of energy from other sources than geothermal, the best option would be a dualfluid-hybrid power plant with R236fa as a working fluid for the ORC cycle.

1.4. Fluid Selection and Parametric Optimization for Transcritical Rankine Cycles

Organic Rankine cycles are reviewed for low grades of heat conversion into power. If a working fluid with subcritical Organic Rankine cycles does not have a good thermal match with its heat sources, the same working fluid, can be compressed directly to its supercritical pressures and heated to its supercritical state before expansion, so as to obtain a better thermal match with the heat source. Unfortunately a supercritical Rankine cycle normally needs higher operating pressures.

Chen et al. (2010) indicates that a review of the literature shows that a transcritical Rankine cycle can achieve higher efficiency than the conventional ORC, and they conduct a rigorous comparative study between a CO_2-based, R32-based, and transcritical Rankine cycles for the conservation of low-grade heat. The results show that the R32-based transcritical Rankine cycle has many advantages over the CO_2-based transcritical Rankine cycle.

One problem with CO_2 is that it has a much lower critical temperature (304.13K, 31°C) and the design of a condenser for CO_2 could be hard to achieve economically and effectively, because in the summer condition the temperature of the sea water is 32°C and it is not possible to remove the heat from the condenser. Instead, R32 has a much higher critical temperature (351.26K), making it much easier to condense. Also, R32 has a higher thermal conductivity in both liquid and vapor phases, which may indicate a smaller heat exchanger for R32.

In this paper energetic and exergetic analyses of transcritical Rankine cycles show that:

I. The thermal efficiency of R32-based transcritical Rankine cycle is higher that CO_2-based cycle for the cycle high temperature of 393-453K and R32 works at much lower pressures.

II. R32 has higher exergy density and lower mass flow rate.

III. With a high temperature of 433 K the exergy efficiencies of CO_2 and R32 based transcritical Rankine cycles are in the range of 0.15-0.51 and 0.56-0.61 respectively, over a wide range of the cycle high pressure.

If we compare the pressure between He et al. (2011) work and the result of the work of Chen et al (2011), we discover that the working pressure at the maximal net power output for the CO_2 is 22 MPa, for the R23 is around 11 MPa, instead of 1.2 MPa with R114 He et al. (2011) like according to the paper Chen H. et al (2010).

Schuster et al. (2010) evaluated the performance of ORCs operating at supercritical pressures. They compared different fluids using both the thermal efficiency and the total heat-recovery efficiency. They showed that the advantage in adopting a supercritical pressure compared to a subcritical operation are: lower exergy destruction in the evaporator and lower exergy losses in the exhausts, it means a low temperature differences between the heat source and the working fluid, thus it require larger U·A values for the heat exchangers.

High pressure and larger U·A are two reasons that render difficult the installation on board.

1.5. Conclusions based on the Literature Review

The brief review presented above clearly shows that the selection of an appropriate working fluid is very important for maximum waste heat recovery in actual output electric power. Amlaku et al. (2010) suggest R227ea for heat source temperature ranging from 80°C-160°C and R245fa for that ranging from 160-200°C. Moreover he stated that the R134a has the lowest turbine size. Instead Wang et al. (2011) wrote that the best choice for the range from 100°C to 180°C is R123 (in agreement with Roy (2010) and R141b when the temperature is higher than 180°C. Chao et al. (2011) took heat transfer capacity and the turbine size for working fluids in consideration and they suggested fluids like R114, R113, R245fa, R123, R600a, n-pentane, R141b. Boursukiewiciz-Gozdur (2010) suggest R236fa as working fluid for ORC cycle. Huijuon et al. (2010) indicated that the supercritical ORC gives higher efficiency than simple ORC but in the same time high working pressure. As indicated in Section 1.2.4 like R113, R114 are phased out and others like R21, R22, R123, R124, R141b, R142b will be phased out in 2020 or 2030. Considering all this information, the possible fluids are R227ea, R245fa, R134a, R236fa.

Table 1-11 Properties of working fluids.

ASHRE number	Name	Formula	Molecular weight	T_c (K)	p_c (MPa)	ζ	ODP	GWP_{100}	Comment
Prohibited in the new installation after 2005									
R113	1,1,2-Trichloro-1,2,2-Trifluoroethane	CCl_2FCClF_2	187.38	487.3	3.257	0.37	0.8	5000	It is suggested by He et al. (2012)
R114	1,2-Dichloro-1,1,2,2-Tetrafluoroethane	$CClF_2CClF_2$	170.92	418.9	3.392	0.62	1	9300	Best choice with source temperature is 150°C (He et al. 2012)
Prohibited in new installation after 2020									
R21	Dichlorofluoromethane	$CHFCl_2$	102.92	451.48	5.18	0.78			
R22	Chlorodifluoromethane	$CHClF_2$	86.47	369.30	4.99	-1.33	0.055	1700	
R123	2,2-Dichloro-1,1,1-Trifluoroethane	CF_3CHCl_2	152.93	456.83	3.66	0.26	0.02	120	Mainline in marine applications. Suggested by He et al. (2012). Minimum area for temp 120°C (Lakew et al. 2010) and best choice for range 100°C to 180°C and minimum payback (Wang et al. 2011)
R124	2-Cholo-1,1,1,2-Tetrafluoroethane	CF_3CHClF	136.48	395.17	3.62	0.26	0.026	620	minimum area for heat source 80°C (Amalaku et al. 2010)
R142b	1-Chloro-1,1-Difluoroethane	$C_2H_3F_2Cl$	100.50	410.26	4.06	0	0.06	2400	Best choice with temperature high than 180°C (Wang et al. 2011)

ASHRAE number	Name	Formula	Molecular weight	T_c (K)	p_c (MPa)	ζ	ODP	GWP_{100}	Comment
Fluids without restrictions									
R32	Difluoromethane	CH_2F_2	52.02	351.26	5.78	-4.33	0	580	Better choice than $C0_2$ for supercritical Rankine cycle Chen(2010)
R134a	1,1,1,2 Tetrafluoroethane	CF_3CH_2F	102.02	374.21	4.06	-0.39	0	130	Mainline in marine application, The smaller turbine size factor (Amlakuet al. 2010), the superheating is not at all beneficial Roy J.O. et al. (2010). It is used for LT loop on Wang et al. (2012)
R227ea	1,1,1,2,3,3,3-Heptafluoropropane	CF_3CHFCF_3	170.03	375.95	3.00	0.76	0	3500	Mainline marine application. Highest power for th range (80-160)°C Amlaku et al.(2010)
R236fa	1,1,1,3,3,3 Hexafluoropropane	$C_3H_2F_6$	152.04	397	3.19		0	9810	
R245fa	1,1,1,3,3 Pentafluoropropane	$C_3H_3F_5$	134.05	427.20	3.64	0.19	0	950	Mainline marine application. It is suggested by Chao et al. (2011) It is used by Smolen (2011), Wang E.H. et al (2012) Highest power range (160-200°C), Lakew et al.2010
R600	Butane	C_4H_{10}	58.12	425.13	3.80	1.03	0	3	Mainline marine application. It is suggested by He et al. (2012)
R600a	Isobutene	$CH(CH_3)_3$	58.12	407.81	3.63	1.03	0	3	Mainline marine application It is suggested by Chao et al. (2011)
R601	Pentane	$CH_3CH_2CH_2CH_2CH_3$	72.15	469.70	3.37	1.51	0	-	It is suggested by Chao and it is considered flammable J.P.Roy et al (2010).
R717	Ammonia	NH_3	17.03	405.4	11.33	-10.48	0	<1	Mainline marine application

ASHRAE number	Name	Formula	Molecular weight	T_c (K)	p_c (MPa)	ζ	ODP	GWP_{100}	Comment
R717	Ammonia	NH_3	17.03	405.40	11.33	-10.48	0	<1	Mainline marine application
R744*	Carbon dioxide	CO_2	44.01	304.13	7.38	-8.27	0	1	Mainline in marine application. T_c around 31.1°C disadvantage for the condensation process
R1270	Toluene	C_3H_6	92.14	591.75	4.13	-0.21	0	1.8	The pressure of condensation is much lower than atmospheric , it means more cost. He et al. (2010)

* The critical temperature of the fluid is below 320K and the data is given based on 290K.

2. Literature Review of Various ORC Systems

2.1. Introduction

The aim of this chapter is to describe various ORC cycles that they are found in literature in order to find the best choice or suggest a plant design to apply in the ship that is studied.

2.2. Thermal efficiency and total heat recovery efficiency.

A new metric was introduced by Liu B.T et al. (2004) to better characterize the performance of ORCs called "total heat-recovery efficiency". According with Liu, Manente (2011) wrote that the parameter thermal efficiency does not show how effectively the heat carrier is cooled since it only considers the heat transferred from the heat source to the working fluid. Instead the total heat-recovery efficiency (η_T) takes into account the whole thermal energy of the heat carrier and it is defined by the following equation:

$$\eta_T = \frac{\dot{W}}{\dot{Q}_{av}} \tag{2.1}$$

where $\dot{W}$ is the power output and $\dot{Q}_{av}$ is the available thermal power in the heat carrier. The thermal efficiency (η_{TH}) is the ratio between the power output and the input thermal power to the thermodynamic cycle:

. $$\eta_{TH} = \frac{\dot{W}}{\dot{Q}_{in}} \tag{2.2}$$

The heat recovery efficiency (ϕ) is defined as the ratio between the thermal power transferred to the cycle and the thermal power that is effectively available in the working fluid.

$$\phi = \frac{\dot{Q}_{IN}}{\dot{Q}_{av}} \tag{2.3}$$

Hence, the total heat-recovery efficiency is the product of the thermal efficiency and the heat recovery efficiency:

. $$\eta_T = \eta_{TH} \cdot \phi \tag{2.4}$$

The analysis of total heat recovery is different from the conventional analysis which focused on thermal efficiency. In general, the maximum value of total heat-recovery efficiency occurs at the appropriate evaporating temperature that is between the inlet temperature of waste heat and the condensing temperature. The maximum value of total heat recovery efficiency increases with the increase of the inlet temperature of the waste heat and decreases it by using working fluids of the lower critical temperature.

Analysis using a constant waste heat temperature, or based on thermal efficiency may result in considerable deviation regarding the system design of the varying temperature conditions of the actual waste heat recovery.

2.3. Simple ORC

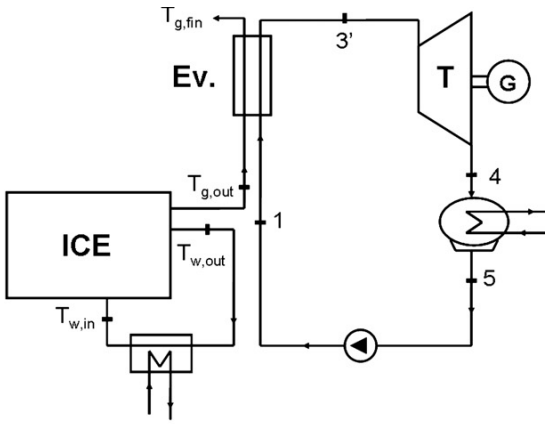

Figure 2-1 Flow diagram of simple ORC.

Vaja et al. (2010) propose a cycle like in Figure 2-1 and Figure 2-2, which consists of a working fluid pump, an evaporator driven by the exhaust gas, an expander and a water cooled condenser. Working fluid is pumped to the evaporator where it is heated and vaporized by the exhaust heat. The generated high pressure vapor flows into the expander and its heat energy is converted to mechanical work. Simultaneously, the expander drives the generator and electric energy is generated. Then, the exhaust vapor exits the expander and is led to the condenser where it is condensed. The condensed working fluid is pumped back to the evaporator and a new cycle begins.

The graphs outlined in Figure 2-2 and Figure 2-8 show the thermodynamic cycle on T-$\dot{S}$ diagram. The curve regarding the engine exhaust gas is described by *T* and $\dot{S}_{gas}$ axis. Moreover the exhaust gases trend have been calculated with this composition on the basis of mass: CO_2=9.1%, H_2O=7.4%, N_2=74.2%, O_2=9.3%.

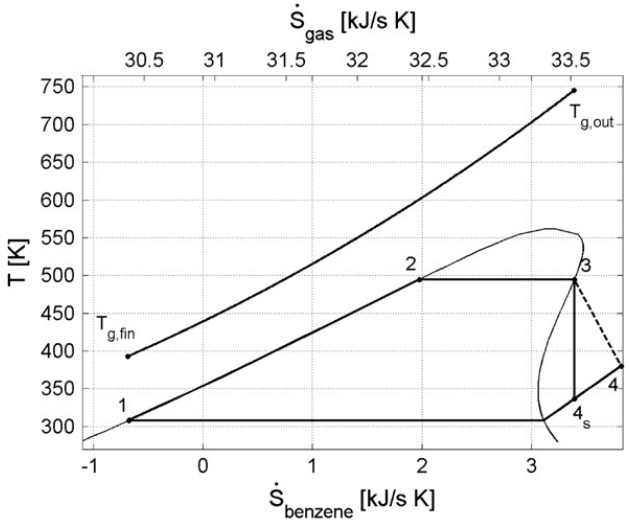

Figure 2-2 diagram T-s simple ORC.

The heat source includes 1700 kW_t from exhaust gas (from 340°C to 120°C). If the simple ORC configuration in Figure 2-2 is used, the power output is 376 kW for benzene, 290 kW for R11, and 147 kW for R134. With regard to the cycle efficiencies, the maximum value of 0.215 is achieved with benzene, 0.165 with R11 and 0.085 with R134a.

The temperature difference between gases and organic fluid induces irreversibility, that is the main cause for low thermodynamic efficiencies with R11 and R134a. Benzene has a critical temperature of 288.9°C and it is closer to inlet exhaust gas temperature than the other two fluids.

2.4. ORC with Use of Heat Available from the Engine Cooling System

In a typical diesel engine, less than 45% of the fuel energy might be converted into useful work output, and the remaining energy is mainly lost through exhaust gas, jacket water and lubricating oil. For this reason Vaja et al. (2010) suggest as well as a partial preheat of the organic fluids, (it is shown in Figure 2-3) using jacket water as heat source. The thermodynamic cycles are the same as defined in the previous section but it is added one more exchange liquid- liquid upstream the main evaporator.

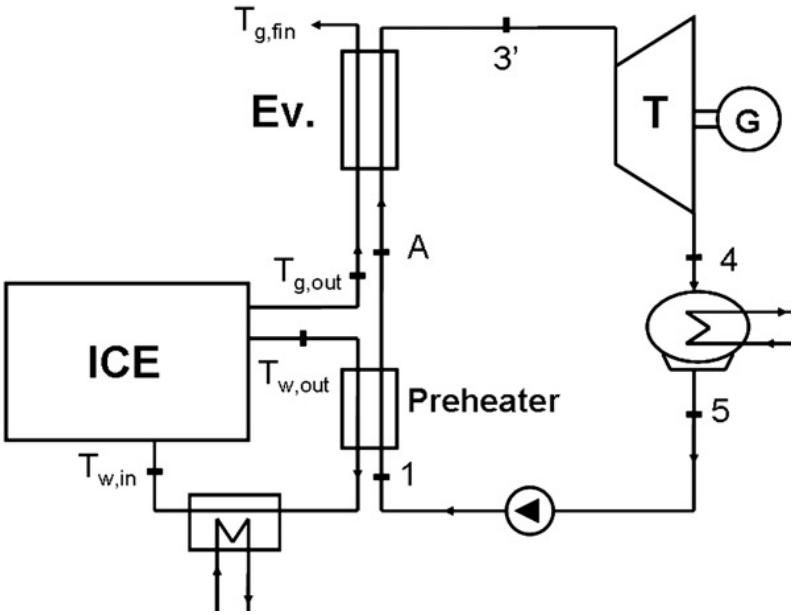

Figure 2-3 Flow diagram of ORC with engine cooling system.

The heat source includes 1700 kW_t from exhaust gas (from 340°C to 120°C) and 1000 kW_t from engine cooling water. If the configuration in Figure 2-3 is used, the power output value is 386 kW for benzene, 332.5 kW for R11, and 199.5 kW for R134. The net

power output compared to the simple ORC increases by 9.9% with benzene, 14.5% with R11 and 34.8% with R134a.

2.5. Dual loop system

Wang et al. (2012) describe another system. The authors combine a gasoline engine with a duel loop ORC, which recovers the waste heat from both the exhaust and coolant system. A high temperature (HT) loop recovers the exhaust heat while a low temperature (LT) loop recovers both the residual high temperature loop heat and the coolant heat (Figure 2-4).

The HT loop consists of Pump 1, Evaporator 1, Expander 1, Preheater, Reservoir 1, and the connecting pipes. The LT loop consists of Pump 2, Preheater, Evaporator 2, Expander 2, Condenser, Reservoir 2, and the connecting pipes. The LT loop is coupled with HT loop via the preheater.

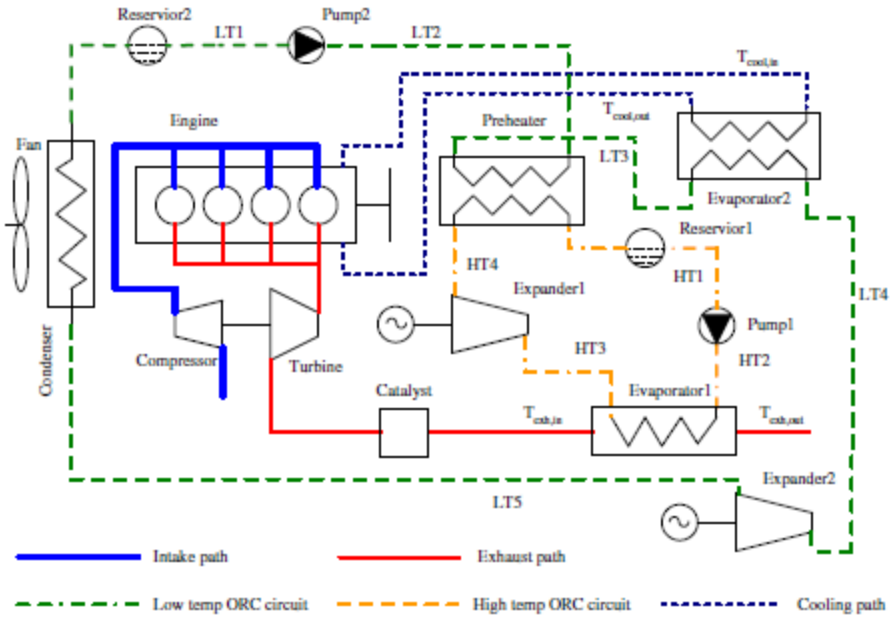

Figure 2-4 flow diagram dual loop system.

The dual loop ORC designed for this study is shown in Fig.2.3.1-1 and Fig. 2.3.1-2. The waste heat from the exhaust is then added and working fluid is evaporated to a saturated vapor state HT3. Subsequently the R245fa is expanded in Expander 1 and the useful work in output to generate electricity. R245fa is a dry working fluid: thus, it changes to a superheated state HT4 after expansion. In the preheater R245fa is transformed into a saturated liquid state HT1 after transferring its heat to the R134a working fluid. Then the working fluid returns to Reservoir 1 and waits for the next

circulation cycle. Meanwhile, in the LT loop, Pump 2 pressurizes the R134a from Reservoir 2 to the preheater. Then the coolant flows out of the engine jacket, evaporates, and heats the R134a to a superheated state LT4 in Evaporator 2. Superheating is required because R134a is a wet working fluid and superheating guarantees that no liquid is generated during the subsequent expansion process. The R134a is slightly superheated at LT5 after expanding in Expander 2 later the fluid is condensed to a saturated liquid state LT1 in the condenser and flows back to Reservoir 2. At the rated power output, the heat recovery from the HT loop is 133 kW whereas that of the LT loop is 365 kW. The thermal efficiency of the HT loop is 7.16%, slightly lower than the efficiency of the LT loop (7.72%). For this reason, the net power of the LT loop is higher than that of the HT loop (9.57 kW for the HT loop and 26.39 kW for the LT loop).

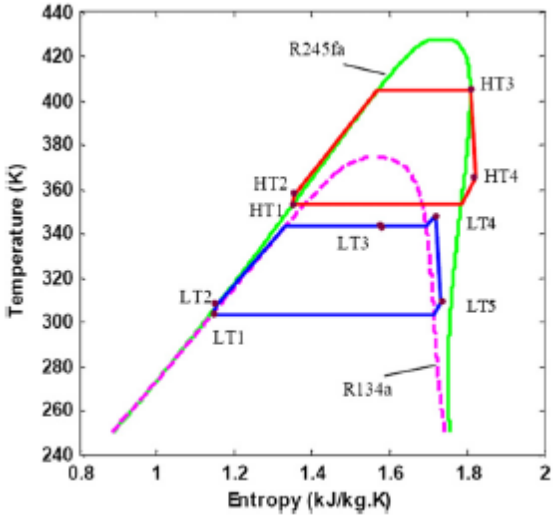

Figure 2-5 T-s plots of the HT and LT loops.

2.6. Recovery system by Yue et al. (2012)

Yue et al. (2012) suggest another type of system to recover energy from exhaust gas and at the same time from jacket water, but in this case the exhaust gas exchanges heat with cooling water by heat exchanger. The organic fluid (in this paper the authors analyze Isopentane) was pressurized by the fluid pump and then it was heated to saturated steam by the heated cooling water. The organic fluid vapor expanded and accelerated in turbine converted the thermal energy into mechanical energy. The turbine drives a generator, which produces electricity. Outlet gas was condensed into the liquid state in cooled condenser.

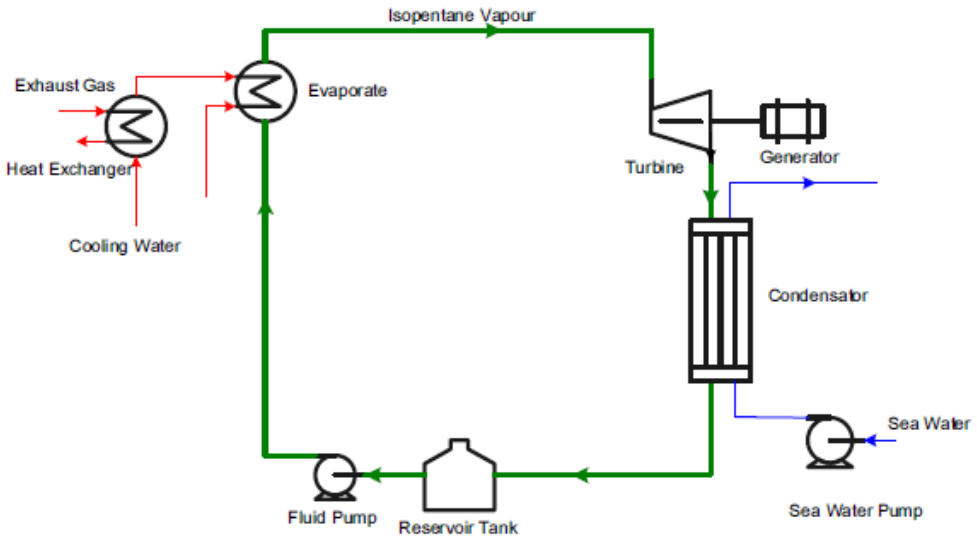

Figure 2-6 flow diagram of system by Yue et al. (2012).

The maximum temperature of exhaust gas is 370°C and the outflow temperature is 150°C. The whole available energy is 1542.82 kW by exhaust gas. The inlet temperature of cooling water is 63°C and the outlet temperature is 73°C. Thermal energy from cooling water is 2286.67 kW. The choice of evaporating temperature is the key point in the waste heat recovery system. Cycle efficiency (η_{TH}) and working pressure increased with the increase of evaporating temperature, and mass flow decreased with the increase of evaporating temperature. When the working pressure increases, the flow field of the turbine and evaporator will become more complicated and the cost of the components will be higher. Given the above problems, the evaporating temperature was set at 105°C. The results show a cycle efficiency of 13.6% and the design turbine power is 300 kW.

2.7. Regenerated ORC

Vaja et al. (2010) analyses also the regenerated cycle Figure 2-7, it consists of one pump , one evaporator, one expander, one heat exchanger for energy recovery, and the connecting pipes.

The cycle is quite similar to the cycle described in Section 2.3, but before the evaporator the fluid transfers heat to the superheated vapor at the turbine outlet.

The authors worked at this cycle with three different fluids (benzene, R134, R11), among which, only benzene is suitable for direct regeneration, this is because at the exit of the turbine benzene has high temperature and high enthalpy. Moreover, the authors suggest to use the regenerated design with turbines with low adiabatic efficiency. In fact, a low efficiency expander leads to a temperature and enthalpy increase of the

superheated vapor at the turbine outlet and this energy is partly recovered in the exchange.

The regenerate heat exchange requires a liquid-gas, it is not simple than the heat exchange liquid-liquid. Vaja et al. (2010) shows in the Section 1.3 that the increase power output from the regenerated cycle and from simple cycle with preheat is the same, so it is suggested the second choice, thus simplifying the design of the heat exchanger required.

The heat source includes 1700 kWt from exhaust gas (from 340°C to 120°C). If the configuration in Figure 2 8 is used, the power output is 392.6 kW for benzene, and the net power increases with respect to the simple ORC by 12.4 %.

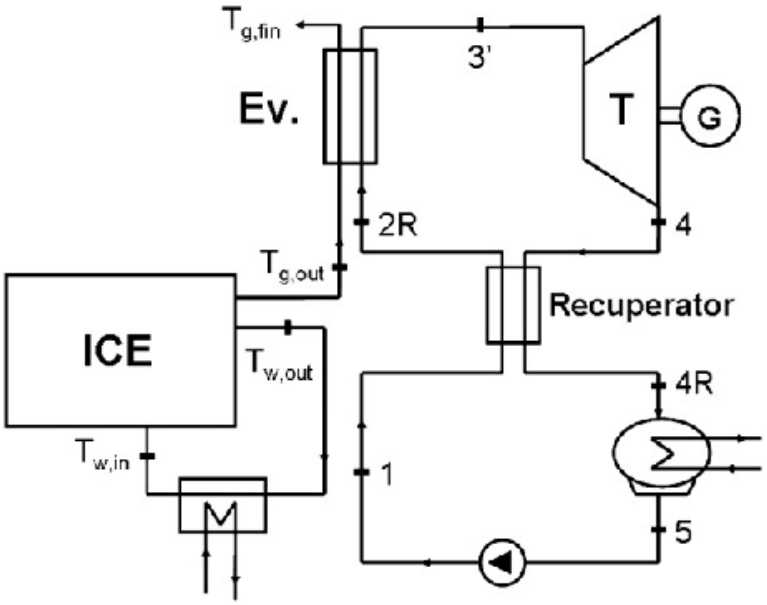

Figure 2-7 flow diagram of regenerated ORC.

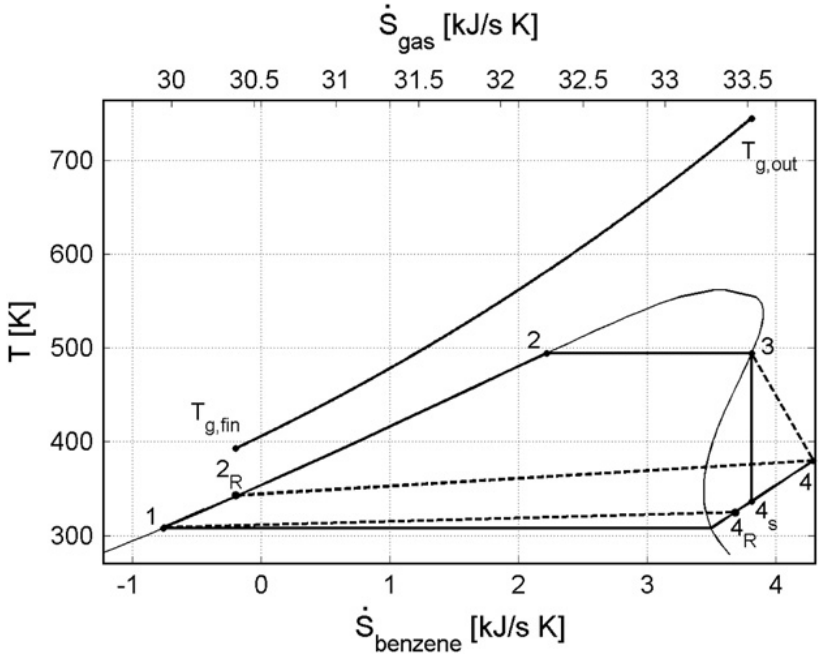

Figure 2-8 benzene regenerated cycle, T-s diagram.

Vaja consider that the recuperator is a counterflow type heat exchanger and it required a $\Delta T_{appr,R} = 15\ K$. Under these hypotheses the temperature of the vapor at the heat exchanger outlet can be evaluated.

$$T_{4R} = T_1 + \Delta T_{app,R} \tag{2.5}$$

In Figure 2-8 the two dotted lines are referred to the internal heat exchange process.

2.8. Two-stage Organic Rankine Cycle

Smolen et al. (2011) present a similar idea for a two-stage ORC of Wang et al. (2012), but using another coupling concept. In Figure 2-9 and in Figure 2-10 there is a simplified view of the two-stage ORC process.

The ORC system concept also mentioned comprises two heat input stages and two expansion stages. The two temperature levels of heat input correspond to the heat transfer temperatures and ratios in the exhaust gas heat exchanger of a combustion engine specifically a gas motor in a biogas plant, and in the cooling system of the engine. High pressure expansion is carried out in a micro-turbine, and the residual expansion is coupled with the expansion of the working fluid from the low temperature heat input in a screw engine.

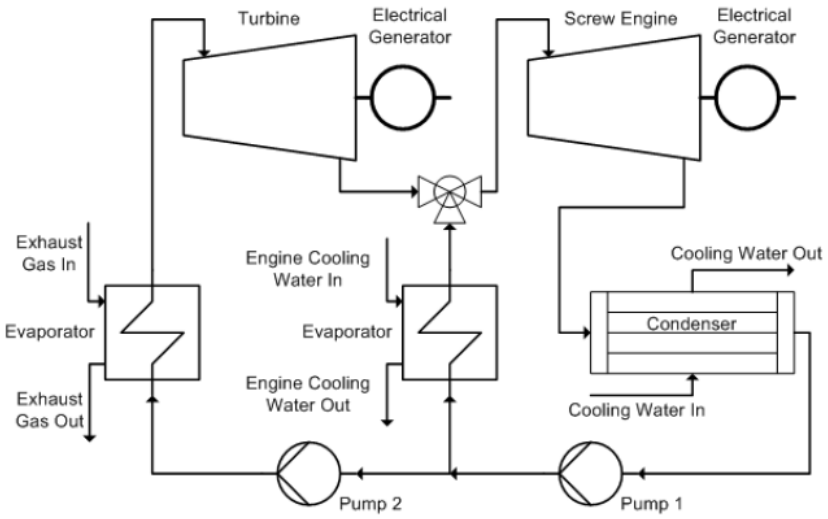

Figure 2-9 Flow diagram for a two stage ORC system.

The waste heat used by ORC system is 131 kW from exhaust gas and 143.67 kW from cooling system of engine. The output power is 5.39 kW for the turbine and 22.69 kW for the screw engine. The cycle efficiency is 0.098.

Although this complicates, the system as a whole, it permits a better operational exploitation of the power. The variant with two pumps and two expansions is more efficient and advantageous due to flexible operation but also more expensive and it needs more space.

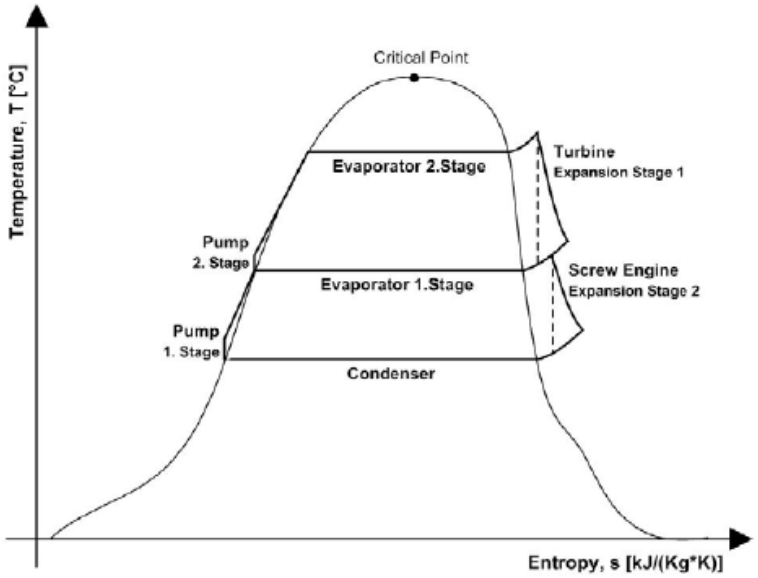

Figure 2-10 Two-stage ORC process in form of a T-s diagram.

2.9. Effect of using Diathermic Oil

Yu et al. (2013) use a thermal oil circuit between exhaust gas and ORC circuit to prevent decomposition of working fluid R245fa.

Vaja et al. (2010) describe that the effect of using diathermic oils as heat transfer media between engine gases and organic fluid will also be considered in order to reduce risks related to the flammability of some of the fluids that may be employed and to ensure higher stability for the operation of the ORC due to the oil thermal inertia. This design would however introduce further irreversibility in the main heat exchange process that is the cause for a reduction in the global ORC system efficiency.

3. Energy Balance of the Main Engine

3.1. Introduction

The aim of this chapter is to explain the whole method that was used to evaluate the energy balance of the main engine (M/E) for a Tanker. The results are obtained combining information from various sources: official shop test results for Main Engine (there are data for 110%, 100%, 90%, 75%, 50%, 25% engine load), results of sea trials, F.W (fresh water)/S.W (sea water) heating balance calculation, and steam balance. In addition, the values of several operating parameters at various loads (not given in the aforementioned documents) have been obtained using software available on the website of the manufacturer. Thus, using the available data and formulating some assumptions the energy balances for the main engine loads are evaluated.

3.2. Main Engine System

In Figure 3-1, the Main Engine system is shown. Within main engine (box number 1) the fuel thermal power is converted into useful mechanical power ($\dot{W}$). The remaining fuel thermal power is lost through lubricating oil (box number 3), jacket water (box number 4), air cooling (box number 6), radiation losses ($\dot{Q}_r$) and exhaust gas (point g1). Part of the exhaust gas heat is actually recovered in the turbocharger (box number 2) and in the exhaust gas boiler (box number 7). The turbocharger's compressor draws in ambient air (point a1) and compresses it (point a2) before it enters into the air cooler system (box number 6). Using part of the thermal power from the jacket water, fresh water generator (box number 5) produces fresh water (water used for steam production, domestic consumption). Cooling system is composed by a water loop which extracts heat from lubricating oil, jacket water and supercharging air and then reject it to seawater in a central cooler (box number 8).

.

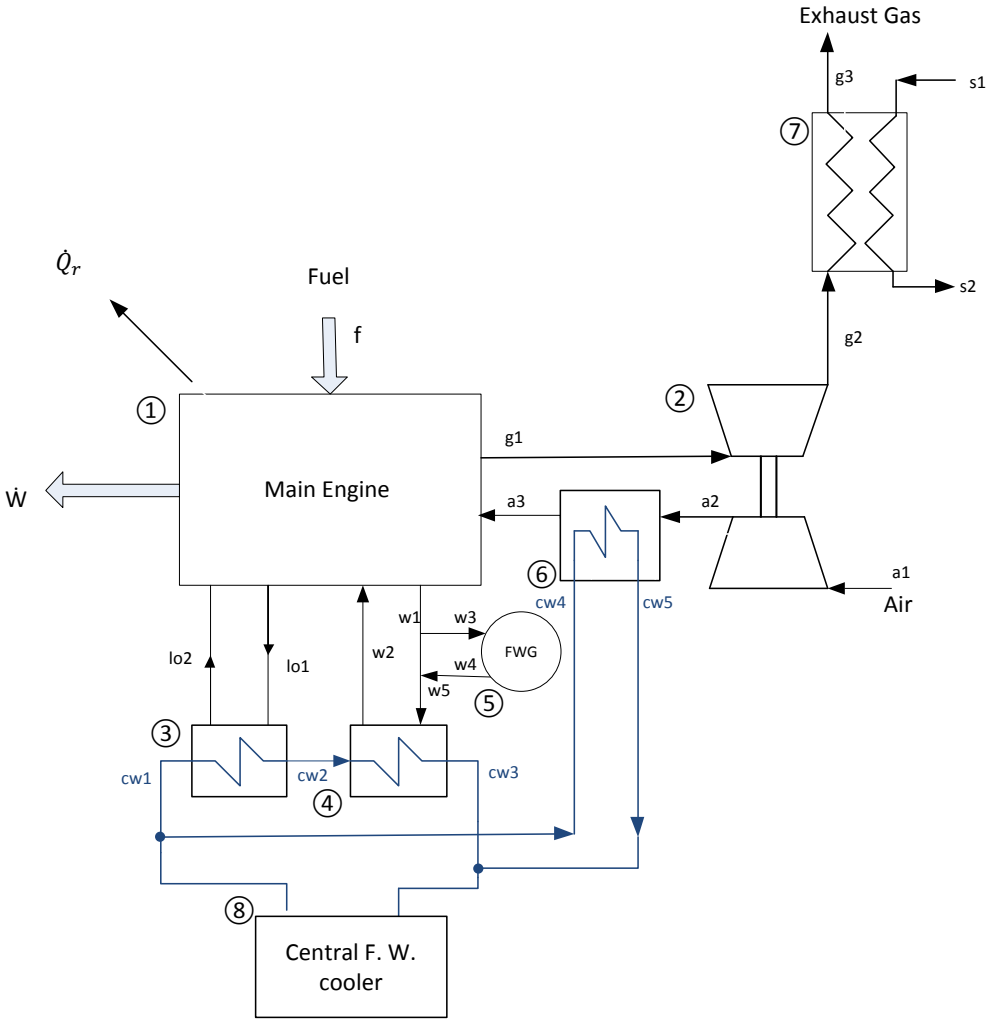

Legend:

1 Main Engine
2 Turbocharger
3 Lubricating oil exchanger
4 Jacket water exchanger
5 Fresh water generator
6 Supercharging air cooler
7 Exhaust gas boiler
8 Central fresh water cooler
Q_r=radiation power
$\dot{W}$=mechanical power

a=air
eg=exhaust gas
w=water
lo=lubricating oil
s=water / steam
cw=cooling water

Figure 3-1 Arrangement of the main engine in ships of relatively low power without steam turbine.

3.3. Explanation of the Main Components of the Main Engine System.

Figure 3-1 shows eight main components (eight boxes). They are: main Engine, Turbocharger, Lubricating oil cooler, jacket water cooler, fresh water generator, supercharging air cooler, exhaust gas boiler and central fresh water cooler. Using the available documents (official shop test results for Main Engine, results of sea trials, heating balance calculation and steam balance, and fresh water generator manual), this paragraph explains in detail all these main components.

3.3.1. Main Engine

Information of the Main Engine are: type 6S60MC, number of cylinders 6, diameter of the cylinder (bore) 600 mm; power 15400 BHP (11325 kW) at 97 RPM. The engine (Diesel Engine) is fed with Marine Diesel Oil (MDO). The fuel consumption rate as measured is 2169 l/hr, if the fuel has the following features: density of 0.962 kg/l, low calorific value of 9609 kcal/kg and the engine load is 92.84% (10516 kW).

3.3.2. Turbocharger

Supercharging air is supplied to the engine by one or more turbochargers, located on the exhaust side of the engine (see Figure 3-1). There are two turbochargers equipping the Main Engine having the following features: maximum speeds (20400 RPM and 19380 RPM) and maximum exhaust gas inlet temperatures (550°C and 520°C, respectively).

The compressor of each turbocharger draws air from the engine room, through an air filter, and the compressed air is cooled in the supercharging air cooler (box number 6). The supercharging air cooler is provided with a water mist eliminator, which prevents condensate water from being carried with the air into the supercharging air receiver and to the combustion chamber.

3.3.3. Lubricating oil cooler and jacket water cooler

The cooling water is pumped through the heat exchanger with the lubricating oil and then in the heat exchanger with the jacket water (see Figure 3-1). At 100% engine load, the inlet temperature of the lubricating oil to the Main Engine (point lo2) is 46°C and the outlet temperature is 50.8°C (point lo1), the inlet temperature of the jacket water to the Main Engine (point w1) is 70°C and the outlet temperature (point w2) is 79.3°C. The inlet temperature of the cooling water coming from the central cooler is 36°C (point cw1

in Figure 3-1); after the heat exchanger with the lubricating oil the temperature reaches 42.5°C (point cw2). Through the heat exchanger with the jacket water the temperature increases further until 53.7°C (point cw3). All these data are for the 100% engine load. Mass flow rate and thermal power for all these hot streams are not given in the available documentation.

3.3.4. Fresh water generator

Fresh water generator is an important equipment on board. Fresh water (i.e., desalinated water) produced by the fresh water generator is used for steam production, cooling circuits, as well as for domestic consumption .

The fresh water is produced by heating and evaporation of the sea water. The heat exchanger in the freshwater generator is connected to the jacket cooling water system of the Diesel engine, and it, therefore, works as an extra cooler (see box 5 in Figure 3-1).

Looking at Figure 3-2, the jacket cooling water, which may reach a temperature around 80°C, flows outside the tubes of the heat exchanger. During this passage the temperature will drop between 4 to 10°C depending on the amount of jacket cooling water that is used. The controlled amount of sea feed water flows within the heat exchanger tubes, where it is heated under vacuum (-0.085 MPa) and evaporates by rising film evaporation, meaning that optimum conditions are achieved and scale formation is minimized. The vacuum required is obtained by means of a water ejector which automatically ensures correct conditions.

The generated vapor passes through the separator, in which the sea water droplets are separated. The brine is discharged by means of a water ejector.

The saturated vapor reaches the sea water heat exchanger, it cools off, and it is condensed outside the tubes into fresh water, which is collected in a shell and discharged by the freshwater pump, (see FigureFigure 3-2).

The model of fresh water generator is KE25 of Sakura Engineering, the capacity of distillate is 25 t/day, and the heat balance is described in Figure 3-2. It requires 704.5 kW from jacket water thermal power.

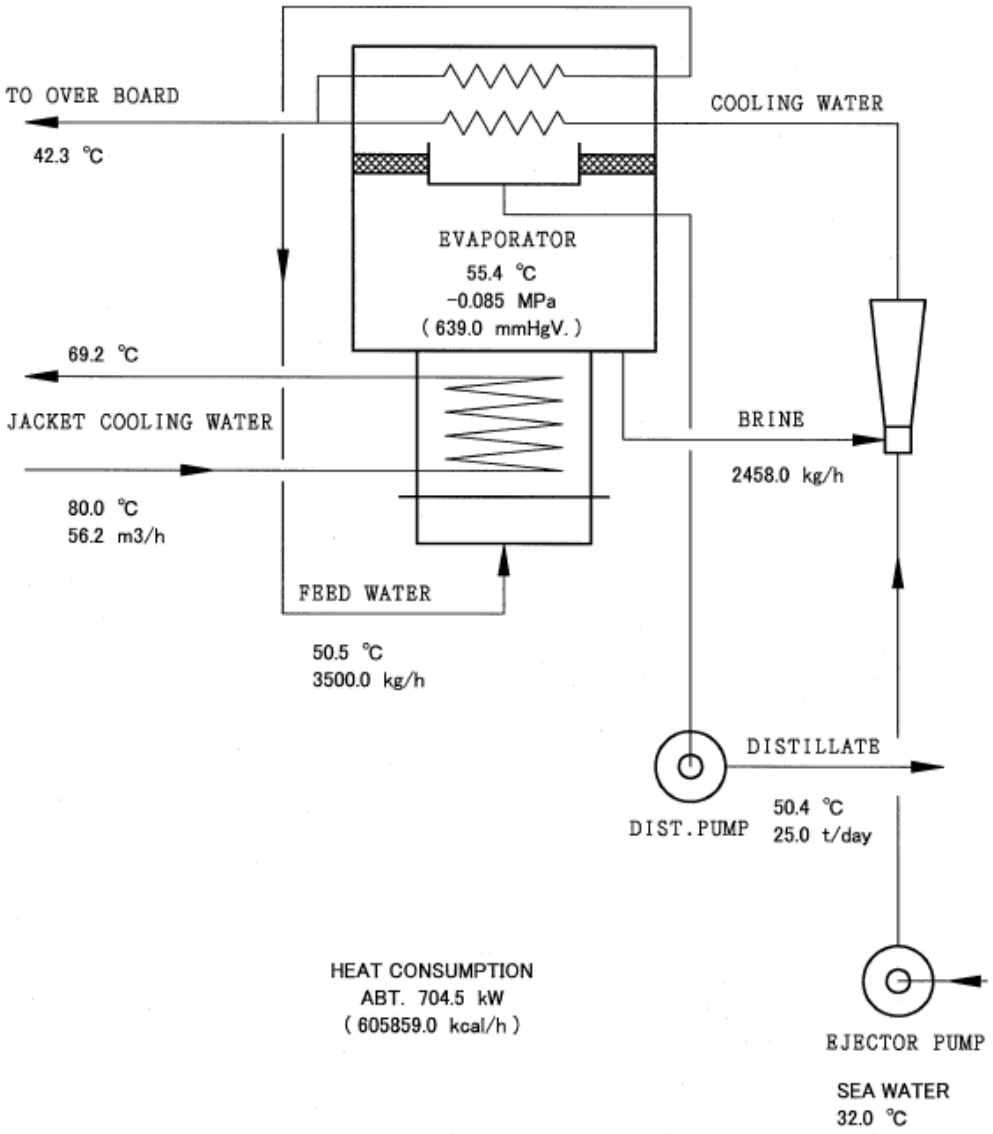

Figure 3-2 Fresh Water Generator.

3.3.5.Scavenge Air cooler

The Turbocharger increases charge air density, and intake manifold temperature as well. High temperature can lead to reduced charge density and higher combustion temperature, which can affect torque, power and emissions. If intake manifold temperature could be reduced, the intake density could be further increased and more air could be supplied to the engine without necessarily increasing the intake manifold pressure. By cooling the air with a heat exchanger, the temperature will be low and the density will be higher. While this would require a compressor capable of higher flow, the cost would be considerably less than a compressor that was also capable of higher pressures. Cooling the air with a heat exchanger as soon as it leaves the compressor, is a common way to achieve this supercharging air cooling. At 100% engine load, the cooler

system (see box 6 Figure 3-1) uses water directly from central cooler, thus the inlet temperature is 36°C (point cw4) and the outlet temperature is around 60°C (point cw5).

3.3.6. Exhaust gas Boiler

The steam consumers in this vessel consist of steam driven pumps, oil heaters for E/R machinery, steam heated F.O tanks, slop tanks (cleaning tanker), domestic consumers, etc.. The steam consumption is divided into three different pressure levels: 16 kg/cm^{2}G (16.7 bar), 10 kg/cm^{2}G (9.8 bar) and 6 kg/cm^{2}G (5.88 bar). Three different steam generators supply these demands. Two of them are auxiliary boilers fed with heavy fuel oil: each of them produces 25000 kg/h of saturated steam at two pressure levels at 16 kg/m^{2}G (16.7 bar) and 6 kg/m^{2}G (5.88 bar). The other one is an Exhaust gas boiler (box 7 in Figure 3-1) which recovers heat from exhaust gas of the engine and produces 1400 Kg/h of saturated vapor at 6 kg/m^{2}G (5.88 bar). In all cases the feed water temperature is 60°C (point s1) because it comes from the fresh water generator.

According to the available information, there are three different pressure levels of steam, in four different operating modes. These modes are “normal voyage”, “tank heating”, “tank cleaning” and “cargo unloading”. Each of these operating modes is associated with different steam demands. “Tank heating” is a normal practice to heat up cargo for 2-3 days before arriving at the discharge port. “Tank cleaning” is the preparation of ship for dry docking. The tanks must be fully and thoroughly cleaned to avoid hydrocarbon release when the ship is in the repair yard, (otherwise the vessel will not receive the gas free certificate). The duration but also the temperature and hence steam consumption will depend not only on internal tank geometry but also on the type of cargo, the viscosity and the existence of any constituents which cling on the internal structure and is difficult to be removed. This operation takes place only once a year or every two years. “Cargo unloading” is the process of moving oil off a tanker: the transfer starts at low pressure to ensure that equipment is working correctly and that connections are secure. Then a steady pressure is achieved and held during all the operation.

To complete the energy balance the ISO conditions are taken into consideration and only the exhaust gas boiler is considered, because it operates with heat from exhaust gases of the main engine.

The steam consumption at 6 kg/m^{2}G (5.88 bar) is 767 kg/h during the normal voyage, 1105 kg/h during tank cleaning, 1149 kg/h during tank heating, 43292 kg/h during cargo unloading. Using 1400 kg/h of steam, produced by the exhaust gas boiler, it is possible to cover the steam demand for all of the three operating conditions. Nevertheless, in “normal voyage”, exhaust gas heat is only partially used and a part of it would be used for ORC system.

In this study “cargo unloading” is not considered, because in this operating mode the engine does not operate.

In “steam balance” documentation a safety factor of about 5% per consumption (2% of the pipe loss and 3% of safety secure) is considered, i.e. the steam consumption is assumed 5% higher than the values reported above. In the Table 3-1 the whole steam demand of the Tanker is reported which included the safety factor.

Table 3-1 Steam consumption (kg/h).

NORMAL VOYAGE	VOYAGE TANK CLEANING	VOYAGE TANK HEATING	CARGO UNLOADING
806	1161	1207	45457

3.3.7. Central Fresh Water Cooler

The water cooling can be arranged in several configurations, the system in this ship is a central cooling water system (box number 8 in Figure 3-1).

The main advantages of the central cooling system are three. There is only one heat exchanger cooled by seawater, in this way there is only one heat exchanger to be overhauled. All the other heat exchangers are freshwater cooled and can therefore be made of a less expensive material (Cu-Ni pipes).The central cooling system needs few corrosive-resistance pipes to be installed (only for the seawater heat exchanger), and thus the needs for maintenance of coolers and components are reduced. On the other hand, the disadvantages of the central cooling system are the need of three sets of cooling water pumps (seawater, central water and jacket water) and the high initial cost.

The cooling system is made up of two sets of central F.W.(fresh water) coolers and three sets of central cooling F.W. (fresh water) pumps, two sets of pumps for the main / COPT condenser, and one set of auxiliary cooling S.W (sea water) pump.

During the voyage, the outlet temperature (point cw1) of the fresh water is kept constant by thermostatic valves at 36°C.

Figure 3-3 shows the temperature of the fresh water cooler in parenthetical at 100% engine load.

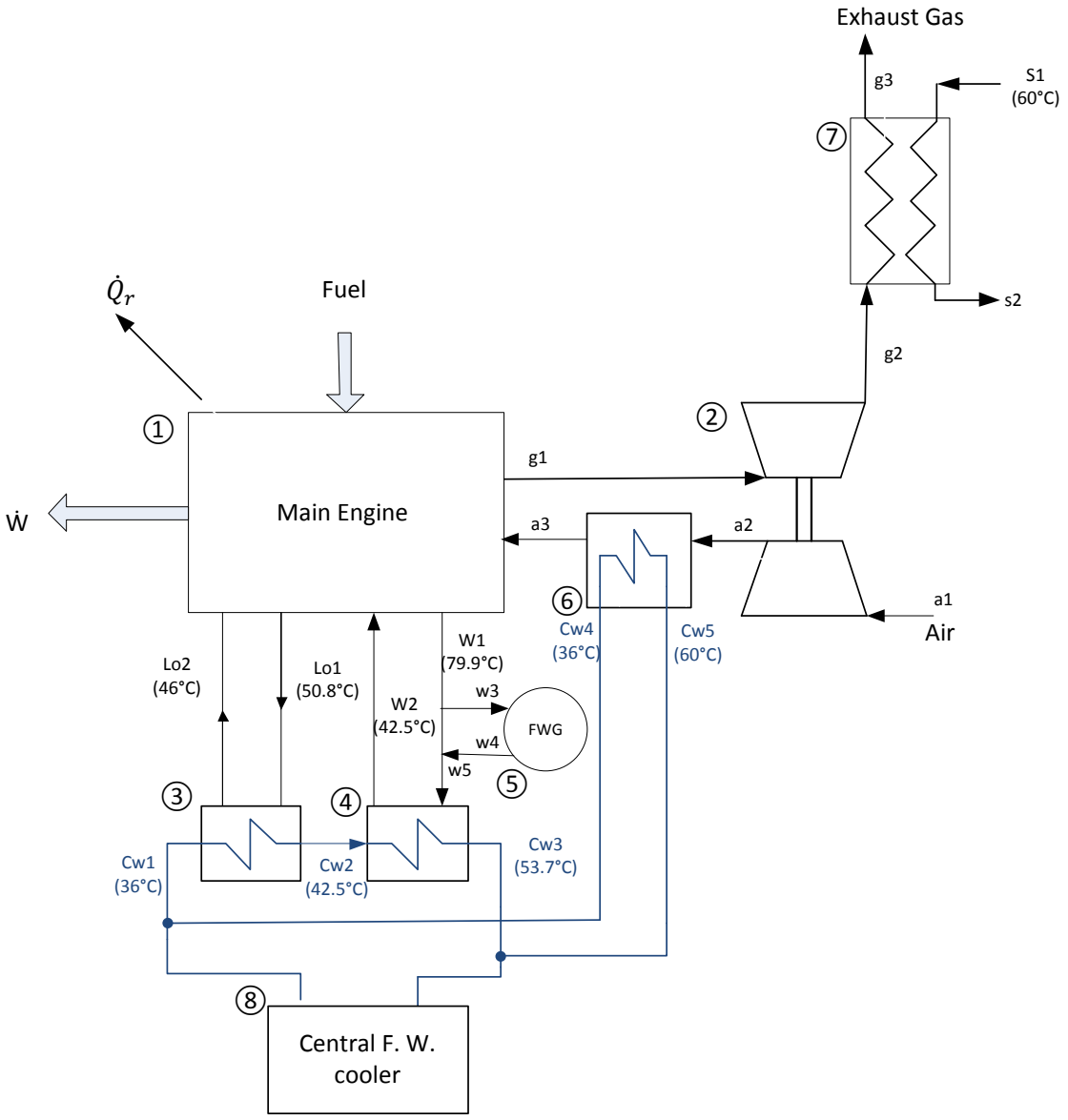

Legend:

1 Main Engine	a=air
2 Turbocharger	eg=exhaust gas
3 Lubricating oil exchanger	w=water
4 Jacket water exchanger	lo=lubricating oil
5 Fresh water generator	s=water / steam
6 Supercharging air cooler	cw=cooling water
7 Exhaust gas boiler	Q_r=radiation power
8 central fresh water cooler	$\dot{W}$=mechanical power

Figure 3-3 Arrangement of the main engine in ships of relatively low power with steam turbine. The temperature of fresh water cooler are shown in parenthetical.

3.4. Operating Profile of the Main Engine

The vessel operates at various conditions throughout a year. However, for the purposes of this study, the operating profile presented in Table 3-2 is considered.

Table 3-2 Operating Profile.

	Hr/year	Load	Type of voyage
	[-]	%	[-]
1	3039	80	Normal
2	2752	70	Normal
3	482	55	Normal-Reduced speed

In this table, there are three different main loads of the engine. During the voyage from charge port to discharge port, the engine usually operates at 80% of load, and when it comes back, the load is usually at 70%.

A reduced speed is used, for example when there is information from the authorities of the port that there is no space in this case it is preferred to reduce the speed instead of arriving at the destination and waiting outside the port.

Speed reduction has been increasingly common in the shipping market in recent years. It yields significant reductions in operational expenses. The main principle that makes speed reduction interesting is that hull resistance increases exponentially with speed. Thus, even a modest speed reduction can substantially decrease the required propulsion thrust. Lower required thrust results in lower fuel consumption, reduced emissions to the air and cost reduction [Eide et al. (2012)].

The operating profile in Table 3-2 is considered, thus the energy balance is evaluated for these three main engine loads: 80, 70 and 55%.

3.5. Model of the Main Engine Balance

In Figure 3-4 the red line is the boundary control of the Engine assumed for the energy balance calculations. The temperatures of the cooling loop are known from Section 3.3. In the points cw1, cw2, cw3, cw4, cw5 the temperatures are 36, 42.5, 53.7, 36 60°C, respectively. According to Wang et al. (2012) when the heat source temperature is lower than 100°C, ORC-technology is uneconomical. Thus, the evaluated ship does not allow a convenient heat recovery from the cooling circuit because the working fluid cannot reach temperature higher than 100°C (maximum temperature of the cooling loop is 60 °C, point cw5 in Figure 3-1). For this reason, the component boundary does not include the three heat exchangers (air cooler, lubricating oil, jacket water). The possibility to recover directly heat from these hot streams is examined in study, so the working fluid could reach higher temperature than 100°C.

The energy balance of the main engine is expressed as follows

$$\dot{m}_f\left[H_u + c_{pf}\left(T_f - T_0\right)\right] + \dot{m}_a c_{pa}(T_{a1} - T_0) = \dot{W} + \dot{Q}_c + \dot{Q}_{eg} + \dot{Q}_r \quad (3.1)$$

$$\dot{Q}_c = \dot{Q}_{jw} + \dot{Q}_{lo} + \dot{Q}_{ca} \quad (3.2)$$

Then:

$$\dot{m}_f\left[H_u + c_{pf}\left(T_f - T_0\right)\right] + \dot{m}_a c_{pa}(T_{a1} - T_0) = \dot{W} + \dot{Q}_{jw} + \dot{Q}_{lo} + \dot{Q}_{ca} + \dot{Q}_{eg} + \dot{Q}_r \quad (3.3)$$

where:

$\dot{m}_f$ fuel mass flow rate
H_u Lower calorific value
c_{pf} Isobaric specific heat of the fuel
T_f Inlet fuel temperature
T_0 Reference temperature
$\dot{m}_a$ Air mass flow rate
c_{pa} Isobaric specific heat of the air
T_{a1} Inlet air temperature
$\dot{W}$ Mechanical Power
$\dot{Q}_c$ Cooling power
$\dot{Q}_{eg}$ Exhaust gas power
$\dot{Q}_r$ Radiation power
$\dot{Q}_{jw}$ jacket water power at the exit of the main engine
$\dot{Q}_{lo}$ lubricating oil power
$\dot{Q}_{ca}$ Air cooler power

where:

$$\dot{Q}_{jw} = \dot{m}_{w1}(h_{w1} - h_{w2}) \quad (3.4)$$

$$\dot{Q}_{lo} = \dot{m}_{lo}c_{plo}(T_{lo1} - T_{lo2}) \quad (3.5)$$

$$\dot{Q}_{ca} = \dot{m}_{a}c_{pa}(T_{a2} - T_{a3}) \quad (3.6)$$

$$\dot{Q}_{eg} = \dot{m}_{g}c_{pg}(T_{g2} - T_{0}) \quad (3.7)$$

$\dot{Q}_r$: approximately 1% of the fuel energy. (3.8)

Note that $\dot{Q}_{eg}$, as defined by Eq. (3.7), is the thermal energy contained in exhaust gas measured above the reference temperature T_0. The actual available heat from exhaust gas is given by the equation:

$$\dot{Q}_{eg1} = \dot{m}_{g}c_{pg}(T_{g2} - T_{g4}) \quad (3.9)$$

where T_{g4} is the lowest allowed temperature for the exhaust gases at the exit of the boiler (the value used here is 180°C). Part of this thermal energy (down T_{g3} in Figure 3-4) is recovered in the exhaust gas boiler to generate low pressure steam and the useful heat of the exhaust gas boiler is given by the equation:

$$\dot{Q}_{s} = \dot{m}_{s}(h_{s2} - h_{s1}) \quad (3.10)$$

or

$$\dot{Q}_{s} = \eta_{EGB}\dot{m}_{g}c_{pg}(T_{g2} - T_{g3}) \quad (3.11)$$

The heat that would be available for the ORC from the exhaust gas boiler is given by the following equation

$$\dot{Q}_{eg,ORC} = \dot{Q}_{eg1} - \dot{Q}_{s} \quad (3.16)$$

where $\dot{Q}_s$ is given by Eq.(3.11). Practically, the required mass flow rate of steam in various modes of operation is given in Table 3-1. In order to use the whole available thermal power contained in exhaust gas for the production of the steam, Qs is equal to 975 kW, which is the power required for the production of 1400 Kg/h of steam, that is the maximal capacity of the exhaust gas boiler when the main engine is operating.

The thermal energy required by the fresh water generation is:

$$\dot{Q}_{FWG} = \dot{m}_{w3}(h_{w3} - h_{w4}) \quad (3.17)$$

The thermal energy that remains to be rejected through the jacket water cooler (box number 4):

$$\dot{Q}_{JWC} = \dot{Q}_{jw} - \dot{Q}_{FWG} = \dot{m}_{w1}(h_{w5} - h_{w2}) \quad (3.18)$$

All the points, symbols described in section 3.5 are showed in Figure 3-4.

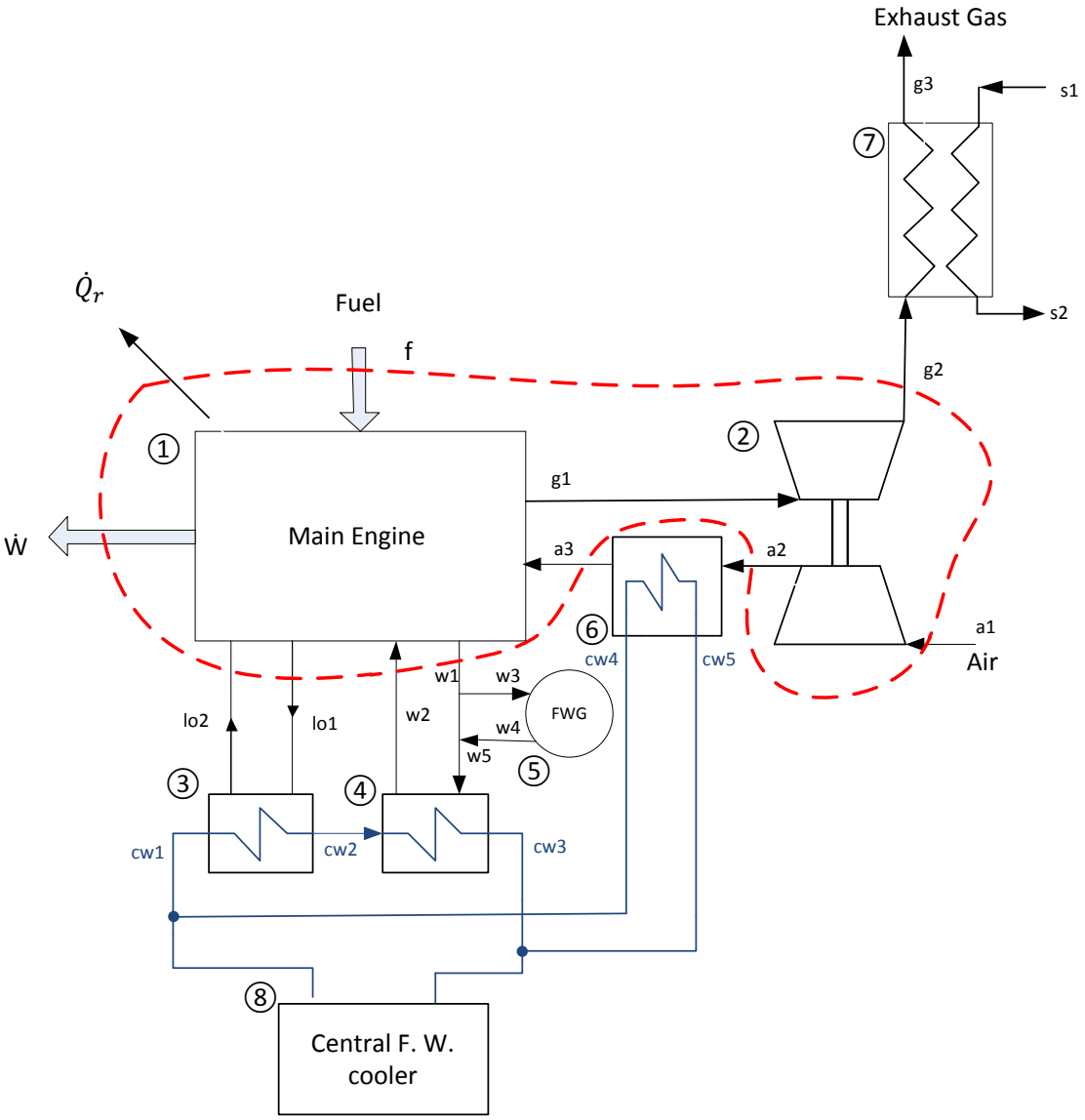

Legend:

1 Main Engine	a=air
2 Turbocharger	eg=exhaust gas
3 Lubricating oil exchanger	w=water
4 Jacket water exchanger	lo=lubricating oil
5 Fresh water generator	s=water / steam
6 Charge air cooler	cw=cooling water
7 Exhaust gas boiler	Q_r=radiation power
8 Central fresh water cooler	$\dot{W}$=mechanical power

Figure 3-4 Arrangement of the main engine in ships of relatively low power without steam turbine. The boundary control is shown with a red dashed line.

3.6. Data and Assumptions

This section explains the data and the assumptions needed to evaluate the energy balance referring to Figure 3-4 . Mechanical power ($\dot{W}$), fuel consumption ($\dot{m}_f$), low calorific value of the fuel (H_u), mechanical efficiency (η_{engine}), thermal power required by the fresh water generation ($\dot{Q}_{FWG}$), isobaric specific heat of the fuel (c_{pf}), inlet temperature of the fuel (T_f), temperatures T_{w1}, T_{w2} of the jacket water, temperatures T_{lo1}, T_{lo2} of lubricating oil, temperatures T_{a1}, T_{a2} of the air, and the temperature of the exhaust gas at point g2 are given from the documentation available at 100, 90, 75, 50, 25% engine loads. These data will be used to find out the temperatures at 80, 70, 55% engine loads, which are the most frequent engine loads (see Table 3-2). Efficiency (η_{EGB}) of the exhaust gas boiler, reference temperature (T_0) and inlet temperature of the air (T_{a1}), are assumptions made for this work. Efficiency (η_{EGB}) is equal to 0.95, the reference temperature and the air temperature are equal to 25°C. According to Marindagen and Potentialer (2011) the condensation of sulfuric acid is avoided when the exhaust gas outlet temperature is kept higher than 180°C. Table 3-3 summarizes all these data for five engine load (100, 90, 75, 50, 25%).

Table 3-3 shows that on varying of engine load, the air temperature (T_{a2}) varies in a wide range (from 189.5°C at 100% engine load to 43.5°C at 25% engine load), instead of jacket water and lubricating oil. The outlet temperature of the lubricating oil from the Main Engine (T_{lo1},) varies from 50.8°C at 100% engine load to 48°C at 25% engine load. The range of the outlet temperature of jacket water from Main Engine (T_{w1}) is from 70°C at 100% engine load to 60°C at 25% engine load. There is the maximum engine efficiency at 75% engine load where η_{engine} is equal to 0.481. At the 75% engine load the exhaust gas temperature (T_{g2}) is the lowest (229°C) of other engine loads. Lower exhaust gas temperature means lower exhaust gas power, thus less fuel thermal power lost and more mechanical efficiency (η_{engine}). In detail, Figure 3-11 shows that there is the minimum exhaust gas temperature (T_{g2}) at 80% engine load. For this reason, the Main engine operates at 80% engine load from charge port to discharge port and at 70% engine load when the tanker comes back to the charge port (when the mechanical efficiency reaches the highest values).

Table 3-3 Available data and Assumptions.

Parameter		Main Engine load (%)				
Symbol	**Units**	**100**	**90**	**75**	**50**	**25**
$\dot{W}$	**kW**	11327	10200	8494	5663	2832
$\dot{Q}_{FWG}$	**kW**	704.5	704.5	704.5	704.5	704.5
H_u	**kJ/kg**	42700	42700	42700	42700	42700
$\dot{m}_f$	**kg/s**	0.556	0.498	0.413	0.284	0.143
η_{engine}	**-**	0.477	0.48	0.481	0.467	0.137
η_{EGB}	**-**	0.95	0.95	0.95	0.95	0.95
c_{pf}	**kJ/kgK**	1.7	1.7	1.7	1.7	1.7
T_f	**°C**	40	40	40	40	40
T_{w1}	**°C**	79.3	78.5	75.5	70.7	64.7
T_{w2}	**°C**	70	70	68	63	60
T_{lo2}	**°C**	46	40	42	40	40
T_{lo1}	**°C**	50.8	49.8	49.5	49.5	48
T_{a2}	**°C**	189.5	171.0	147.0	96.0	43.5
T_{a3}	**°C**	39.0	34.0	30.5	25.5	20.0
T_{g2}	**°C**	240	230	229	247	252
T_0	**°C**	25	25	25	25	25
T_{a1}	**°C**	25	25	25	25	25

Energy balances at 80, 70 and 55% engine load are required in this study (see Table 3-2). The documentation provides the temperatures T_{w1}, T_{w2}, T_{lo1}, T_{lo2}, T_{a1}, T_{a2}, T_{g2} at different loads than the required ones (see Table 3-3). Using these available temperatures, for each hot stream (as explained in Chapter 4) it is possible to derive a trend from which all the temperatures at different loads are estimable as shown in Figure 3-5 to 3-11.

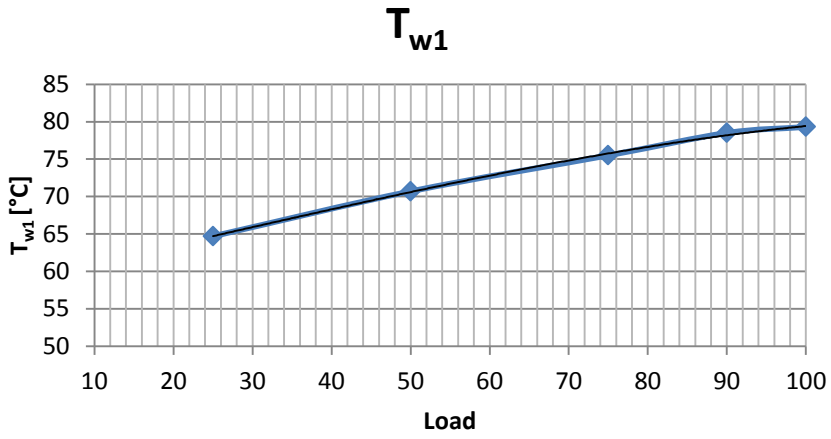

Figure 3-5 Outlet temperature of jacket water from M/E as a function of engine load.

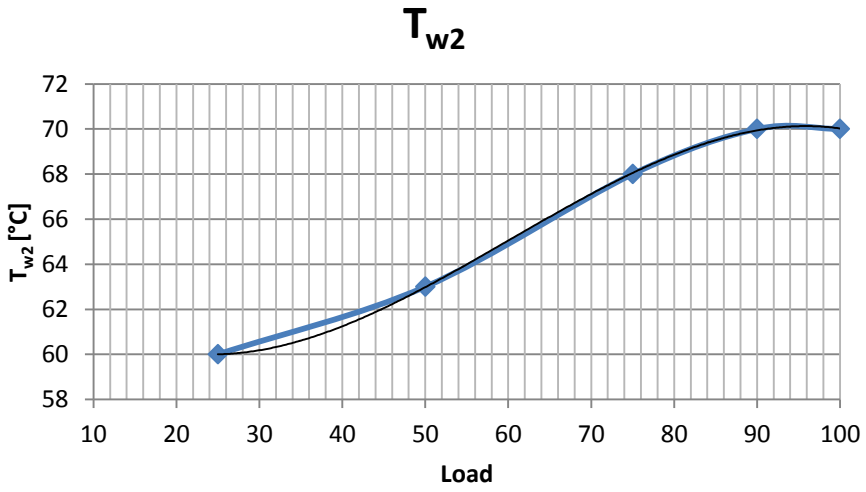

Figure 3-6 Inlet temperature of jacket water to the M/E as a function of load.

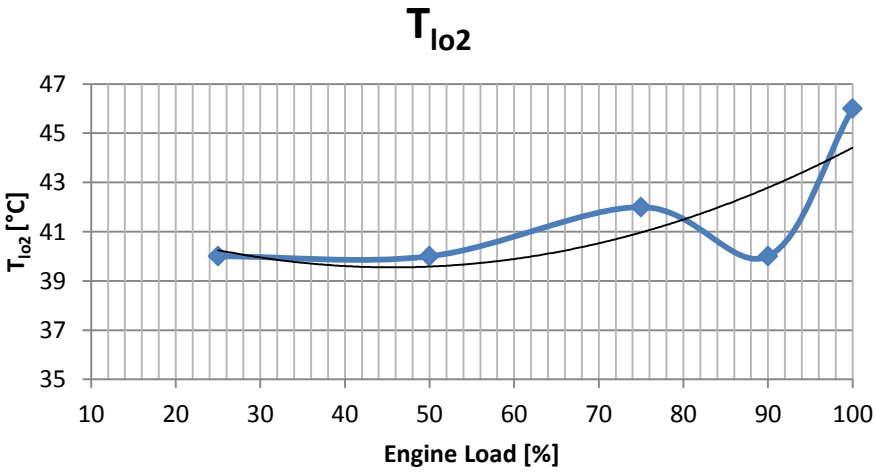

Figure 3-7 Inlet temperature of lubricating oil to the M/E as a function of load.

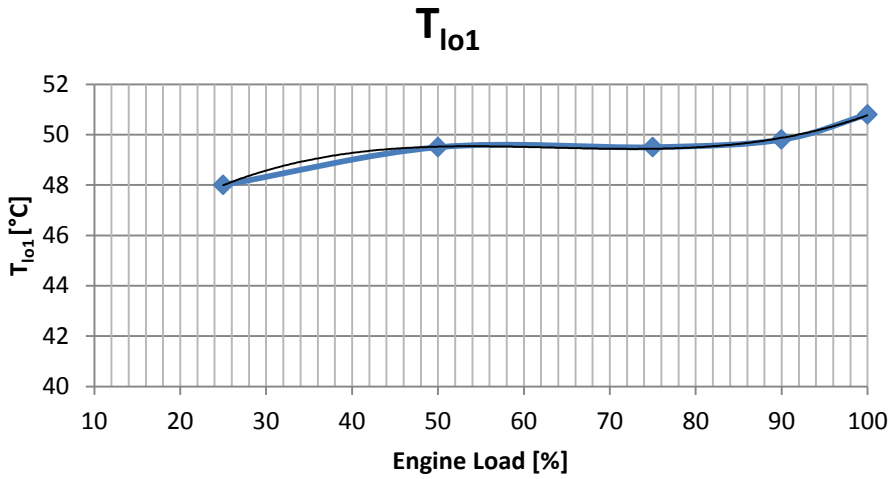

Figure 3-8 Outlet temperature of lubricating oil as a function of load.

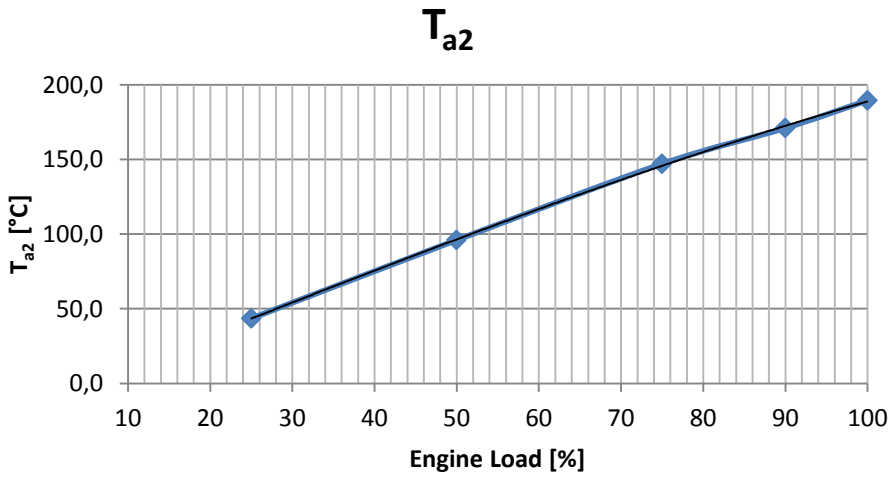

Figure 3-9 Air inlet temperature to the supercharging air cooler.

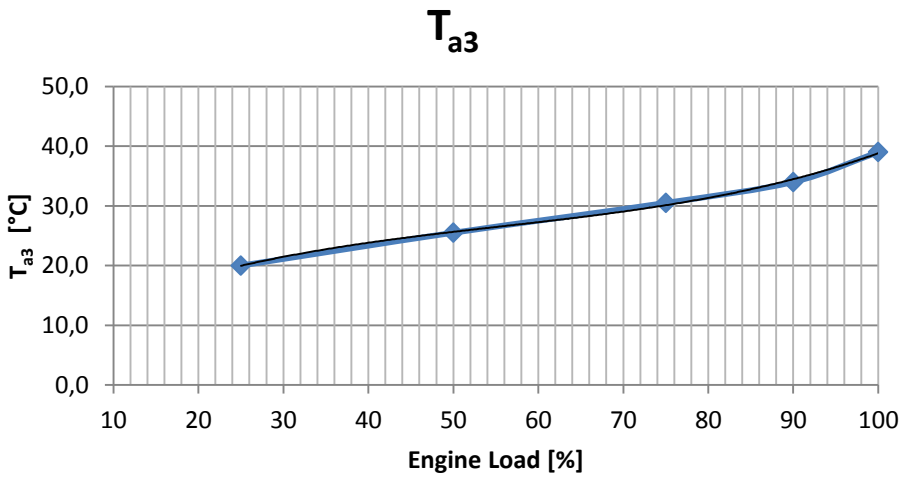

Figure 3-10 Air outlet temperature from the supercharging air cooler.

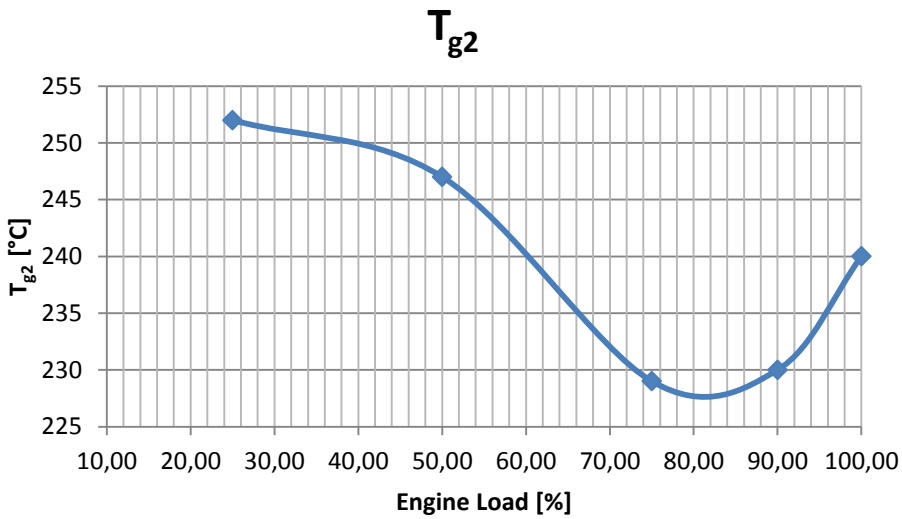

Figure 3-11 Exhaust gas temperature from turbocharger.

The fuel mass flow rate and the exhaust gas temperature, after the turbocharger for the main loads, are found out by interpolation from the data in Table 3-3. Figure 3-11 shows that there is the minimum exhaust gas temperature around 80% engine load, and so lower exhaust gas temperature means lower thermal power lost by exhaust gas. For this reason Main Engine frequently operates at that condition (80% engine load). Fuel thermal power ($\dot{Q}_f$) is given by Eq. (3.19). Taking into consideration the assumptions that the inlet air temperature is equal to the reference temperature, Eq.(319) can be reedited in Eq.(3.20).

$$\dot{Q}_f = \dot{m}_f\left[H_u + c_{pf}\left(T_f - T_0\right)\right] \tag{3.19}$$

$$\dot{Q}_f = \dot{m}_f H_u \tag{3.20}$$

Fuel thermal power ($\dot{Q}_f$) minus mechanical power gives the amount of power lost which is sum of exhaust gas, cooling and radiation power. The radiation power ($\dot{Q}_r$) is assumed to be 1% of the fuel power at all engine loads. Using the software available on MAN website (www.mandieselturbo.com), the proportion of cooling power compared to fuel thermal power ($\dot{Q}_c/\dot{Q}_f$) is found out for several engine loads (see Table 3-4). Exhaust gas power is evaluated by the following equation:

$$\dot{Q}_{eg} = \dot{Q}_f - \dot{Q}_c - \dot{Q}_r - \dot{W} \tag{3.21}$$

Figure 3-12 and Table 3-4 show the c^* coefficient as a function of the engine load. C^* is given by the equation:

$$c^* = \frac{c_L}{c_{100}} = \frac{(\frac{\dot{Q}_C}{\dot{Q}_f})_L}{(\frac{\dot{Q}_C}{\dot{Q}_f})_{100}} \quad (3.22)$$

Eq.(3.22) describes the ratio between cooling power and the thermal fuel power at generic engine load (L) compared to the ratio between the cooling power and the fuel power at 100% engine load. Eq. (3.23) describes c^* as a function of the engine load.

Table 3-4 Cooling heat as a function of load.

Load	$\dot{Q}_c$	$\dot{Q}_f$	$c = \frac{\dot{Q}_c}{\dot{Q}_f}$	c^*
[%]	[kW]	[kW]	[-]	[-]
100	6790	26420	0.257	1.000
90	6070	23619	0.259	1.006
80	5350	20693	0.258	1.002
70	4590	17824	0.251	0.977
60	3850	15333	0.243	0.945
50	3110	12805	0.231	0.900
40	2400	10376	0.218	0.850
25	1520	6958	0.208	0.810

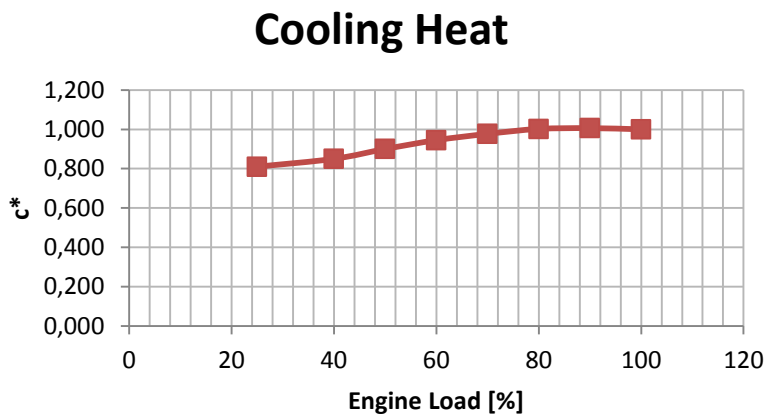

Figure 3-12 c* as function of engine load.

Eq. (3.23):

$$c^* = 1.82 \cdot 10^{-8} \cdot L^4 - 5{,}522 \cdot 10^{-6} \cdot L^3 + 5{,}481 \cdot 10^{-4} \cdot L^2 - 1.768 \cdot 10^{-2} \cdot L + 0.988$$

Cooling power is the sum of three thermal powers: jacket water power, lubricating oil power, air cooler power (see Eq. 3.2). In the available documentation there is no information regarding how to split the cooling power. For this reason, the same proportion given for the engine 6S60MC-C7.1 (available on the official MAN website) is used. Tables 3-4 to 3-6 show these proportions as a functions of the engine load.

Table 3-5 Jacket water trend.

Load	$\dot{Q}_{jw}$	$\dot{Q}_c$	$jw = \frac{\dot{Q}_{jw}}{\dot{Q}_c}$	jw^*
[%]	[kW]	[kW]	[-]	[-]
100	1540	6790	0.227	1.00
90	1420	6070	0.234	1.03
80	1310	5350	0.245	1.08
70	1190	4590	0.259	1.14
60	1080	3850	0.280	1.24
50	970	3110	0.311	1.37
40	850	2400	0.354	1.56
25	680	1520	0.447	1.97

Table 3-5 shows that the jacket water thermal power increases in percentage at decreased engine loads. At 25% engine load it represents almost 45% of the overall cooling load, i.e. around twice its value at 100% engine load.

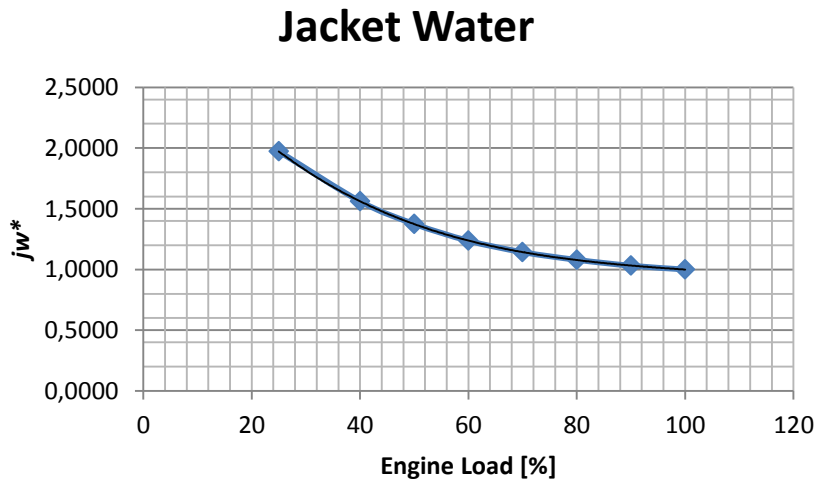

Figure 3-13 Jacket water trend.

Eq. (3.24):

$$jw^{x} = 5.579 \cdot 10^{-9} \cdot L^{4} - 3.248 \cdot 10^{-6} \cdot L^{3} + 6.659 \cdot 10^{-4} \cdot L^{2} - 6.098 \cdot 10^{-2} \cdot L + 3.129$$

Figure 3-13 and Eq. (3.24) describe jw*: the ratio between jacket water power and the cooling power at certain engine load *L* compared to the ratio between the jacket water power and the cooling power at 100% engine load as a function of the engine load.

Table 3-6 Lubricating oil trend.

Load	$\dot{Q}_{lo}$	$\dot{Q}_{c}$	$lo = \frac{\dot{Q}_{lo}}{\dot{Q}_{c}}$	lo^{*}
[%]	[kW]	[kW]	[-]	[-]
100	850	6790	0.125	1.000
90	830	6070	0.137	1.092
80	800	5350	0.150	1.195
70	760	4590	0.166	1.323
60	720	3850	0.187	1.494
50	660	3110	0.212	1.695
40	600	2400	0.250	1.997
25	480	1520	0.316	2.523

Table 3-6 shows that the lubricating oil thermal power increases in percentage at decreased engine loads as the jacket water thermal power in percentage (see Table 3-5). At 25% engine load it represents almost 31% of the overall cooling load, i.e. around twice and a half its value at 100% engine load.

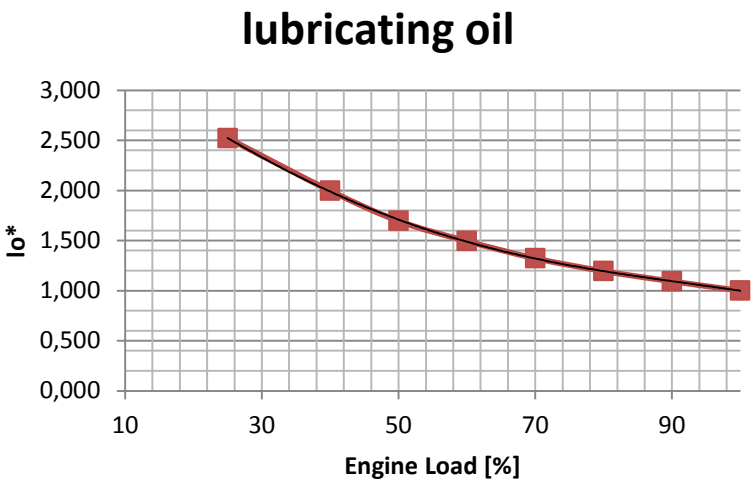

Figure 3-14 Lubricating oil trend.

Eq.(3.25):

$$lo^* = -2.034 \cdot 10^{-8} \cdot L^4 + 3.391 \cdot 10^{-6} \cdot L^3 + 9.7 \cdot 10^{-5} \cdot L^2 - 14.995 \cdot 10^{-2} + 3.667$$

Figure 3-14 and Eq. (3.25) describe lo*: the ratio between lubricating oil power and the cooling power at a generic engine load compared to the ratio between the lubricating oil power and the cooling power at 100% engine load as a function of the engine load.

Table 3-7 Charge air cooling as function of load.

Load	$\dot{Q}_{ca}$	$\dot{Q}_c$	$ca = \frac{\dot{Q}_{ca}}{\dot{Q}_c}$	ca^*
[%]	[kW]	[kW]	[-]	[-]
100	4400	6790	0.648	1.00
90	3820	6070	0.629	0.91
80	3240	5350	0.606	0.95
70	2640	4590	0.575	0.88
60	2050	3850	0.532	0.82
50	1480	3110	0.476	0.74
40	950	2400	0.396	0.61
25	360	1520	0.237	0.35

Table 3-7 shows that the air cooler thermal power decrease in percentage at decreased engine loads. At 25% engine load it represents almost 23.7% of the overall cooling load, i.e. around less than a half its value at 100% engine load.

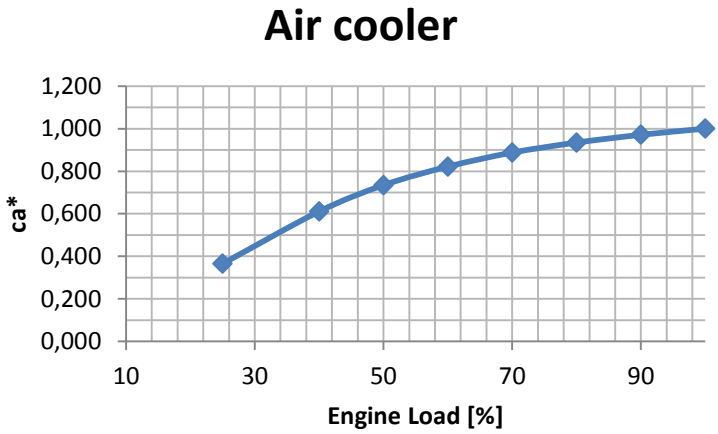

Figure 3-15 Air cooler Trend.

Eq.(3.26):

$$ca^{x} = 9.777 \cdot 10^{-7} \cdot L^{3} - 2.955 \cdot 10^{-4} \cdot L^{2} + 3.258 \cdot 10^{-2} \cdot L - 0.2799$$

Eq. (3.25) describes ca*: the ratio between air cooler power and the cooling power at a certain engine load *L* compared to the ratio between the air cooler power and the cooling power at 100% engine load as a function of the engine load.

At low engine load, the thermal power that can be recovered is higher from jacket water than from air cooler. Fortunately the engine never works at low load. The 55% engine load is the lowest load, where air cooler power is still the highest than the lubricating oil and jacket water. From tables 3.5 to 3.7 at 50% engine load, air cooler thermal power is equal to 1480 kW, lubricating oil and jacket water are 660 kW and 970 kW.

In Table 3-4, it is shown that the cooling heat decreases as the load engine decreases and the mechanical efficiency decreases (see Table 3-3). In fact jacket water heat (Figure 3-13) and lubricating oil heat (Figure 3-14) increase in percentage as the engine load decreases whereas air cooler heat decreases (Figure 3-15). At low loads, the exhaust gas flow rate decreases and the speed of turbocharger decrease as well, thus pressure outlet of the air compressor decreases. This means low air temperature and less demand of air cooler. For this reason the *c* coefficient does not increase with low engine load.

3.7. Energy Balance at 100% Engine Load

The following paragraph presents the complete procedures to compute the energy balance at 100% engine load of the M/E. The energy balance is performed using data given in the documents described in Section 3.6.

In the first step, the fuel mass flow rate and mechanical power are extrapolated from Table 3-3, while the second step is to calculate the fuel power.

The fuel consumption at 100% load is:

$$\dot{m}_f = 0.555 \ \frac{kg}{s}$$

The mechanical power at 100% engine load is:

$$\dot{W} = 15401 \ bhp = \ 11327 \ kW$$

The fuel power is given by the following equation (take into consideration the assumption that the inlet air temperature is equal to the reference temperature):

$$\dot{Q}_f = \dot{m}_f[H_u] = 23736 \ kW \tag{3.25}$$

The efficiency of the engine:

$$\eta_{engine} = \frac{\dot{W}}{\dot{Q}_f} = \frac{11327}{23736} = 0.477$$

The radiation losses $\dot{Q}_r$ are assumed to be 1% of the thermal fuel power $\dot{Q}_f$ at all engine loads:

$$\dot{Q}_r = \frac{1}{100} \cdot \ \dot{Q}_f = \frac{1}{100} \cdot 23736 = 237 \ kW$$

The coefficient *c* defined as the ratio between cooling and fuel power is found from data of 6SM60MC (see Table 3-4). For 100% load, its value is 0.257.

$$\begin{aligned} &c = 0.257 \\ &\dot{Q}_c = \dot{Q}_f \cdot c = 23736 \cdot 0.257 = 6100 \ kW \\ &\dot{Q}_{eg} = \dot{Q}_f - \dot{Q}_c - \dot{Q}_r - \dot{W} = 6072 \ kW \end{aligned} \tag{3.26}$$

In the next step we need to define the values of jacket water, lubricating oil, air cooler thermal power ($\dot{Q}_{jw}$, $\dot{Q}_{lo}$, $\dot{Q}_{ca}$) which on the whole, form the cooling power ($\dot{Q}_c$)

see Eq. (3.2). As already seen in the previous section for different engine loads, the value of $\dot{Q}_c$ is known but no information is available regarding how to split the cooling power. So the proportions for the engine 6S60MC-C7.1 are applied. At 100% engine load the coefficients: *jw*, *lo*, *a* are 0.227, 0.125, 0.648, respectively (see Table 3-5, Table 3-6, Table 3-7), then:

$$\dot{Q}_{jw} = \dot{Q}_c \cdot jw = \dot{Q}_c \cdot 0.227 = 1385\ kW$$
$$\dot{Q}_{lo} = \dot{Q}_c \cdot lo = \dot{Q}_c \cdot 0.125 = 762\ kW$$
$$\dot{Q}_{ac} = \dot{Q}_c \cdot a = \dot{Q}_c \cdot 0.648 = 3953\ kW$$

The energy balance of the main engine is expressed as follows (the left side of the equation depicts input power, the right side the output power):

$$\dot{m}_f\left[H_u + c_{pf}\left(T_f - T_0\right)\right] = \dot{W} + \dot{Q}_{jw} + \dot{Q}_{lo} + \dot{Q}_{ca} + \dot{Q}_{eg} + \dot{Q}_r$$

$$23736 = 11327 + 1385 + 762 + 3953 + 6072 + 237$$

$$23736\ kW = 23736\ kW$$

From the previous finding, the energy balance is satisfied. The input power is equal to the output power in the composite boundary in Figure 3-4.

3.8. Operating data and results at 100%, 80%, 70% and 55% Load

In the previous sections: the method, the component boundary (see the red line Figure 3-4), available data, assumptions and the energy balance at 100% engine load were explained. Using previous information and procedure (Section 3.7), it is possible to fill Table 3-8. It summarizes the results of the energy balances and the properties observed at various points as shown in Fig. 3-4 at 100% engine load and at 80%, 70%, 55% engine load which on the whole, form the operating profile .

Due to the lack of sufficient information and because of inconsistencies in some data of the available documents the product of the mass flow rate and isobaric specific heat is evaluated instead of the mass flow rate of the same stream, using the following equation:

$$\dot{m}_i c_{pi} = \frac{\dot{Q}_i}{\Delta T_i} \tag{3.27}$$

where $\dot{Q}_i$ are the thermal power evaluated by the procedure in Section 3.7, and ΔT_i is calculated using the temperatures in Figs. 3-5 to 3-11.

According to Marindagen and Potentialer (2011) thermal power from exhaust gas cannot be recovered from the ORC system, because output temperature of exhaust gas from exhaust gas boiler (T_{g3}) are close to 180°C. To avoid sulfuric condensation, T_{g3} has to be above up 180°C. From Table 3-8, T_{g3} are equal to 186, 185, 185°C for 80,70,55% engine load. (the most frequent engine loads). Moreover, the available exhaust gas power ($\dot{Q}_{eg,ORC}$) after the exhaust gas boiler is negligible if compared to jacket water power, lubricating oil and air cooler power, as shown in Table 3-8. At 80% engine load (the most frequent engine load), the available exhaust gas power for the ORC ($\dot{Q}_{eg,ORC}$) is equal to 146 kW and the available thermal power from jacket water, lubricating oil, air cooler are 1186, 729, 3941 kW, respectively.

Because of lack of exact information regarding the duration of the various modes appearing in Table 3-1 and regarding the low power recovered from exhaust gas for ORC system, we decided to study the ORC taking into consideration the heat available from the cooling circuits of the engine only and ignoring any heat available from the exhaust gases.

For each engine load, thermal power from air cooler ($\dot{Q}_{ca}$) is higher than the thermal powers from jacket water ($\dot{Q}_{jw}$) and lubricating oil ($\dot{Q}_{lo}$). Moreover the temperature level of $\dot{Q}_{ca}$is the highest. At 80% engine load, it is around 154°C (see T_{g2} Table 3-8,). The temperature range of jacket water is between 70°C and 60°C (see T_{w2}, T_{w1}), and the temperature level of lubricating oil is between 50°C and 40°C (see T_{lo1}, T_{lo2}).

In Figure 3-16, 3-17, 3-18, values of fuel thermal power ($\dot{Q}_{th}$) mechanical power ($\dot{W}$), radiation losses ($\dot{Q}_r$), mass flows rate of jacket water ($\dot{m}_w$,$\dot{m}_{w3}$), temperatures , thermal capacity of lubricating oil ($\dot{m}_{lo}c_{plo}$), air cooler ($\dot{m}_a c_{pa}$), exhaust gas ($\dot{m}_g c_{pg}$)are shown. Figure 3-16 depicts engine balance at 80% engine load. Figure 3-17 energy balance at 70% engine load. Figure 3-18 energy balance at 55% engine load.

Table 3-8 Energy balance.

Parameter		Main Engine load (%)			
Symbol	**Units**	**100**	**80**	**70**	**55**
H_u	kJ/kg	42700	42700	42700	42700
$\dot{Q}_{th}$	kW	23736	18842	16577	13245
$\dot{W}$	kW	11327	9062	7929	6230
$\dot{Q}_{eg}$	kW	6072	4736	4306	3729
$\dot{Q}_r$	kW	237	188	166	132
$\dot{Q}_{jw}$	kW	1385	1186	1081	929
$\dot{Q}_{lo}$	kW	762	729	693	627
$\dot{Q}_{ca}$	kW	3953	2941	2402	1598
$\dot{m}_f$	kg/s	0.555	0.441	0.388	0.310
$\dot{m}_s$	kg/s	0.39	0.39	0.39	0.39
$\dot{m}_w$	kg/s	35.6	36.8	33.1	28.8
$\dot{m}_{w3}$	kg/s	18.1	21.8	21.6	21.8
$\dot{m}_{lo}c_{plo}$	kW/K	158.7	82.84	103.4	78.4
$\dot{m}_a c_{pa}$	kW/K	26.3	23.81	22.53	19.98
$\dot{m}_g c_{pg}$	kW/K	27.6	23.35	21	17
T_0	°C	25	25	25	25
T_{a1}	°C	25	25	25	25
T_f	°C	40	40	40	40
T_{w1}	°C	79.3	76.6	74.8	71.7
T_{w2}	°C	70	68.9	67.0	64.0
T_{w3}	°C	79.3	76.6	74.8	71.7
T_{w4}	°C	70	68.9	67.0	64.0
T_{w5}	°C	74.5	72	70	66
T_{lo1}	°C	50.8	49.5	49.5	49.6
T_{lo2}	°C	46	40.7	42.8	41.6
T_{a2}	°C	189.5	154.9	136.3	106.7
T_{a3}	°C	39	31.4	29.7	26.7
T_{g1}	°C	436	390	381	372
T_{g2}	°C	240	228	232	243
T_{g3}	°C	205	186	185	185
h_{s1}	kJ/kg	251	251	251	251
h_{s2}	kJ/kg	2762	2762	2762	2762
$\dot{Q}_s$	kW	975	975	975	975
$\dot{Q}_{eg1}$	kW	1656	1121	1092	1071
$\dot{Q}_{eg,ORC}$	kW	681	146	117	96

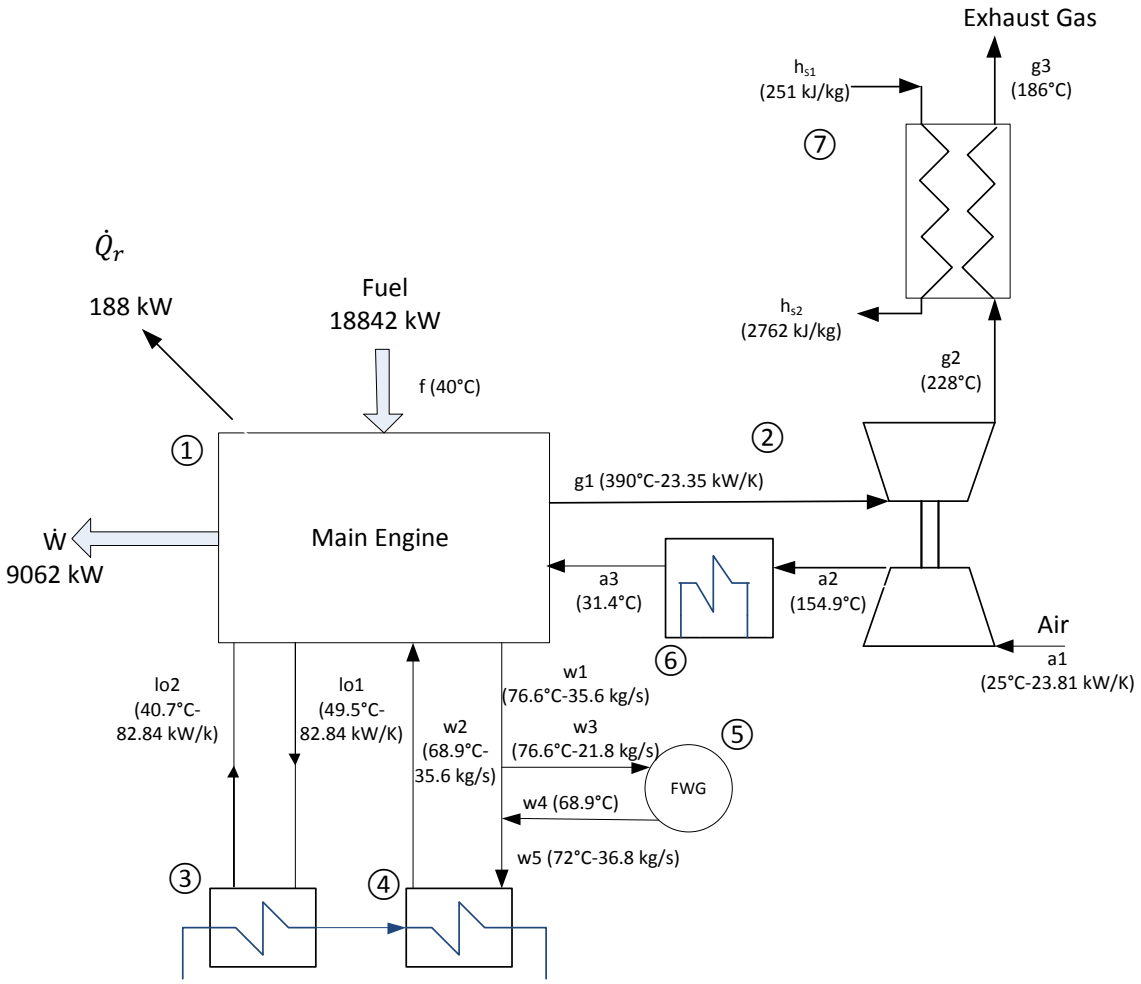

Legend:

1 Main Engine
2 Turbocharger
3 Lubricating oil exchanger
4 Jacket water exchanger
5 Fresh water generator
6 Supercharging air cooler
7 Exhaust gas boiler
8 Central fresh water cooler
Q_r=radiation power
$\dot{W}$=mechanical power

a=air
eg=exhaust gas
w=water
lo=lubricating oil
s=water / steam
cw=cooling water

Figure 3-16 Energy balance at 80% engine load.

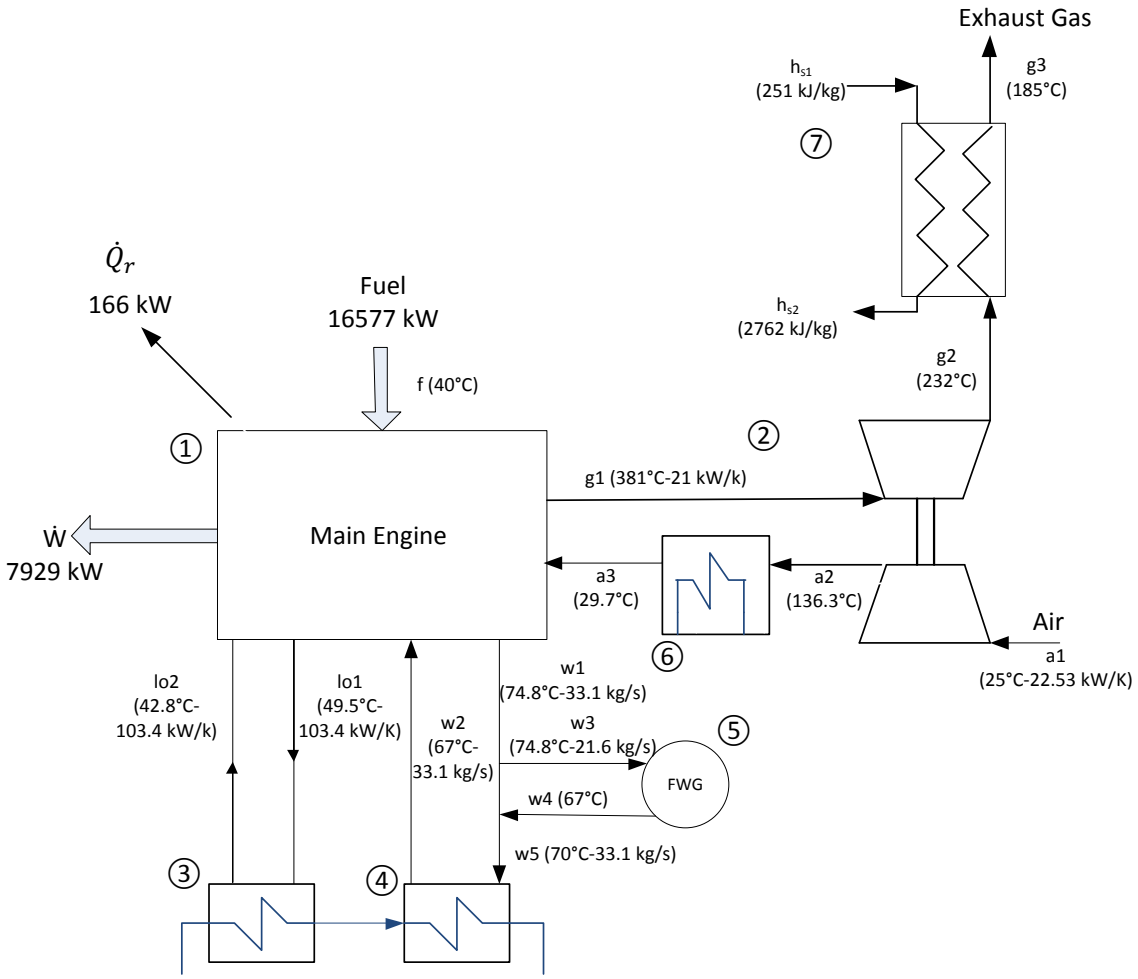

Legend:

1 Main Engine
2 Turbocharger
3 Lubricating oil exchanger
4 Jacket water exchanger
5 Fresh water generator
6 Supercharging air cooler
7 Exhaust gas boiler
8 Central fresh water cooler
Q_r=radiation power
$\dot{W}$=mechanical power

a=air
eg=exhaust gas
w=water
lo=lubricating oil
s=water / steam
cw=cooling water

Figure 3-17 Energy Balance at 70% Engine load.

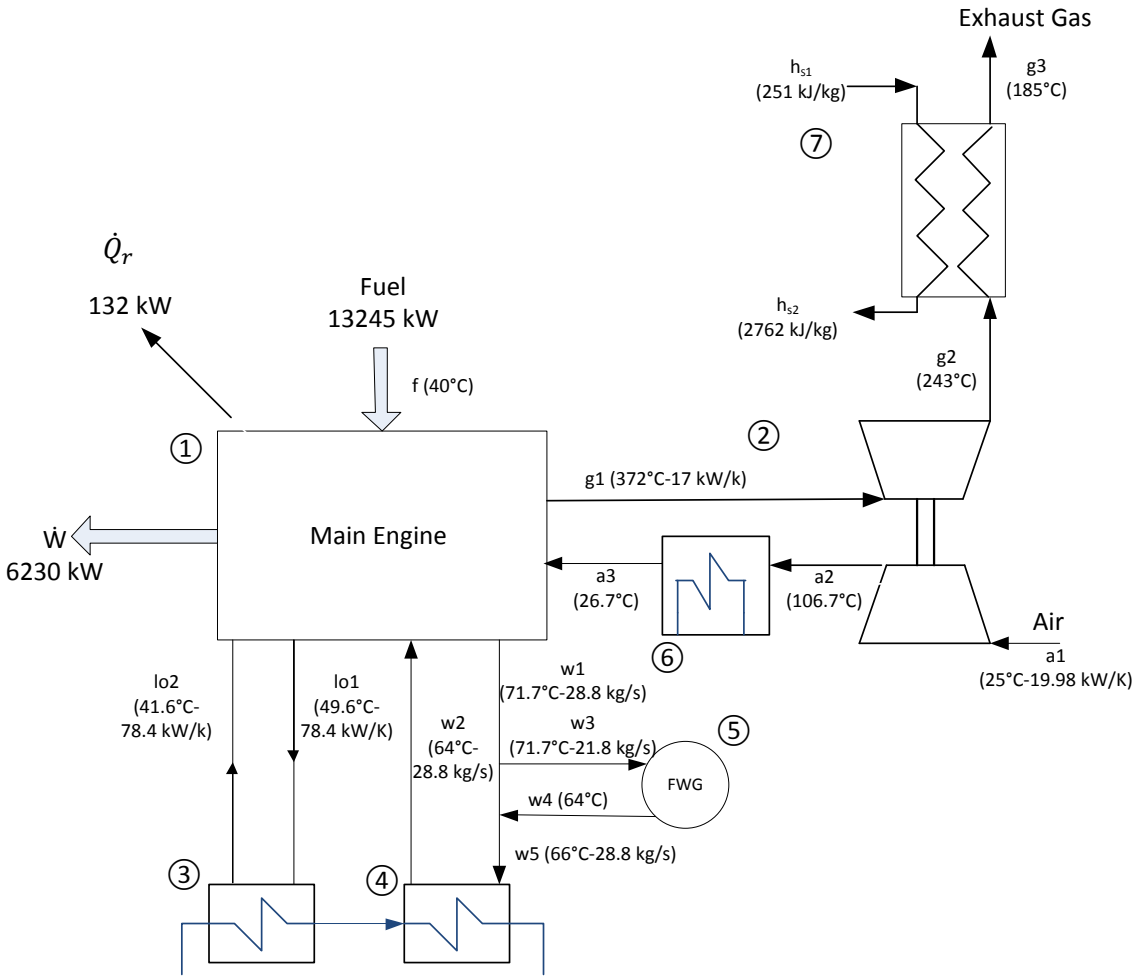

Legend:

1 Main Engine
2 Turbocharger
3 Lubricating oil exchanger
4 Jacket water exchanger
5 Fresh water generator
6 Supercharging air cooler
7 Exhaust gas boiler
8 Central fresh water cooler
Q_r=radiation power
$\dot{W}$=mechanical power

a=air
eg=exhaust gas
w=water
lo=lubricating oil
s=water / steam
cw=cooling water

Figure 3-18 Energy Balance at 55% Engine load.

4. Hot Composite Curves

In Chapter 3, energy balances for main engine loads were evaluated. Table 3-8 and Figure 3-4 show the four hot streams of the main engine: exhaust gas, jacket water, air cooler, lubricating oil. As previously stated (Section 3.5), the temperatures of the cooling circuit are known. Looking at Figure 3-4, the temperatures T_{cw1}, T_{cw2}, T_{cw3}, T_{cw4}, T_{cw5}, are 36, 42.5, 53.7, 36, 60°C respectively. The possibility to recover heat from the cooling circuit is not convenient. According to Wang et al. (2012) when heat source temperature is lower than 100°C ORC technology is uneconomical. Also the possibility to recover power from the exhaust gas is not considered here, for reason explained in the preceding, even if the exhaust gas temperature (T_{g3}) is higher than 100°C. Indeed the 100°C temperature is not a reference temperature for what concern the exhaust gas of the Main Engine due to the formation of sulfuric acid below 180°C. In this case it is not possible to extract power because the temperature T_{g3} is close to 180°C, see Table 3-8. Moreover, the available exhaust gas power after the exhaust gas boiler is negligible if compared to jacket water power, lubricating oil and air cooler power, as shown in Table 3-8. At 80% engine load (the most frequent engine load), the available exhaust gas power for the ORC ($\dot{Q}_{eg,ORC}$) is equal to 146 kW and the available thermal power from jacket water, lubricating oil, air cooler are 1186, 729, 3941 kW, respectively.

Because of the lack of exact information regarding the duration of the fresh water generator operation, the fresh water generator is considered in steady working condition.

After these preliminary considerations, it was decided to use as feasible ORC system hot streams, the thermal power rejected through the jacket water cooler $\dot{Q}_{jw}$, from the scavenge air cooler $\dot{Q}_{ca}$ and from the lubricating oil cooler $\dot{Q}_{lo}$. Thus these hot streams change heat directly with working fluid of the ORC system. The three thermal powers are shown in Figure 4-1.

Table 4-1 summarizes the properties of three hot streams: $\dot{Q}_{ca}$, $\dot{Q}_{jw}$, $\dot{Q}_{lo}$ (and Table 3-8) for the three main operating loads.

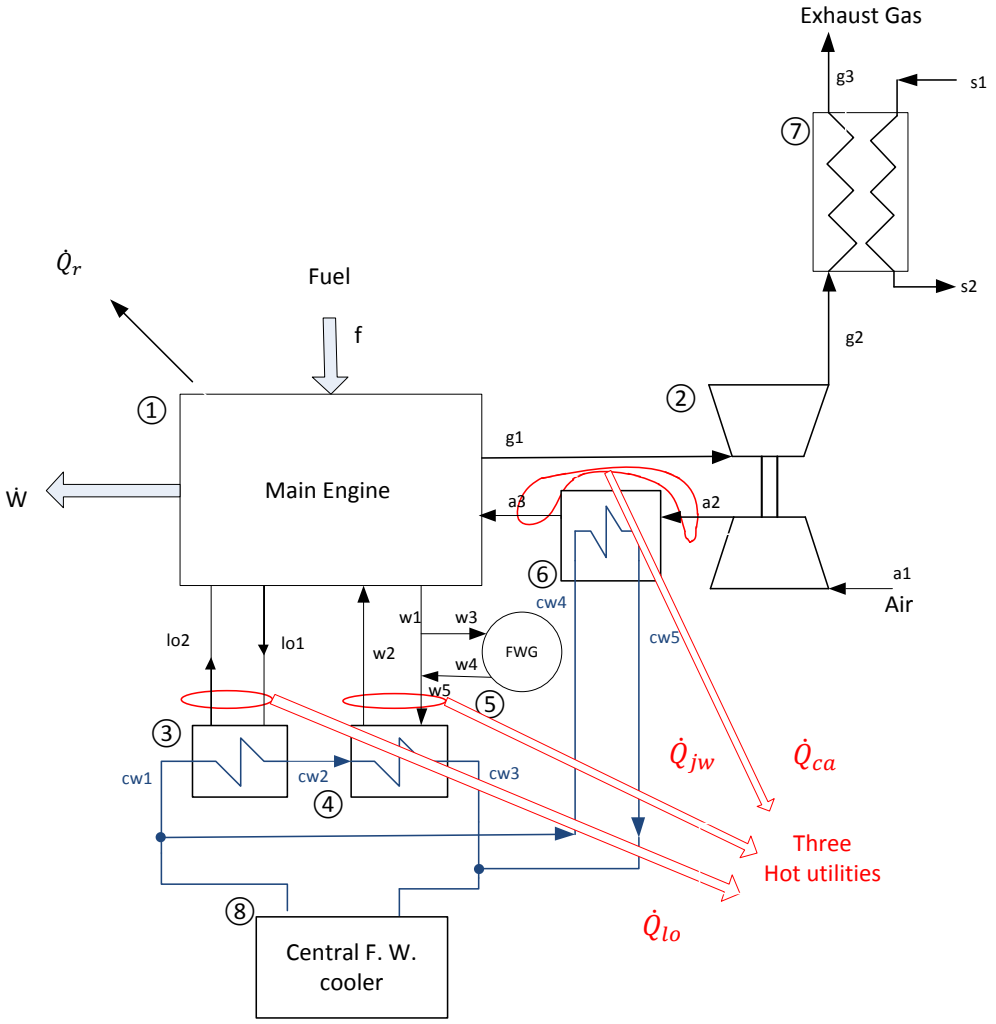

Legend:

1 Main Engine	a=air
2 Turbocharger	eg=exhaust gas
3 Lubricating oil exchanger	w=water
4 Jacket water exchanger	lo=lubricating oil
5 Fresh water generator	s=water / steam
6 Charge air cooler	cw=cooling water
7 Exhaust gas boiler	Q_r=radiation power
8 central fresh water cooler	$\dot{W}$=mechanical power

The red circles are hot utilities.

Figure 4-1 Three Hot utilities chosen.

Table 4-1 Hot utility properties.

Parameter		Main Engine load (%)		
Symbol	**Units**	**80**	**70**	**55**
$\dot{Q}_{ca}$	kW	2941	2402	1598
$\dot{Q}_{jw}$	kW	477.5	415	241
$\dot{Q}_{lo}$	kW	729	693	627
T_{a2}	°C	154.9	136.3	106.7
T_{a3}	°C	31.4	29.7	26.7
T_{w5}	°C	72	70	66
T_{w2}	°C	68.9	67.0	64.0
T_{lo1}	°C	49.5	49.5	49.6
T_{lo2}	°C	40.7	42.8	41.6
$\dot{m}_a c_{pa}$	kW/K	23.81	22.53	19.98
$\dot{m}_{lo} c_{plo}$	kW/K	82.84	103.4	78.4
$\dot{m}_w c_{pw}$	kW/k	154	138	120

To build the hot composite curves is necessary to combine the temperature characteristics of all hot streams into a single hot composite curve.

Each of The following three graphs shows the hot composite curves at three main engine loads, in the order: 80-70-55%, where for each segment the sources are shown.

Thermal power available for the ORC system is 4147 kW at 80% engine load, 3510 kW at 70% engine load and 2466 kW at 55% engine load. In each graphs, thermal power from air cooler covers all temperature range. At 80% engine load, $\dot{Q}_{ca}$ covers the temperature range from 154.9°C to 31.4°C. HCC is made by the combination of two streams, supercharging air and jacket water between 72°C and 68.9°C . and by lubricating oil and supercharging air from 49.5°C to 40.7°C . There is the same situation also at 70% and 55% of engine load. In each HCC, the temperature range can be divided in three parts, top, middle and bottom. In the top part, thermal power is supplied by air cooler, in the middle part by air cooler combine jacket water (range from 70°C to 64°C), and in the bottom part, thermal power is supplied by the combination of lubricating oil and air cooler (range between 50°C and 40°C)

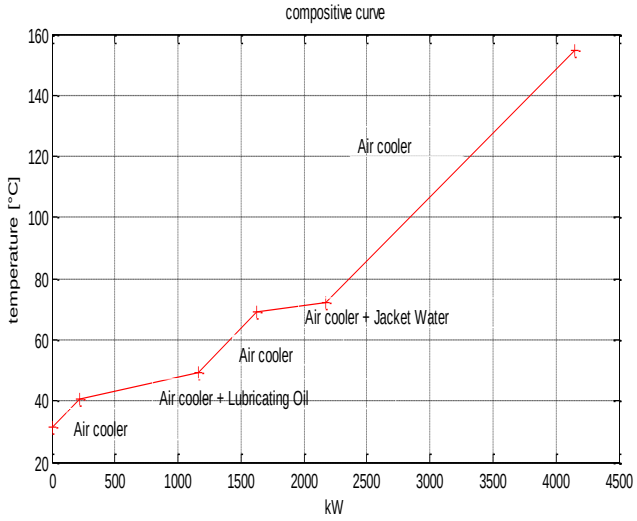

(a)

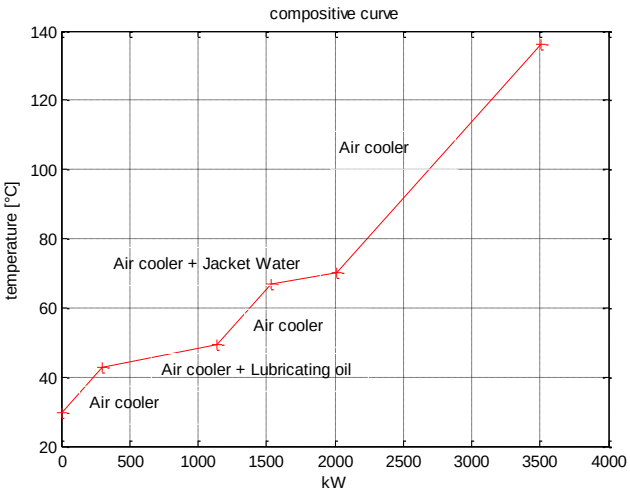

(b)

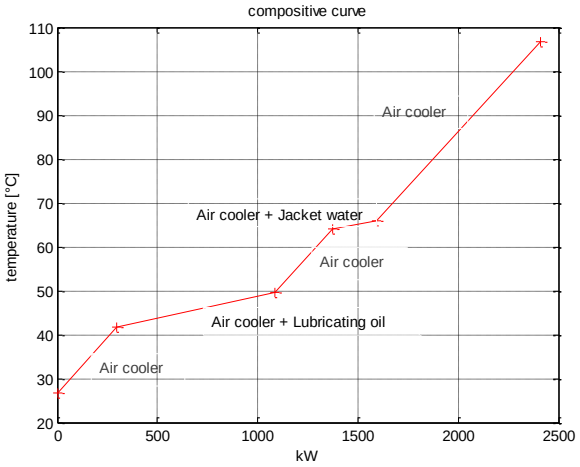

(c)

Figure 4-2 Hot composite curve: a) 80% engine load, b) 70% engine load, c) 55% engine load.

5. ORC Model

5.1. Introduction

In chapter four the following three hot utilities: jacket water, lubricating oil, supercharging air were selected as input for the ORC system and composed in three hot composite curves corresponding to the three engine loads (80%, 70%, 55%). Chen et al. (2011) and Schuster et al. (2010) conducted a study of a supercritical system and showed that a supercritical cycle requires larger U.A values (product overall heat transfer coefficient and heat transfer area) for the heat exchanger with the heat source and higher maximum pressures compared to subcritical cycles. This means that it is difficult to install a supercritical system on board. Hence, a subcritical ORC system is preferred and it is considered in the following sections. Chapter 5 describes the ORC thermodynamic model. The optimization function is defined and the function to be maximized is the power output ($\dot{W}_{net}$ see Section 5.2). After that, the assumptions made during the performance analysis and the procedure of the optimization are defined.

5.2. Thermodynamic Model of ORC

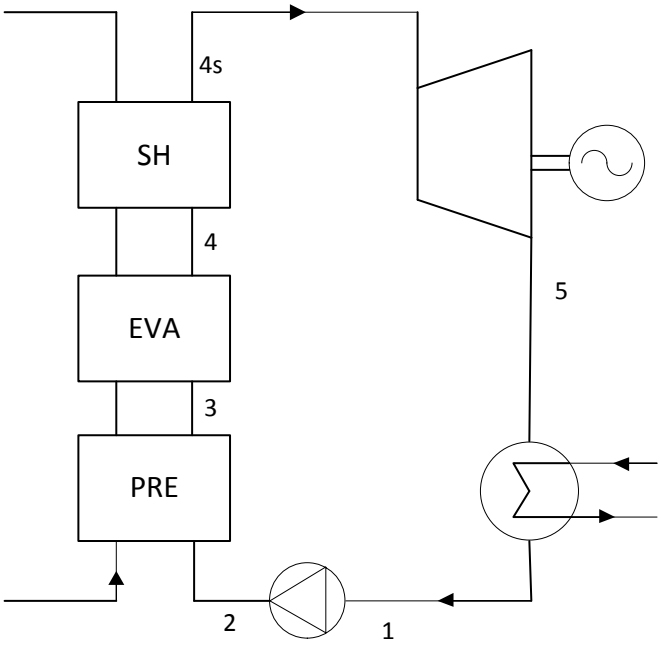

Figure 5-1 Model of the ORCs.

A simple Rankine cycle with subcritical configuration is considered, which consists of a pump, preheater (PRE), evaporator (EVA) and superheater (SH) exchangers , turbine and condenser. The working fluid is saturated liquid at the exit of the condenser; it is then pumped to the evaporator, where it gains heat from the heat source. Hot pressurized vapor expands in the turbine thereby producing useful work. The flow diagram of the system is shown in Fig. 5-1.

The thermodynamic equations for the components in the ORC are the following.
Available thermal power:

$$\dot{Q}_{av} = \dot{Q}_{jw} + \dot{Q}_{lo} + \dot{Q}_{ca} \tag{5.1}$$

Pump:

$$\dot{W}_p = \dot{m}_{orc} \cdot (h_2 - h_1) \tag{5.2}$$

$$\eta_{is,p} = \frac{h_{2,is} - h_1}{h_2 - h_1} \tag{5.3}$$

Input thermal power:

$$\dot{Q}_{in} = \dot{m}_{orc}(h_{4s} - h_2) \tag{5.4}$$

Turbine:

$$\dot{W}_T = \dot{m}_{orc} \cdot (h_{4s} - h_5) \tag{5.5}$$

$$\eta_{is,t} = \frac{h_{4s} - h_5}{h_{4s} - h_{5,is}} \tag{5.6}$$

The power output is:

$$\dot{W}_{net} = \eta_g \eta_m \cdot \dot{W}_T - \frac{\dot{W}_P}{\eta_{mt}\eta_m} \tag{5.7}$$

Total net system efficiency:

$$\eta_{net} = \frac{\dot{W}_{net}}{\dot{Q}_{av}} \tag{5.8}$$

The Rankine cycle efficiency:

.

$$\eta_R = \frac{\dot{W}_{net}}{\dot{Q}_{in}} \tag{5.9}$$

The heat recovery efficiency:

$$\phi = \frac{\dot{Q}_{in}}{\dot{Q}_{av}} \tag{5.10}$$

5.3. Optimization Function

The objective function to be maximized is the power output:

$$max(\dot{W}_{net}(x)) \tag{5.11}$$

where:

$$x = [\, \dot{m}_{ORC,}\ p_{max,}\ \Delta s_{sup}] \tag{5.12}$$

We consider the following as independent variables for the system optimization:

$\dot{m}_{orc}$ mass flow rate of the organic fluid.

p_{max} cycle maximum pressure.

Δs_{sup} According to Toffolo et al. (2010), the degree of superheating is measured in terms of entropy. The degree of superheating is measured from the entropy of the point on saturated vapor curve for subcritical cycle.

In addition the following bounds are specified for the three independent variables:

$$0\,\tfrac{kg}{s} < \dot{m}_{orc} < 50\,\tfrac{kg}{s} \tag{5.13}$$

$$p_{cond} < p_{max} < p_c \tag{5.14}$$

$$0\,\tfrac{kJ}{kgK} < \Delta s_{sup} < 0.20\tfrac{kJ}{kgK} \tag{5.15}$$

The model of the basic plant configuration was built in the Matlab/Simulink environment and the working fluid properties are calculated with REFPROP.

In this work the following assumptions are made during the optimization and performance analysis. The values of isentropic (η_{is}) and mechanical (η_m) efficiency of pump (indicated by p subscript) and turbine (indicated by t subscript), generator efficiency (η_g) and motor efficiency of the pump (η_{mt}) are fixed:

$$\eta_{is,p} = 0.70 \tag{5.13}$$

$$\eta_{is,t} = 0.85 \tag{5.14}$$

$$\eta_g = 0.96 \tag{5.15}$$

$$\eta_{m,p} = \eta_{m,t} = 0.90 \tag{5.16}$$

$$\eta_{mt} = 0.90 \tag{5.18}$$

Sea water at 25°C (ISO conditions) is used as cold utility in the condenser; and also the possibility to use water from cooling system at 36°C is investigated. The minimum

approach temperature (ΔT_{min}) is set at 10°C in the evaporator and 5°C in the condenser in accordance with Lakew and Bolland (2010).

5.4. Simulation Procedure

This section describes how the simulation code works. At each point the thermodynamic properties are calculated by REFPROP. The positions of the points appear in Section 5.2 and in the T-s diagram in Figure 5-2. For each point REFPROP needs at least two independent variables to define the thermodynamic state. In the following description the decisions made and the two independent variables are highlighted at each point.

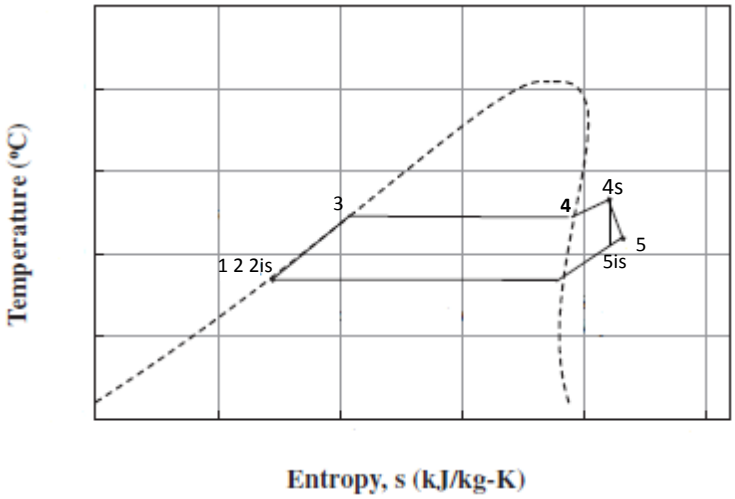

Figure 5-2 Circuit of ORC.

First Decision: the temperature of the cold utility (T_c) in the condenser can be 25°C using sea water or 36°C using water cooling:

Point 1:

$$T_c = 25°C \; or \; 36°C \tag{5.19}$$

$\Delta T_{cond} = 5°C$ in accordance with Lakew and Bolland (2010). (5.20)

$$T_1 = T_c + \Delta T_{cond} \;\; [°C] \tag{5.21}$$

$x_1 = 0$ vapor fraction (quality of the gas) (5.22)

$$[PROPERTIES] = REFPROP(T_1, x_1)$$

Point 2is:

$$s_{2,is} = s_1 \quad [\tfrac{kJ}{kgK}] \text{ specific entropy} \tag{5.23}$$

$p_{2,is} = p_{max}$ second decision variable [bar] (5.24)

$$[PROPERTIES] = REFPROP(p_{2,is}, s_{2,is})$$

Point 2:

$$h_2 = \frac{(h_{2,is} - h_1)}{\eta_{is,p}} + h_1 \quad [\tfrac{kJ}{kg}] \tag{5.25}$$

$p_2 = p_{max}$ second decision variable [bar] (5.26)

$$[PROPERTIES] = REFPROP(p_{2,} h_2)$$

$\eta_{is,p}$ assumption from Section 5.2

Point 3:

$$x_3 = 0 \tag{5.27}$$

$$p_3 = p_{max} \text{ second decision variable [bar]} \tag{5.28}$$

$$[PROPERTIES] = REFPROP(p_{3,} x_3)$$

Point 4:

$$x_4 = 1 \tag{5.29}$$

$$p_4 = p_{max} \text{ second decision variable [bar]} \tag{5.30}$$

$$[PROPERTIES] = REFPROP(p_{4,} x_4)$$

Point 4s:

$$s_{4s} = s_4 + \Delta s_{sup} \quad [\tfrac{kJ}{kgK}] \quad (\Delta s_{sup} \text{ is the third decision variable}) \tag{5.31}$$

$$p_{4s} = p_{max} \text{ second decision variable [bar]} \tag{5.32}$$

$$[PROPERTIES] = REFPROP(p_{4s,} s_{4s})$$

Point 5is:

$$s_{5is} = s_{4s} \quad [\tfrac{kJ}{kgK}] \text{ specific entropy} \tag{5.33}$$

$$p_{5is} = p_{cond} \quad \text{[bar]} \tag{5.34}$$

$$[PROPERTIES] = REFPROP(p_{5is,} s_{5is})$$

Point 5:

$$h_5 = h_{4s} - \eta_{is,t} \cdot (\ h_{4s} - h_{5is}) \ [\tfrac{kJ}{kg}] \tag{5.35}$$

$$p_5 = p_{cond} \text{ [bar]} \tag{5.36}$$

$$[PROPERTIES] = REFPROP(p_{5,} h_5)$$

$\eta_{is,t}$ assumption from section 5.3.

A h_c vector with all the specific enthalpies of the cold composite curve (C.C.C) is created:

$$h_c = [h_2, h_3, h_4, h_{4s}] \tag{5.37}$$

The h_c vector is multiplied by mass flow rate $\dot{m}_{orc}$ (first decision variable):

$$H_c = h_c \cdot \dot{m}_{ORC} \tag{5.38}$$

H_c describes the x-axis value (enthalpy multiplied mass flow rate) of the cold composite curve.

Another vector with temperatures is made of the cold composite curve

$$T_c = [T_2, T_3, T_4, T_{4s}] \tag{5.39}$$

T_c vector represent the y-axis value of the cold composite curve.

:

In the last step, the code controls the position of the cold composite curve (C.C.C). The temperatures of the cold composite curve made by the vector T_C have to be lower than the hot composite curve (hot composite curve are described in Figure 4-2 and Table 4-1) considering also 10°C as minimum approach temperature (the minimum approach temperature is defined in accordance with Lakew and Bolland (2010).).

The range of the H_c vector (enthalpies multiplied by mass flow rates) of the C.C.C has to fit within the range of enthalphies multiplied by mass flow rate. of the H.C.C.
This procedure is shown in the Figure 5-3. Heat recovery between hot and cold composites curves is feasible when the hot composite curve is above the cold composite curve. Assuming a minimum approach temperature (ΔT_{min}) value, the cold composite curve may be shifted horizontally until the smallest vertical distance between the two composite curves reaches the ΔT_{min} value. In the Figure 5-3 the azure curve (dashed line) is made by the vector H_c and the vector T_c. The vectors H_c and T_c are the results of the simulation with Simulink. The azure curve is shifted horizontally in direction of HCC, until it reaches the ΔT_{min}. The blue curve is the result of this control and it represents the final CCC (cold composite curve).

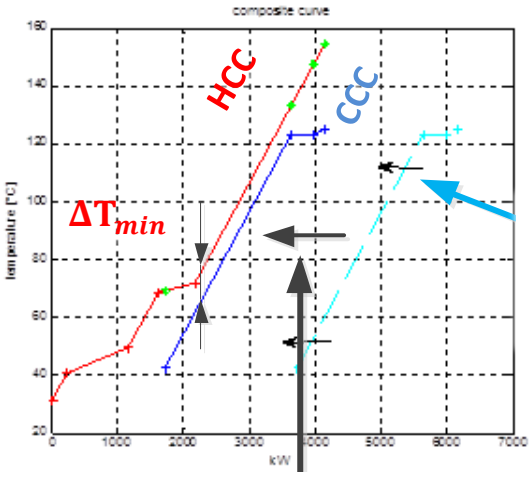

Figure 5-3 Simulation Procedure

6. Selection of Alternative Systems for an Performance Evaluation

6.1. Introduction

A subcritical ORC is evaluated as the power cycle to generate electric power from the cooling of lubricating oil, jacket water and air cooler. The operating condition at 80% engine load is chosen as design point. This operating condition is more frequent than the other two conditions (70% and 55% engine load). Four organic fluids R134a, R245fa, R227ea and R236fa are chosen for this application after the literature review carried out in Chapter 1. Two cold utilities in the condenser are compared, sea water at 25°C and fresh water from cooling system at 36°C. At first a ORC system was evaluated using the hot composite curve at 80% of engine load. Using HCC, the heat exchanger network is not defined and the maximum electric power is estimated. After that, six configurations are studied. The first, second, fourth, fifth configurations are at a single pressure level ORC, the third configuration is a regenerated ORC and a double pressure level ORC is investigated in the last configuration.

6.2. Optimization with Ideal System ORC

In the first simulation the HCC at 80% of load is the input to the ORC system (without details of the heat exchangers network). Thus it is possible to find the maximum power that the ORCs can produce with an ideal system.

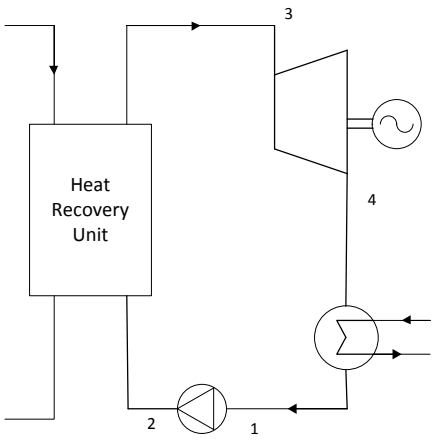

Figure 6-1 Ideal system ORC.

It is called “ideal system” because in this section the configuration of the heat exchanger network is not considered. The best configuration will be defined in the next sections.

The cycle in Figure 6-1 consists of a working fluid pump (1-2), an heat recovery unit (2-3), driven by the hot composite curve, an expander (3-4) and a water cooler condenser (4-1). Working fluid is pumped (1-2) to the heat recovery unit (2-3) where it is heated, vaporized and superheated by the heat source represented by the hot composite curve. The generated high pressure vapor flows into to the expander (3-4), and it drives the generator and electric power is produced ($\dot{W}_{net}$). Then, the working fluid is condensed in the condenser (4-1). The condensed working fluid is pumped back to the heat recovery unit and a new cycle begins.

The thermal power available from hot composite curve is given by Eq. (5.1) and the value is 4147 kW at 80% engine load. Here below the results of the optimization are expressed in tables and graphs referred to the system layout shown in Figure 6-1.

Table 6-1 Results with condensing water temperature at 25°C (see Figure 6-1).

Parameter		Working fluids			
Symbol	**Units**	**R134a**	**R227ea**	**R245fa**	**R236fa**
$\dot{Q}_{av}$	**kW**	4147	4147	4147	4147
$\dot{Q}_{IN}$	**kW**	2684	3016	2021	2697
T_1	**°C**	30	30	30	30
T_2	**°C**	32.17	31.59	30.25	42.67
T_3	**°C**	108.68	99.82	92.9	125
T_4	**°C**	36	36.96	45	43
p_{cond}	**bar**	7.59	5.208	1.75	3.16
p_{evap}	**bar**	38	28	10.66	31
$\dot{m}_{ORC}$	**kg/s**	13.14	23.38	8.76	15.04
Δs	**kJ /kg K**	0.088	0	0	0.027
η_{net}	**[-]**	0.067	0.067	0.054	0.078
η_R	**[-]**	0.104	0.092	0.11	0.12
ϕ	**[-]**	0.63	0.72	0.48	0.65
$\dot{W}_{net}$	**kW**	280.5	280.13	225	323
Sp	**m**	0.255	0.36	0.4	0.36
v_4/v_3		6.011	9.59	6.44	16.98

According to Table 6-1 using the sea water at 25°C as cooling medium in the condenser the maximum power output (323 kW) is achieved by R236fa. The Power output values for the remaining fluids are 280.5, 280.13, 225 kW for R134a, R227ea,

R245fa, respectively. Table 6-2 shows that using fresh water at 36°C as cooling medium in the condenser the maximum power output achievable is 255kW using R236fa. The power output values are 221, 209, 161 kW for R134a, R227ea, R245fa.

Table 6-2 Results with condensing water temperature at 36°C (see Figure 6-1).

Parameter		Working fluids			
Symbol	Units	R134a	R227ea	R245fa	R236fa
$\dot{Q}_{av}$	kW	4147	4147	4147	4147
$\dot{Q}_{IN}$	kW	2419	2571	1794	2433
T_{cond}	°C	36	36	36	36
T_1	°C	41	41	41	41
T_2	°C	43.3	42.67	41.29	42.67
T_3	°C	114.3	104.7	97.8	125
T_4	°C	53	55	55.4	51
p_{cond}	bar	10.29	7.118	2.55	4.44
p_{evap}	bar	39	28.5	11.93	31
$\dot{m}_{ORC}$	kg/s	12.32	20.03	8.2	14.66
Δs	kJ /kg K	0.11	0.039	0	0.03
η_{net}	[-]	0.053	0.05	0.043	0.061
η_R	[-]	0.09	0.081	0.10	0.10
ϕ	[-]	0.58	0.62	0.43	0.586
$\dot{W}_{net}$	kW	221	209	181	255
Sp	-	0.22	0.3	0.33	0.32
v_5/v_4	-	4.4	5.95	5.05	11.86

The use of sea water for condenser cooling results in lower condensation temperatures, and consequently lower condensation pressures. Thus, the turbine operates with higher pressure ratios and for the same flow rate it produces more power. Using sea water in the condenser, the highest total net efficiency (η_{net}) is about 7.8% when R236fa is adopted. The total efficiencies are 6.7, 6.7, 5.4% corresponding to R134a, R227ea, R245fa, respectively (see Table 6-1). If the water cooler is adopted in the condenser, the total net efficiencies are lower than the previously cases (using sea water). They are 6.1, 5.2, 5, 4.3 using R236fa, R134a, R227ea, R245fa, respectively (see Table 1-2).

Sea water (25°C)

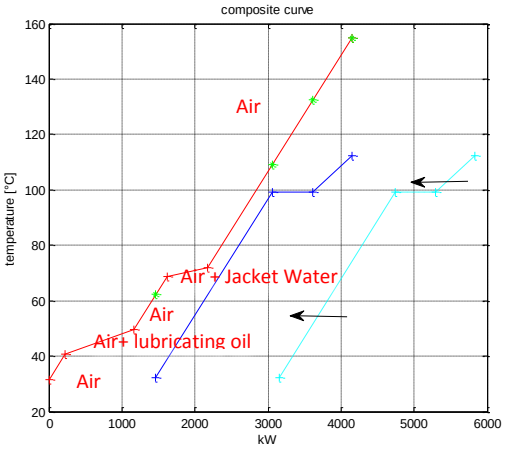

Water cooling (36°C)

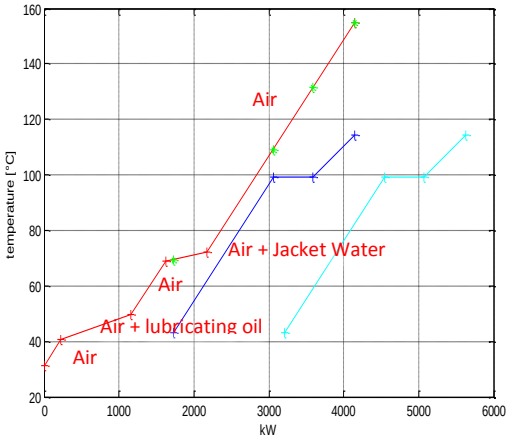

R134a

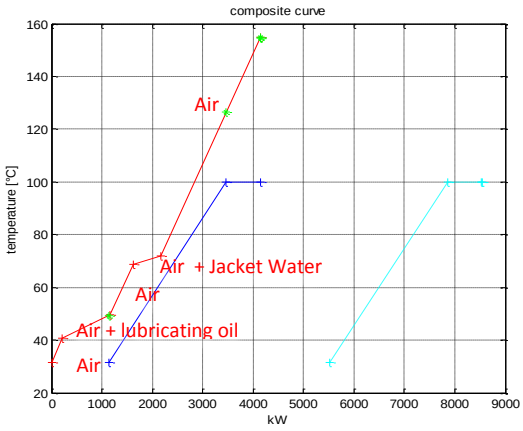

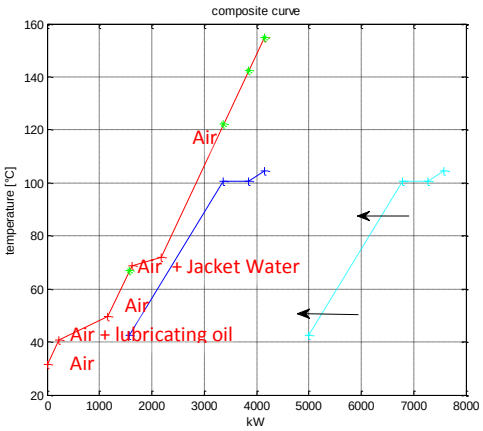

R227ea

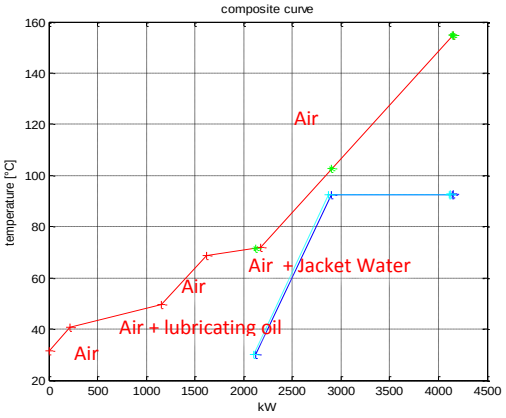

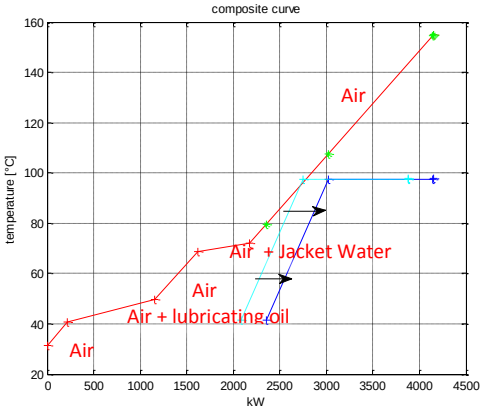

R245fa

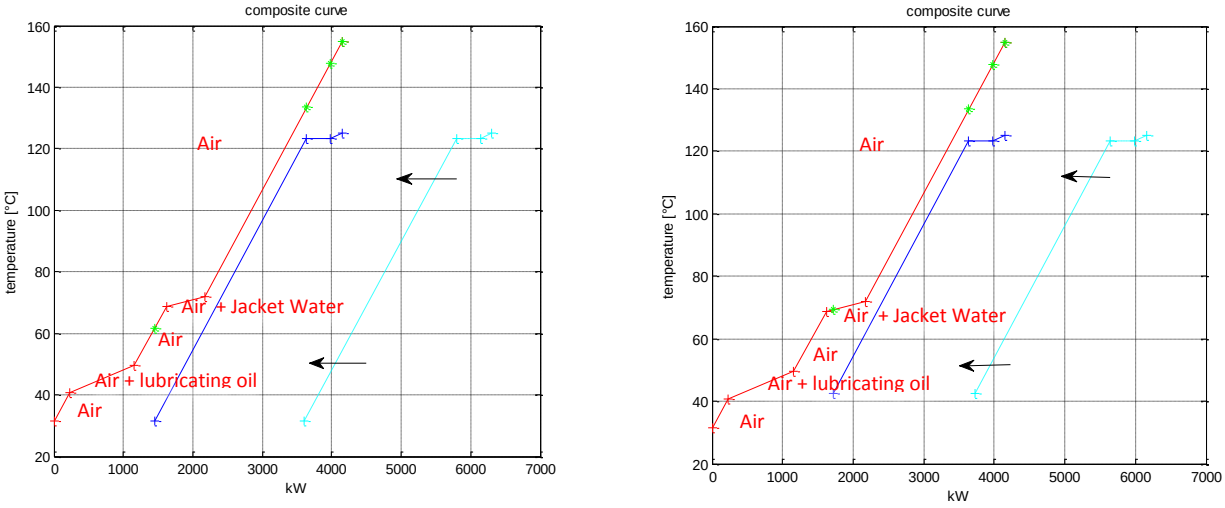

R236fa

Figure 6-2 Composite curves of R134a, R227ea, R245fa, R236fa (see Figure 6-1).

Figure 6-2 is divided in two columns and four rows. Each column represents the cooling medium in the condenser (sea water and fresh water). The four rows refer to the four working fluids. Each graph shows:

- a red curve that is the HCC, relative to the 80% engine load
- an azure curve which defines the thermodynamic condition of the cold utility obtained from the thermodynamic optimization
- a blue curve which is the cold utility shifted horizontally until the smaller vertical distance between the two composite curves is reached.

Figure 6-2 shows working fluids with low critical temperature presenting the superheating. For example, the critical temperature of R134a is 101°C, and R134a box shows such superheating. Instead, with working fluids with high critical temperature, as R245fa, there is no superheating (see R245fa boxes). Moreover, R245fa does not reach high temperature because the critical temperature is high (154°C) and for lower temperature it presents high latent heat levels.

6.3. First ORCs configuration proposed

A possible system for this ship is outlined in Figure 6-3. This configuration does not considered heat exchange between air cooler and working fluid but jacket water is used as heat transfer medium between air cooler and working fluid.

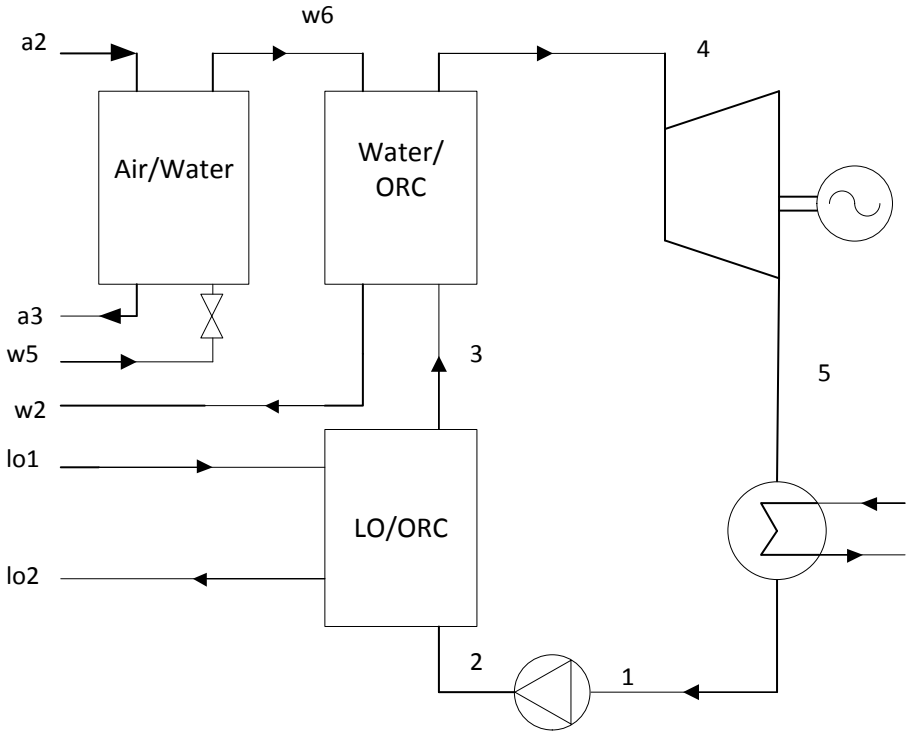

Figure 6-3 ORC system as the one proposed by Yue et al. (2012).

The cycle consists of a working pump (1-2), three heat exchangers (LO/ORC, AIR/water, Water/ORC), an expander (4-5) and a water cooled condenser (5-1). Jacket water is pumped to the Air/water exchanger (w5-w6) and the supercharging air (a2-a3) exchanges heat with jacket water. Working fluid is pumped to the LO/ORC heat exchanger (2-3) and after to Water/ORC heat exchanger (3-4), where it is heated, vaporized and superheated by the lubricating oil and then by jacket water. The generated high pressure vapor flows into the expanders (4-5) where it is expanded and accelerated, converting the thermal energy into mechanical energy. The turbine drives a generator, which produces electric power ($\dot{W}_{net}$). Then, the working fluid is condensed in the condenser (5-1). The condensed working fluid is pumped back to the LO/ORC heat exchanger and a new cycle begins.

The system in Figure 6-3 looks like the system suggested by Yue et al (2012). However, in this case, the jacket water exchanges heat to the air cooler through the AIR/WATER heat exchanger and not through the exhaust gas. This configuration has a

number of advantages which are missing in the first configuration (Section 6.2). The water is pumped in the pipes instead of air and carried around the ship, thus It permits a more compact ORC system.

One problem is that the air temperature outlet cannot be lower than the inlet temperature of the water, thus the air cooling needs two heat exchangers, one for the ORCs and the other one for the cooling system. Air cooler is not used as heat source at low temperature for ORC system, because working fluid is already warm up by lubricating oil.

Thus, if in the Air/Water heat exchanger, the product $\dot{m}_a c_{pa}$ is kept constant and the air outlet temperature (T_{a3}) is supposed to be equal to the water inlet temperature (T_{w5}) plus 5°C, the thermal power available from air cooler decreases if compared to the value in Table 3-8 . At 80% engine load, $\dot{m}_a c_{pa}$ is equal to 23.81 kg/s (see Table 4-1) and T_{a3} is equal to 77°C. The thermal power rejected through Air/Water heat exchanger is 1855 kW (Table 6-3) and the thermal power available from air cooler is 2941 kW (see Table 4-1). This system needs one heat exchanger to cool down the air from 77°C to 31.4°C, which means a thermal power equal to 1086 kW which cannot used for ORCs.

Table 6-3 shows the properties of AIR/WATER exchange.

Table 6-3 Properties of air/water exchange.

Parameter		Main Engine load (%)			
Symbol	**Units**	**100**	**80**	**70**	**55**
$\dot{Q}_{air}$	**kW**	2893	1855	1385	713
cp_{H2O}	**kJ/kgK**	4.186	4.186	4.186	4.186
T_{w5}	**°C**	74.5	72	70	66
T_{w6}	**°C**	94	84	79	71
T_{evap}	**°C**	133	133	133	133
P_{H2O}	**Bar**	2.94	2.94	2.94	2.94
$\dot{m}_w$	**kg/s**	35.6	36.8	33.1	28.8

If the whole water flow rate is used in the Air/Water exchanger, the outlet temperature is low (T_{w6}), and the working fluids cannot reach a high temperature at the outlet of the Water/ORC exchanger (see Table 6-3).

In this section it is proposed to add to the system a valve which can select the quantity of water flow rate at the entry of the AIR/WATER heat exchanger, in order to increase the temperature of the water at the outlet. Indeed, the rest of quantity of jacket water flows in the central fresh water cooler.

The water pressure at point w5 is 2.94 bar (30mTH), which corresponds to an evaporation temperature of 133°C. We need to avoid vapor in the pipes. Therefore the temperature T_{w6} must be lower than 133°C.

Table 6-4 shows this proposed change.

Table 6-4 Air/water exchanger with water valve.

Parameter		Main Engine load (%)			
Symbol	**Units**	**100**	**80**	**70**	**55**
$\dot{Q}_{air}$	**kW**	2893	1855	1385	713
$\dot{m}_w$	**kg/s**	15	10	10	10
T_{w5}	**°C**	74.5	72	70	66
T_{w6}	**°C**	120	115	103	83

At 80% engine load, the water mass flow rate decreases from 36.8 kg/s to 10kg/s and the temperature T_{w6} increases to 115°C. In this ORC configuration, the model is similar to the situation described in the model proposed in Section 5.2 and in the Section 5.3. Only the hot composite curve has changed. There are only two hot inlet streams, one from jacket water (where the flow rate is equal to 10 Kg/s) and the other one from lubricating oil. The heat exchanged in the two heat exchangers (Water/ORC and LO/ORC) is between two liquids, thus a minimum approach temperature of 5°C is chosen in both cases.

The results of the optimization are showed in the

Table 6-5 and Table 6-6.

From Table 6-5 using sea water in the condenser, the maximum output power is about 193 kW, achieved by R227ea. The power output ($\dot{W}_{net}$) are 180, 187.5, 182 for R236fa, R134a, R245fa, respectively. The total net efficiencies (η_{net}) are 4.6, 4.5, 4.5, 4.3 for R227ea, R236fa, R134a, R245fa. From Table 6-6, using fresh water at 36°C from central fresh water cooler, the maximum power output is 140kW adopting R227ea and the output power ($\dot{W}_{net}$) are 136, 134.8, 112 kW for R236fa, R134a, R245fa. The total efficiency values are 3.3, 3.2, 3.2,2.7 for R227ea, R236fa, R134a, R245fa, respectively . These results clearly show that using this configuration (Figure 6-3) the power output and the total net efficiency of all working fluids are strongly reduced, if compared with the results in Section 6.2. This eventuality is described by the fact that the input thermal power ($\dot{Q}_{IN}$) of the ORC system decreases, for example, referring to sea water in the condenser and R227ea as working fluid, $\dot{Q}_{IN}$ in the previous section was 3016 kW (see Table 6-1) where it is only 2236 kW in this configuration (see Table 6-5). Moreover, the maximum temperature of the cycle (see T_4Table 6-5) are low (less than 100°C) for two reasons. Jacket water is used as heat transfer between air cooler and working fluid, and

the temperature of the jacket water is low to avoid steaming in the pipes (see T_{w6} in Table 6-4 and Figure 6-3). Thus the total net efficiencies are strongly reduces.

Table 6-5 Results of the simulations condensing water temperature at 25°C (see Figure 6-3).

Parameter		Working fluids			
Symbol	Units	R134a	R227ea	R245fa	R236fa
$\dot{Q}_{av,total}$	kW	4147	4147	4147	4147
$\dot{Q}_{jw,recovered}$	kW	1929	1929	1929	1929
$\dot{Q}_{lo,recovered}$	kW	255	307	195	245
$\dot{Q}_{IN}$	kW	2184	2236	2124	2174
T_{a2}	°C	154.9	154.9	154.9	154.9
T_{a3}	°C	31.4	31.4	31.4	31.4
T_{w5}	°C	72	72	72	72
T_{w2}	°C	68.9	68.9	68.9	68.9
T_{lo1}	°C	49.5	49.5	49.5	49.5
T_{lo2}	°C	46.5	45.8	47.15	46.5
T_{cond}	°C	25	25	25	25
T_1	°C	30	30	30	30
T_2	°C	31.2	31.3	30.28	31.3
T_3	°C	44.5	44.5	44.5	44.5
T_4	°C	79.99	85.64	73.34	77
T_5	°C	30	43	41	44
p_{cond}	bar	7.59	5.26	1.76	3.16
p_{evap}	bar	26.15	20.81	6.58	11.65
$\dot{m}_{ORC}$	kg/s	11.74	16.72	9.74	12.65
Δs	kJ /kg K	0	0	0	0
η_{net}	[-]	0.045	0.046	0.043	0.045
η_R	[-]	0.085	0.086	0.085	0.086
ϕ	[-]	0.82	0.84	0.80	0.82
$\dot{W}_{net}$	kW	187.55	193	182	188
Sp	m	0.25	0.32	0.45	0.37
v_4/v_3	-	4.01	5.31	3.78	4.12

Table 6-6 Results of the simulations condensing water temperature at 36°C (see Figure 6-3).

Parameter		Working fluids			
Symbol	Units	R134a	R227ea	R245fa	R236fa
$\dot{Q}_{av,total}$	kW	4147	4147	4147	4147
$\dot{Q}_{jw,recovered}$	kW	1929	1929	1678	1929
$\dot{Q}_{lo,recovered}$	kW	48	59	0	40
$\dot{Q}_{IN}$	kW	1977	1988	1678	1969
T_{a2}	°C	154.9	154.9	154.9	154.9
T_{a3}	°C	31.4	31.4	31.4	31.4
T_{w5}	°C	72	72	72	72
T_{w2}	°C	68.9	68.9	75	68.9
T_{lo1}	°C	49.5	49.5	49.5	49.5
T_{lo2}	°C	48.9	48.8	49.5	40.7
T_1	°C	41	41	41	41
T_2	°C	42.16	42.35	41.26	42
T_3	°C	44	44.5	41.26	44.5
T_4	°C	80.67	86.44	74.2	77
T_5	°C	41	50	49	51
p_{cond}	bar	10.29	7.19	2.57	4.44
p_{evap}	bar	26.52	21.17	8.23	11.85
$\dot{m}_{ORC}$	kg/s	11.63	16.5	6.73	12.44
Δs	kJ /kg K	0	0	0	0
η_{net}	[-]	0.032	0.033	0.027	0.032
η_R	[-]	0.068	0.07	0.066	0.07
ϕ	[-]	0.47	0.48	0.40	0.47
$\dot{W}_{net}$	kW	134.8	140	112	136
Sp	-	0.23	0.29	0.375	0.34
v_4/v_3	-	2.98	3.89	2.67	2.97

As previous states, the power output and the total net efficiency of all working fluids are reduced, compared to the results in Section 6.2. Also the maximum temperature of the ORC cycle is reduced. Using R227ea as working fluid, the value of T_4, which is the inlet temperature of the expansion is 86°C (see Table 6-6) instead, in the previous section, the value of inlet temperature of the expansion is 104.7°C (see T_3 in Table 6-2). In both situations of this configuration (using sea water and water fresh as cooling medium in the condenser) there is no working fluid superheating (Δs=0 see Table 6-5 and Table 6-6).

Water cooling system (36°C)

Sea water (25°C)

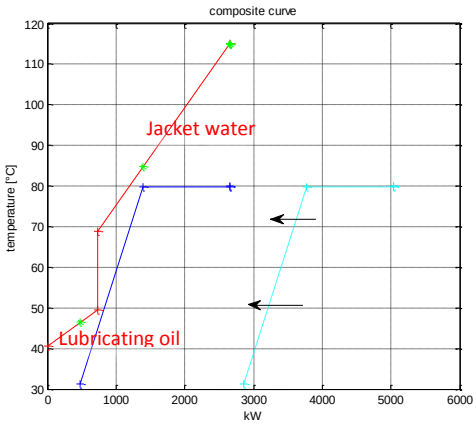

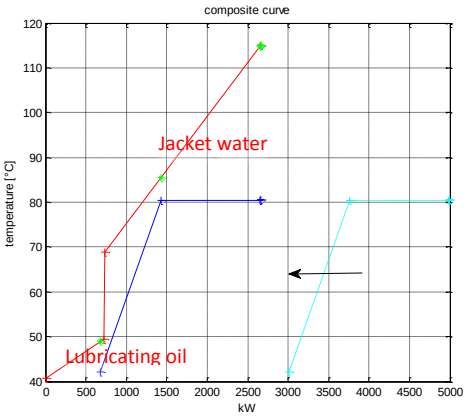

R134a

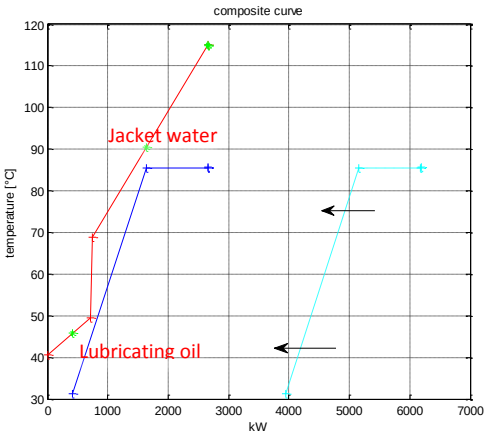

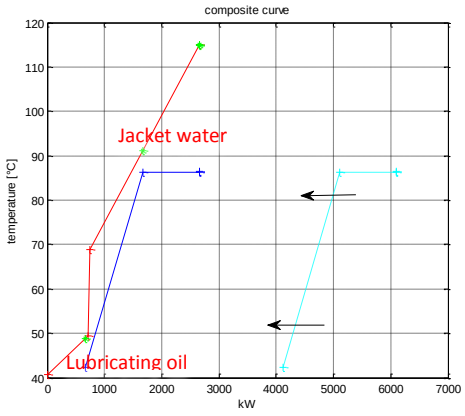

R227ea

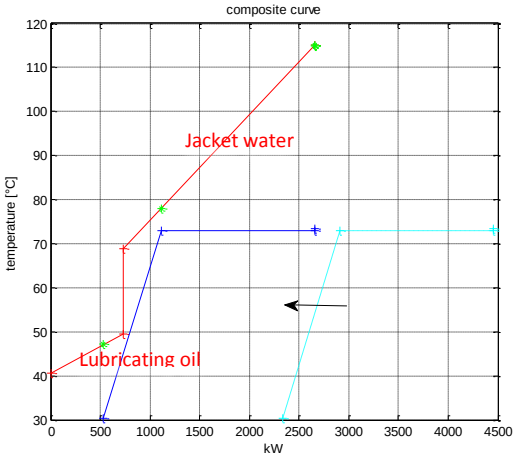

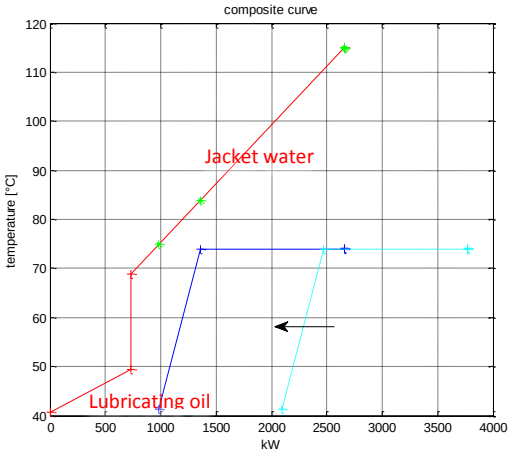

R245fa

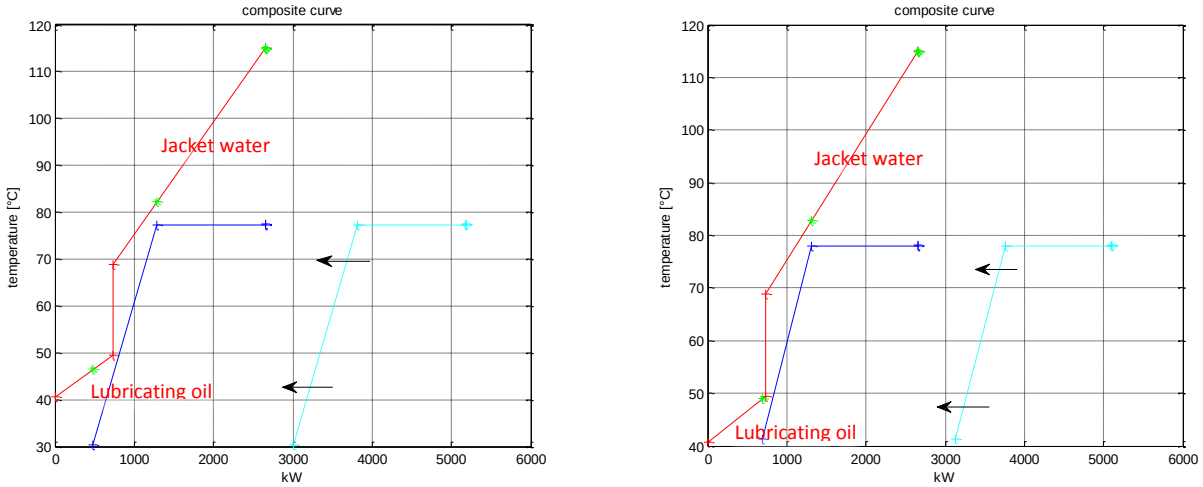

R236fa

Figure 6-4 Composite curve of first configuration (see Figure 6-3).

Figure 6-4Figure 6-2 is divided into two columns and four rows. Each column represents the cooling medium (sea water and fresh water). The four rows refer to the four working fluids. As already seen in the last section for the base case.

Each graph shows:

- a red curve that is the HCC (Hot composite curve).

- an azure curve which defines the thermodynamic condition of the cold utility obtained from the thermodynamic optimization

- a blue curve which is the cold utility shifted horizontally until the smaller vertical distance between the two composite curves is reached.

Using the configuration proposed in Figure 6-3, all working fluids cannot reach high temperature (see composite curves in Figure 6-4). The maximum temperature is around to 86°C achieved by R227ea (see Table 6-2). Moreover Figure 6-4 shows that if freshwater from central cooler is adopted in the condenser as cooling fluid, the thermal power recovered from lubricating oil is negligible compared to the thermal power of jacket water. Especially in the R245fa box (third row and second column) thermal power from lubricating oil is not recovered at all.

6.4. Second configuration of ORCs with two heat exchangers: air cooler and jacket water

This configuration (Figure 6-5) recovers thermal power from air cooler and jacket water. Thermal power from lubricating oil is not adopted. Fresh water at 36°C is adopted as cooling medium in the condenser.

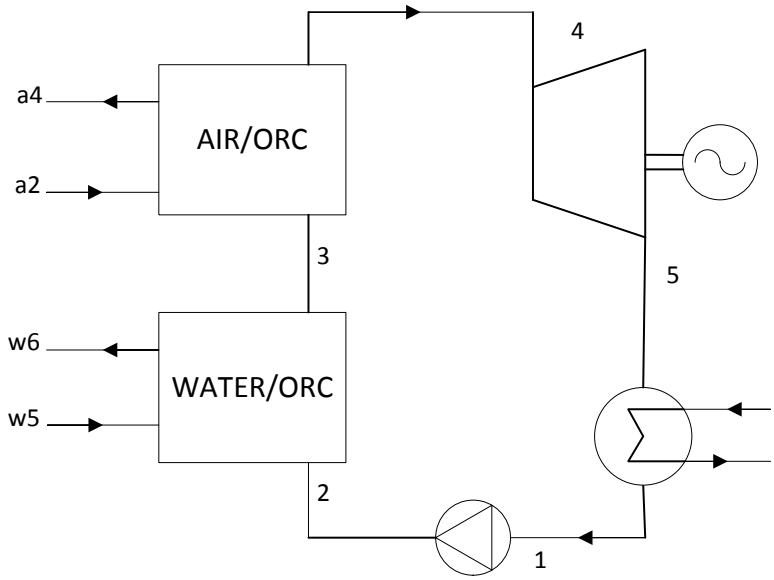

Figure 6-5 ORCs with two heat exchanger (AIR/ORC and WATER/ORC).

The cycle in Figure 6-5 consists of a working fluid pump, two heat exchangers (Water/ORC and Air/ORC), an expander, and a water cooler condenser. Working fluid is pumped (1-2) to the Water/ORC heat exchanger (2-3) and after to the AIR/ORC heat exchanger (3-4), where it is heated, vaporized and superheated by the heat sources represented by jacket water and air cooler. The generated high pressure vapor flows into the expander (4-5), and it drives the generator and electric energy is converted. Then the working fluid is condensed in the condenser (5-1). The condensed working fluid is pumped back to the Water/ORC heat exchanger and a new cycle begins. This configuration does not recover thermal power from lubricating oil.

The analysis of the previous configuration has shown (Figure 6-3) that if fresh water at 36°C is adopted as cooling medium in the condenser, the thermal power recovery from lubricating oil $\dot{Q}_{lo,recovered}$ assumes negligible values equal to 59, 48, 40 kW using R227ea, R134a, R236fa respectively (see in Table 6-6). The lubricating oil temperatures are between 49.5°C and 40.7°C, and the water temperature from the cooling system is 36°C. This difference in temperature is too small and the thermal power $\dot{Q}_{lo,recovered}$ may not

justify the heat exchanger cost. For this reason, the second configuration is made with a condenser temperature equal to 36°C (thus the condenser temperature of working fluid is equal to 41°C from Eq.(5.21)) and without the stream of lubricating oil (see Figure 6-5). A minimum approach temperature of 10°C was chosen for the evaporator. Using this configuration it is impossible to recover the whole supercharging air cooling heat. The air thermal power available is in the temperature range of 154.9°C-73°C (1950 kW), while below 73°C the working fluid is warmed up by jacket water.

The results of the optimization are showed in Table 6-7.

Table 6-7 Second configuration results (see Figure 6-5).

Parameter		Working fluids			
Symbol	Units	R134a	R227ea	R245fa	R236fa
$\dot{Q}_{av}$	kW	4147	4147	4147	4147
$\dot{Q}_{ca,recovered}$	kW	1950	1950	1779	1950
$\dot{Q}_{jw,recovered}$	kW	451	477	0	477
$\dot{Q}_{IN}$	kW	2401	2427	1779	2427
T_{a2}	°C	154.9	154.9	154.9	154.9
T_{a4}	°C	73	73	73	73
T_{w5}	°C	72	72	72	72
T_{w6}	°C	68.9	68.9	68.9	68.9
T_{cond}	°C	36	36	36	36
T_1	°C	41	41	41	41
T_2	°C	43.31	43	41.6	42.67
T_3	°C	62	62	41.6	62
T_4	°C	114.41	112.63	97.96	124.36
T_5	°C	53	70	53	48
p_{cond}	bar	10.29	7.19	2.57	4.44
p_{evap}	bar	39	28	11.96	30.98
$\dot{m}_{ORC}$	kg/s	12.21	16.96	8.14	14.97
Δs	kJ /kg K	0.12	0.074	0	0.02
η_{net}	[-]	0.052	0.048	0.042	0.06
η_R	[-]	0.09	0.082	0.098	0.103
ϕ	[-]	0.57	0.58	0.43	0.58
$\dot{W}_{net}$	kW	217.22	200	175.84	252
Sp	m	0.22	0.28	0.33	0.322
v_5/v_4	-	4.41	5.0741	5.02	12.45

From Table 6-7, the maximum output power is about 252 kW, reached by R236fa. The power outputs ($\dot{W}_{net}$) are 217.22, 200, 175.84 for R134a, R227ea, R245fa, respectively. The total net efficiencies (η_{net}) are 6.0, 5.2, 4.8, 4.2 for R236fa, R134a, R227ea, R245fa.

With this configuration (Figure 6-5) the power output and the total net efficiency of all working fluids are higher than those presented in Section 6.3. This result is explained by the fact that there is not the jacket water as heat transfer medium between air cooler and working fluid (see the Air/water heat exchanger in Figure 6-3) which in the first configuration limited the maximum temperatures achievable by the working fluid.

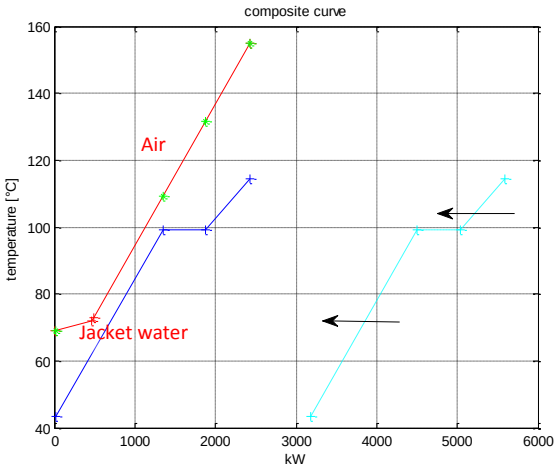

R134a

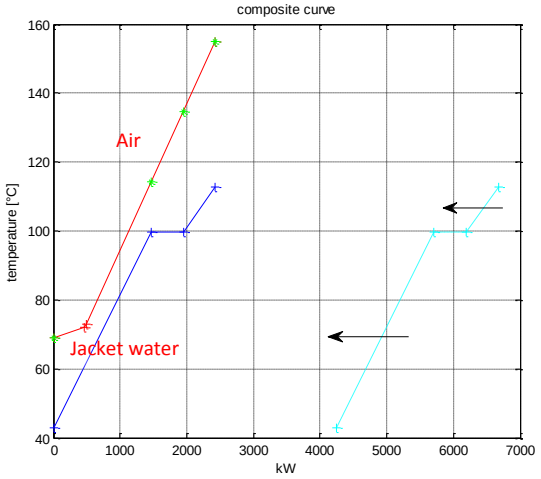

R227ea

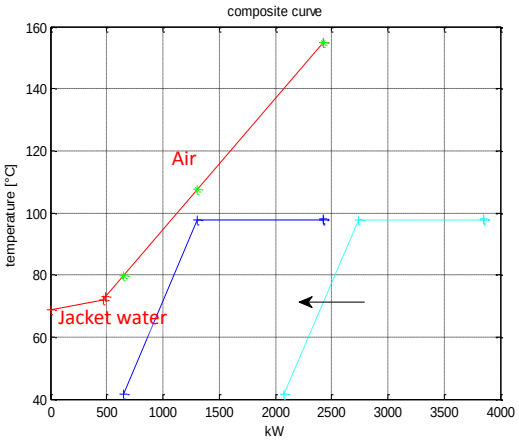

R245fa

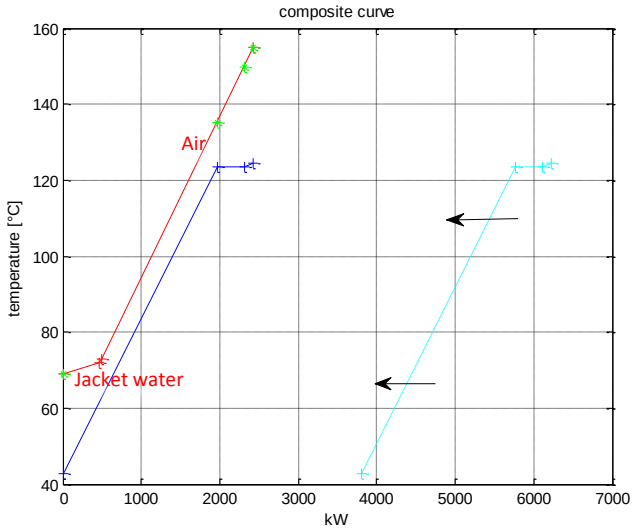

R236fa

Figure 6-6 Composite curves for the second configuration (see Figure 6-5).

Figure 6-6Figure 6-2 is divided in four boxes. Each box represents a working fluid. Into the boxes, each graph shows:

-a red curve that is the HCC (supercharging air and jacket water)

-an azure curve which defines the thermodynamic condition of the cold utility which results from the optimization

-a blue curve which is the cold utility shifted horizontally until the smaller vertical distance (pinch point) between the two composite curves is reached.

In Figure 6-6, Hot composite curve does not allow to recover thermal power from source at low temperature. In the angle between jacket water and air, the blue curve which is the cold utility, reaches the smaller vertical distance between the two composite curves (pinch point). Hence the cold utility cannot shift horizontally in direction of HCC and it recovers thermal power at low temperature. In particular, the configuration does not recover thermal power from jacket water when R245fa is adopted as working fluid (see $\dot{Q}_{jw,recovered}$ in Table 6-5).

6.5. Third configuration: Regenerated ORC

ORCs modules available in the market often use working fluids with superheated vapor. The temperature after expansion in the turbine can be higher than the fluid's condensing temperature. The energy content associated with this temperature difference can be minimized by integrating an additional heat exchanger in the ORC installation. This recovered heat is then used to preheat the ORC fluid that is pumped to the boiler.

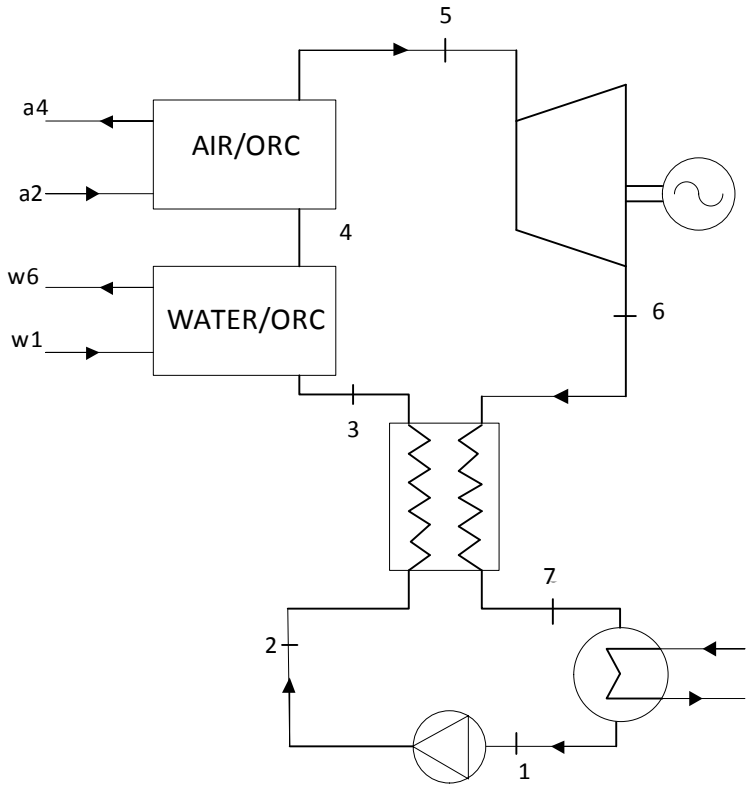

Figure 6-7 Regenerated ORC.

In Figure 6-7, the cycle consists in a working fluid pump, two heat exchangers (Water/ORC, Air/ORC) a heat exchanger for energy recovery, an expander and a water cooled condenser. Working fluid is pumped (1-2) to the recuperator (2-3) where it is heated by the working fluid vapor outlet of the turbine (6-7). After that, the working fluid flows through Water/ORC heat exchanger (3-4) and through to Air/ORC heat exchanger (4-5) and it is heated, vaporized and superheated by the jacket water and by the air cooler. The generated high pressure vapor flows into the expander (5-6), and it drives the generator and electric power ($\dot{W}_{net}$) is produced. Then the working fluid flows into the recuperator (6-7) after that it is condensed in the condenser (7-1). The condensed working fluid is pumped back to the recuperator and a new cycle begins. Fresh water at 36°C is adopted as cooling medium in the condenser.

In the present configuration it is considered that the recuperator is a counter flow type heat exchanger in which $\Delta T_{appr,R}$ is equal to 10°C. Under this hypothesis the temperature of the vapor at the heat exchanger outlet can be evaluated, as well as the available energy for the internal heat exchange process ($\dot{Q}_R$):

$$T_7 = T_2 + \Delta T_{appr} \tag{6.1}$$

$$\dot{Q}_R = \dot{m}_{ORC} \cdot (h_6 - h_7) \tag{6.2}$$

The state of the liquid at the regenerator outlet can be determined, since:

$$h_3 = h_2 + \frac{\dot{Q}_R}{\dot{m}_{ORC}} \tag{6.3}$$

Vaja and Gambarotta (2010) used this method, but they considered a $\Delta T_{appr,R}$ equal to 15°C. In the previous configuration (see Section 6.5) for all working fluids, the output temperatures of turbine (T_5) are not high (the maximum output temperature is 70°C with R227ea, 53°C for R134a and R245fa, 48°C for R236fa, see Table 6-7). As previously stated, fresh water is used in the condenser, thus T_2 is close to 36°C (fresh water temperature) plus 5°C (minimum approach temperature in the condenser see Eq. (5.21)). If the $\Delta T_{appr,R}$ is equal to 15°C, from Eq.(6.1) T_7 would be 56°C, it is higher than almost all output temperatures vapor of expansion found in Section 6.5, which means that the heat exchange is impossible from Eq. (6.2). Thus, in this work $\Delta T_{appr,R}$ equal to 10°C is chosen, so the heat exchange is possible between liquid working fluid and vapor at the end of turbine expansion.

In this simulation one more constraint is added. T_6 has to be equal or higher than T_7.

Table 6-8 shows that the regenerated heat exchanger is useless for R134a and R236fa. The outlet turbine temperatures (T_7) are 53°C for both working fluids, T_7 is equal to T_6, and $\dot{Q}_R$ (available thermal power for the internal heat exchange process) found from Eq. (5.41) is zero. Using R227ea and R245fa as a working fluids, $\dot{Q}_R$ is 79.22 and, 33 kW, respectively. The output power is 246, 217.16, 202, 177 kW for R236fa, R134a, R227ea, R245fa, respectively. If these output powers are compared to the output powers found in Section 6.4, there is an slight improvements for R227ea (from 200 kW to 202 kW) and for R245fa (from 175.84 kW to 177 kW). There is a worsening adopting R236fa (from 252 kW to 246 kW) and using R134a (from 217.22 kW to 217.16 kW) because there is a constraint that T_6 has to be equal or higher than T_7 (using the second configuration the output power is higher because the output temperature of the expansion is lower.)

The total net efficiencies (η_{net}) are 5.9, 5.2, 4.8, 4.2% for R236fa, R134a, R227ea, R245fa. They are almost equal to the total net efficiencies found in section 6.4. In conclusion, using a recuperator, there is not a great improvement.

Table 6-8 Main parameters of regenerated cycle (see Figure 6-7).

Parameter		Working fluids			
Symbol	Units	R134a	R227ea	R245fa	R236fa
$\dot{Q}_{av}$	kW	4147	4147	f4147	4147
$\dot{Q}_{ca,recovered}$	kW	1950	1950	1779	1950
$\dot{Q}_{jw,recovered}$	kW	451	477	0	405
$\dot{Q}_{IN}$	kW	2401	2427	1779	2355
T_{a2}	°C	154.9	154.9	154.9	154.9
T_{a4}	°C	73	73	73	73
T_{w1}	°C	72	72	72	72
T_{w6}	°C	68.9	68.9	68.9	68.9
T_{cond}	°C	36	36	36	36
T_1	°C	41	41	41	41
T_2	°C	43.3	42	41	43
T_3	°C	43.3	46.3	44.34	43
T_5	°C	114.31	104.4	97.83	125.5
T_6	°C	53	57	55	53
T_7	°C	53	53	51	53
p_{cond}	Bar	10.29	7.19	2.55	4.4
p_{evap}	Bar	39.00	28.00	11.93	31
$\dot{m}_{ORC}$	kg/s	12.23	19.4	8.16	14.12
Δs	kJ /kg K	0.119	0.038	0	0.03
η_{net}	[-]	0.052	0.048	0.042	0.059
η_R	[-]	0.09	0.083	0.099	0.104
ϕ	[-]	0.58	0.58	0.43	0.56
$\dot{W}_{net}$	kW	217.16	202	177	246
Sp	M	0.22	0.30	0.337	0.31
v_6/v_7	-	4.41	5.65	50	11.58
$\dot{Q}_R$	kW	0	79.22	33	0

Table 6-8 shows that $\dot{Q}_R$ (available thermal power for the internal heat exchange process) is zero adopting R236fa and R134a. Using R227ea and R245fa as a working fluids, T_3 (the output temperature of the recuperator) is 46.3°C and 44.34°C respectively. Hence, in the best case (R227ea as working fluid) the working fluids cannot be warmed more than 5.3°C after the regenerated.

Figure 6-8Figure 6-2 is divided in four boxes. Each box represents a working fluid. Each graph shows a red curve that is the HCC an azure curve which defines the thermodynamic condition of the cold utility (results of the optimization), a blue curve

which is the cold utility shifted horizontally until the smaller vertical distance (pinch point) between the two composite curves is reached.

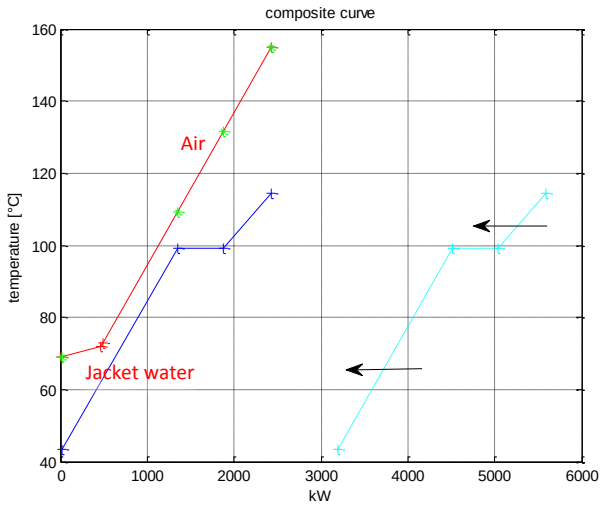

R134a

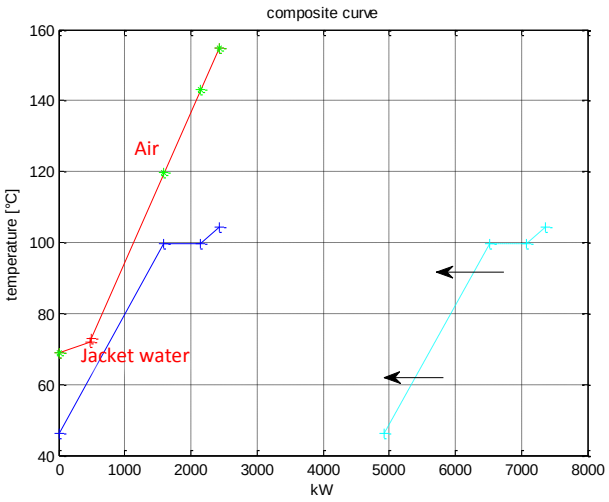

R227ea

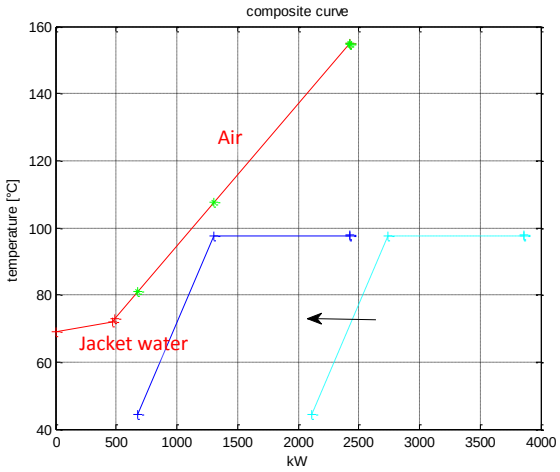

R245fa

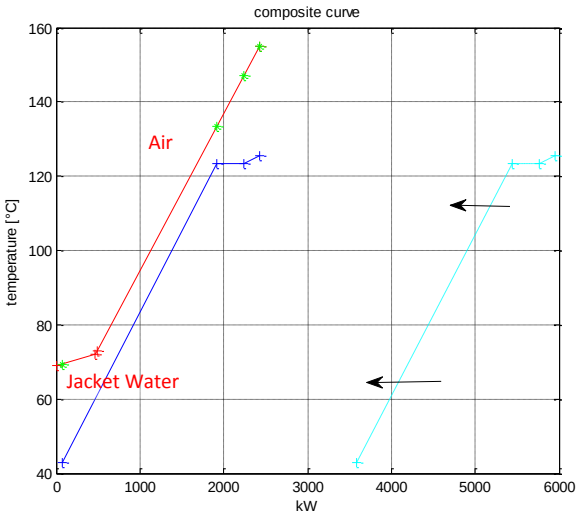

R236fa

Figure 6-8 Composite curves of regenerated system (see Figure 6-7).

In Figure 6-8, even if the hot utility and cold utility are the same of the second configuration, the cold composite curves of R245fa and R227ea are different. Thanks to the recuperator, the lowest temperature of the cold composite curve, which is T_3 (outlet temperature of the recuperator in Table 6-8) is higher than the lowest temperature of the cold composite curve of the second configuration (which is the outlet temperature of the pump).

6.6. Fourth configuration: Simple ORCs with three heat exchanges: air cooler, jacket water and lubricating oil.

A possible system for this ship is outlined in Figure 6-9. This configuration recovers heat from air cooler, jacket water, lubricating oil and sea water is considered as cooling medium in the condenser.

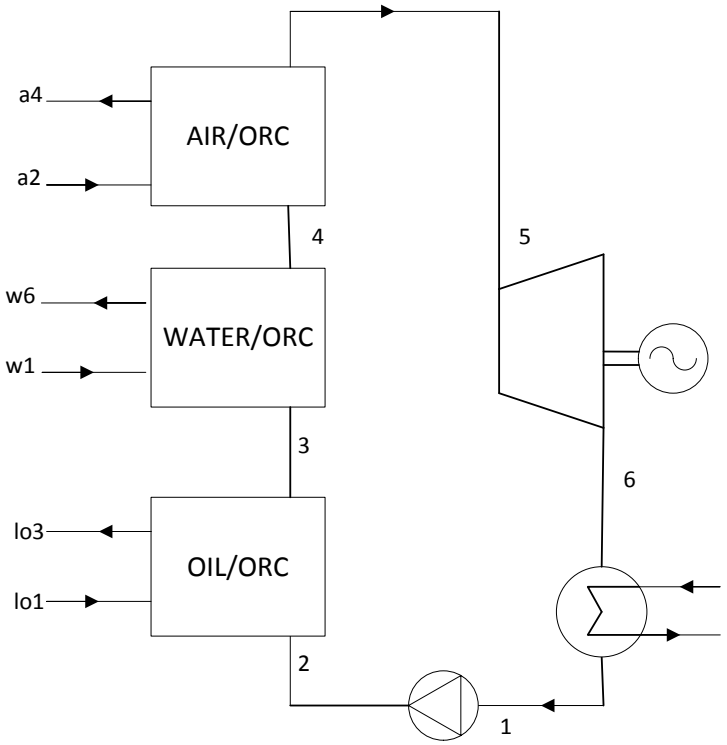

Figure 6-9 Fourth configuration of system.

This configuration (Figure 6-9) consists of a working fluid pump, three heat exchangers (OIL/ORC, WATER/ORC, AIR/ORC), an expander and a water cooled condenser.

Working fluid is pumped (1-2) through OIL/ORC heat exchanger (2-3) after through WATER/ORC heat exchanger (3-4) and then through AIR/ORC heat exchanger, where it is heated, vaporized and superheated by lubricating oil, jacket water and air cooler. The generated high pressure vapor flows into the expander (5-6), and it drives the generator and electric power ($\dot{W}_{net}$) is produced. Then the working fluid is condensed in the condenser (6-1). The condensed working fluid is pumped back to the OIL/ORC heat exchanger and a new cycle begins. The condensation heat is transferred to sea water. A sea water heat exchanger gives lower available temperatures (25°C), therefore, it is possible to recover energy from lubricating oil (49.5-40.7°C). As previously stated in

Section 6.4, the air cooler thermal power available is in the range of 154.9°C-73°C, while down 73°C the working fluid is warmed by jacket water and lubricating oil.

The fact that the surface has to be cleaned regularly to avoid deposition of salts and corrosion and the need for a clever selection of materials (no cooper alloys can be used) represent two disadvantages of sea water cooling. The material is a crucial factor in seawater cooled system. An excellent material is Titanium. It has excellent resistance to corrosion and the Titanium tubes allow higher velocity, which avoids biofouling by suitable increase in the velocity itself. This solution using a sea water is convenient only if the increase of net power output can cover the cleaning cost of the heat exchangers.

Table 6-9 Main parameters of the fourth configuration (see Figure 6-9).

Parameter		Working fluids			
Symbol	Units	R134a	R227ea	R245fa	R236fa
$\dot{Q}_{av}$	kW	4147	4147	4147	4147
$\dot{Q}_{ca,recovered}$	kW	1950	1950	1950	1950
$\dot{Q}_{jw,recovered}$	kW	477	477	63	477
$\dot{Q}_{lo,recovered}$	kW	166	194	0	175
$\dot{Q}_{IN}$	kW	2593	2621	2013	2602
T_{a2}	°C	154.9	154.9	154.9	154.9
T_{a4}	°C	73	73	73	73
T_{w1}	°C	72	72	72	72
T_{w6}	°C	68.9	68.9	68.9	68.9
T_{lo1}	°C	49.5	49.5	49.5	49.5
T_{lo3}	°C	47.5	47.1	49.5	47.4
T_1	°C	30	30	30	30
T_2	°C	32.25	31.97	30.53	31.93
T_3	°C	39	39	30.53	39
T_4	°C	61	59	36	61
T_5	°C	114.41	115.8	93	125.37
T_6	°C	42.87	67	46	45
p_{cond}	bar	7.59	5.26	1.76	3.19
p_{evap}	bar	39	28.5	10.69	31
$\dot{m}_{ORC}$	kg/s	12.2	16.39	8.74	14.44
Δs	kJ /kg K	0.092	0.088	0	0.031
η_{net}	[-]	0.067	0.062	0.054	0.075
η_R	[-]	0.107	0.097	0.11	0.12
ϕ	[-]	0.62	0.63	0.48	0.63
$\dot{W}_{net}$	kW	278.9	259	223	311
Sp	m	0.25	0.31	0.40	0.358
v_5/v_4	-	6.01	7.05	6.40	16.52

Using the configuration in Figure 6-9, Table 6-9 shows the results of the optimization.

The maximal output power is 311 kW with R236fa. Output power ($\dot{W}_{net}$) is 278.9, 259, 223 kW for R134a, R227ea, R245fa, respectively. The total net efficiencies (η_{net}) are 7.5, 6.7, 6.2, 5.4 for R236fa, R134a, R227ea, R245fa, respectively. The fourth configuration leads the higher power than the previous three configurations. This improvement is due to the heat recovery from three hot streams (jacket water, air cooler, lubricating oil) and due to the lower condensation temperature.

The thermal power recovered from lubricating oil (see $\dot{Q}_{lo,recovered}$ in Table 6-9) assumes value equal to 194, 175, 166 kW adopting R227ea, R236fa, R134a. That is a great improvement if compared to the thermal power recovered from lubricating oil in the first configuration where the freshwater is adopted as cooling medium in the condenser . In this case, the values of $\dot{Q}_{lo,recovered}$ are 59, 40, 40 kW for R227ea, R236fa, R134a (see Table 6-6).

Figure 6-10 is divided in four boxes. Each box represents a working fluid. Each graph shows:

- a red curve that is the HCC (supercharging air, jacket water, lubricating oil).

-an azure curve which defines the thermodynamic condition of the cold utility obtained from the thermodynamic optimization.

-a blue curve which is the cold utility shifted horizontally until the smaller vertical distance (pinch point) between the two composite curves is reached.

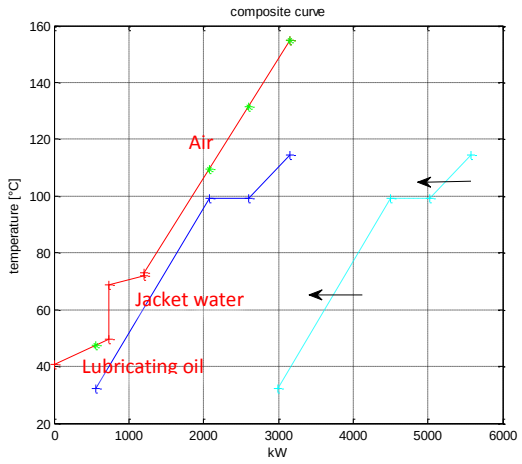

R134a

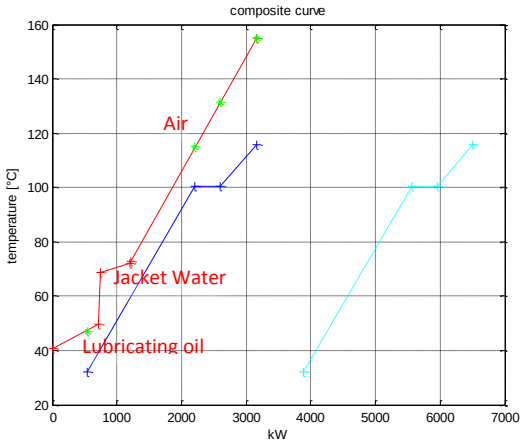

R227ea

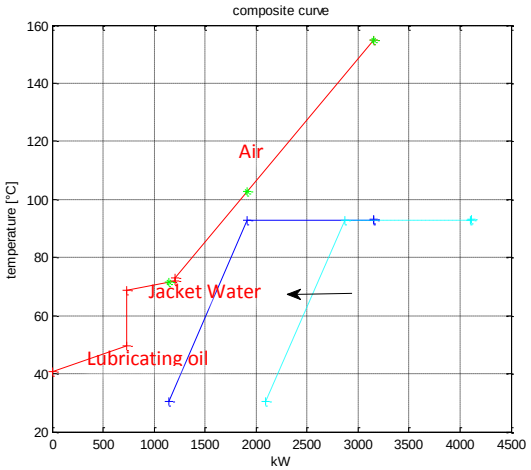

R245fa

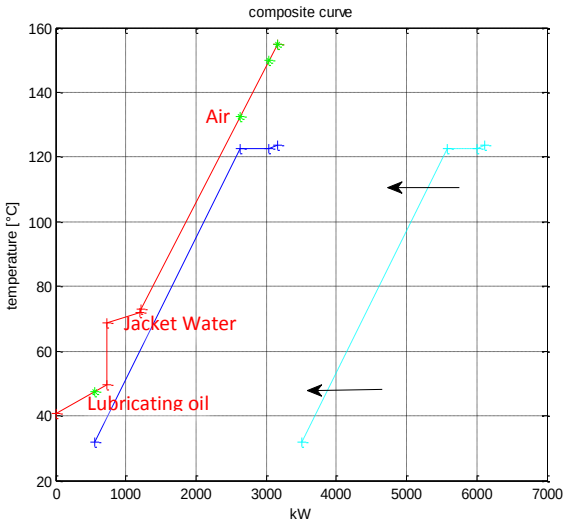

R236fa

Figure 6-10 Composite Curve of fourth configuration (see Figure 6-9).

Using sea water, as cooling medium in the condenser, does not allow to recover thermal power at low temperature for all working fluids. Figure 6-10 shows that using R245fa as working fluid, the maximum power output is obtained recovering thermal power from air cooler, and from jacket water, but not from lubricating oil. The reason is the cold composite curve reaching the pinch point before to recover power from lubricating oil (see R345fa box in Figure 6-10).

6.7. Fifth Configuration: Only Air Heat Exchanger

The fifth configuration explores the possibility to recover energy only from air cooler (Figure 6-11) and sea water at 25°C is adopted as cooling medium in the condenser.

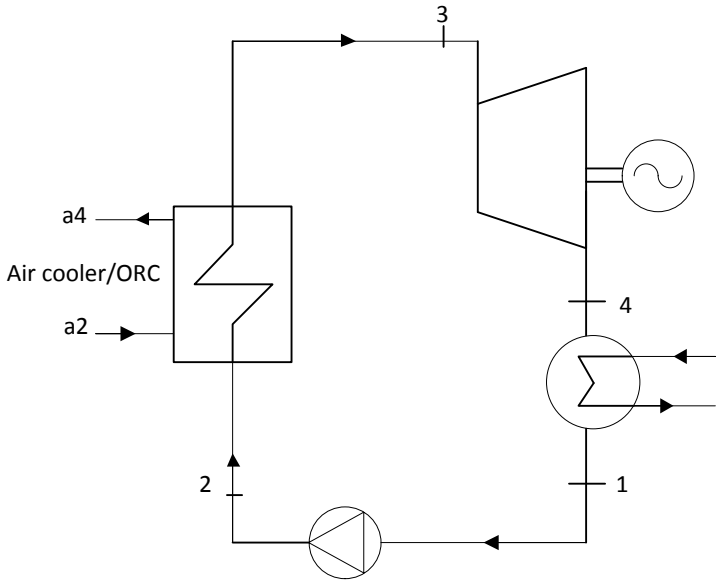

Figure 6-11 Fifth configuration of the system.

The cycle in Figure 6-11 consists of a working fluid pump, one heat exchanger (AIR/ORC), an expander and a water cooled condenser. Working fluid is pumped (1-2) to the AIR/ORC heat exchanger (2-3), where it is heated, vaporized and superheated by air cooler. The generated high pressure vapor flows into the expander (3-4), and it drives the generator and electric power is produced. Then the working fluid is condensed in the condenser (4-1). The condensed working fluid is pumped back to the AIR/ORC heat exchanger and a new cycle begins. The condensation heat is transferred to sea water.
The temperature range is higher than with the other heat sources. The fourth configuration (the best of the previous four configuration studied) in Section 6.6 required several heat exchangers as it is shown in Figure 6-10. For examples, the R236fa needs three preheaters (one for jacket water, one for lubricating oil, and another one for air cooler), one evaporator and one superheater, it means five heat exchangers in total. Instead, using one heat source (supercharging air) only one economizer, one evaporator and one superheater are needed.

Table 6-11 shows the results of the optimization.

Table 6-10 Results of the fifth configuration (see Table 6-11).

Parameter		Working fluids			
Symbol	**Units**	**R134a**	**R227ea**	**R245fa**	**R236fa**
$\dot{Q}_{av}$	**kW**	4147	4147	4147	4147
$\dot{Q}_{ca,recovered}$	**kW**	2675	2688	2019	2690
$\dot{Q}_{IN}$	**kW**	2675	2688	2019	2690
T_{a2}	**°C**	154.9	154.9	154.9	154.9
T_{a4}	**°C**	42.5	42	70	42
T_{cond}	**°C**	25	25	25	25
T_1	**°C**	30	30	30	30
T_2	**°C**	32.52	31.97	30.53	31.87
T_3	**°C**	106	121.9	92.84	121
T_4	**°C**	32	75	46	37
p_1	**bar**	7.66	5.26	1.76	3.19
p_2	**bar**	38	28.5	10.64	30
$\dot{m}_{ORC}$	**kg/s**	13.5	15.97	8.77	15.37
Δs	**kJ /kg K**	0.074	0.11	-	0.0088
η_{net}	**[-]**	0.066	0.064	0.059	0.076
η_R	**[-]**	0.10	0.099	0.11	0.12
ϕ	**[-]**	0.64	0.65	0.48	0.65
$\dot{W}_{net}$	**kW**	273.83	266	223	317.8
Sp	**m**	0.25	0.31	0.40	0.37
v_3/v_4	**-**	6.09	6.74	6.37	17.54

The maximum power output is 317.8 kW when R236fa is adopted. The output power ($\dot{W}_{net}$) is 273.83, 266, 223 kW for R134a, R227ea, R245fa, respectively. Using only the air cooler heat exchanger the output powers are compared with the results of the fourth configuration in Section 6.6. The output powers are equal for R245fa, 223 kW for both configuration. The reason is that the maximum power output is obtained recovering heat from high temperatures. Using R134a, the fifth configuration cannot reach high temperature, because the flow rate is higher than in the fourth configuration. T_3 is 106°C instead of 114.41°C in the fourth configuration. This temperature reduction means lower power output: 273.8 kW against 278.9 kW of the fourth configuration. The power output increases for R227ea and R236fa. The inlet turbine temperature of R227ea is 121.9°C, vs 115.8°C in the fourth configuration. This means higher enthalpy and higher power: 266 kW vs 259 kW of the fourth configuration. The inlet turbine temperature of fluid R236fa does not increase (T_3=121°C) before T_5=125.37°C but in this case the mass flow rate

increases (from 14.44 kg/s to 15.37 kg/s), therefore the power output (from 311 kW to 317.8 kW).

This configuration requires fewer heat exchangers and therefore less space, and the output power in some cases is higher than in the previous configurations. For those considerations, the fifth configuration would be the best solution of the cases studied until this section .

Even if the whole thermal power from air cooler is available (from 154.9°C to 31.4°C), the system in Figure 6 11 cannot cool down the air until 31.4°C because in the heat exchanger, a minimum approach temperature of 10°C is considered. Therefore the minimum temperature of air cooler is around 42°C for all working fluids except for R245fa. In fact, for R245fa the maximum power output is obtained recovering thermal power from high temperature, from 154.9°C to 70°C (see T_{a4} in Table 6 10). Hence, to cool down the air until 31.4°C it has to flow to the scavenge air cooler already installed in the ship.

Figure 6-12 is divided in four boxes. Each box represents a working fluid. Each graph shows:

- a red curve that is the HCC (supercharging air)

-an azure curve which defines the thermodynamic condition of the cold utility obtained from the thermodynamic optimization

-a blue curve which is the cold utility shifted horizontally until the smaller vertical distance (pinch point) between the two composite curves is reached.

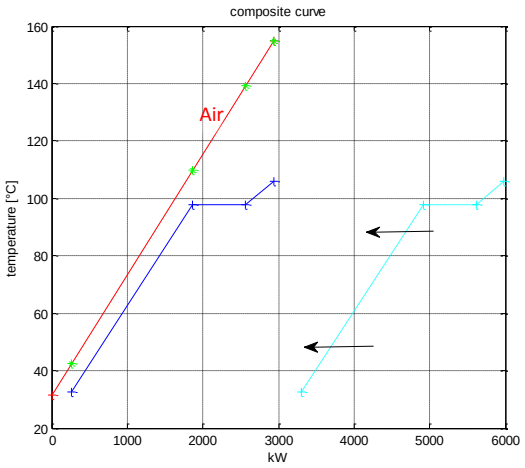

R134a

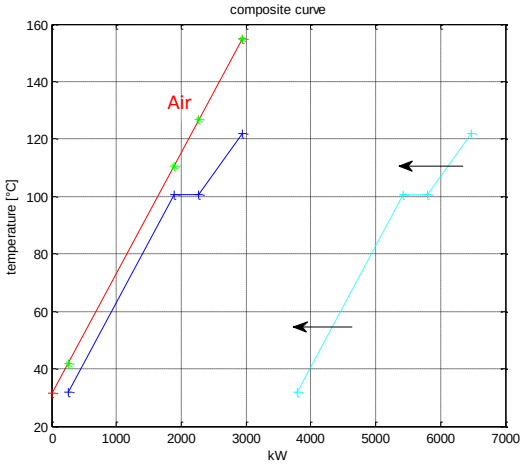

R227ea

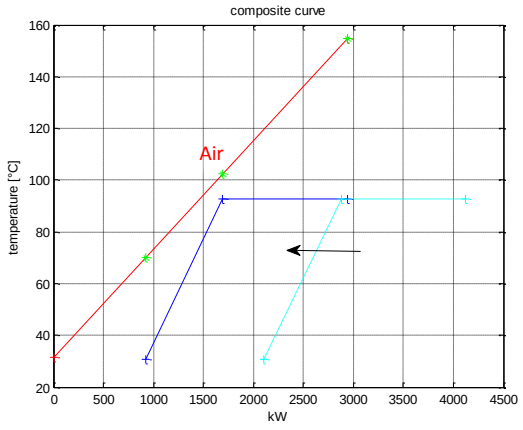

R245fa

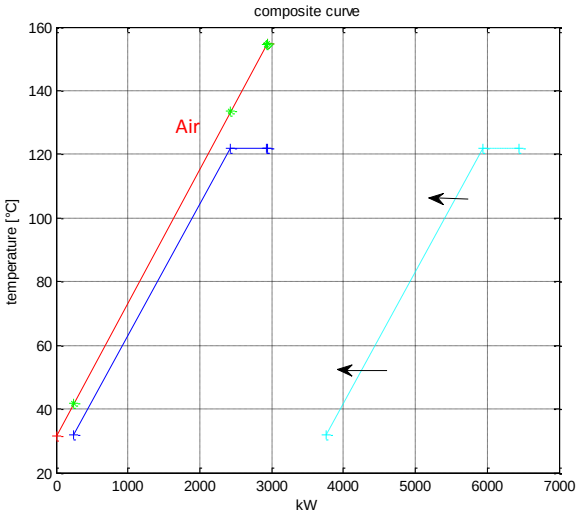

R236fa

Figure 6-12 Composite Curves of the Fifth Configuration (see Figure 6-11).

Figure 6-12 shows that for working fluids with low critical temperature as R134a and R227ea, part of the thermal power is recovered to overheat the working fluids. For working fluid with high critical temperature, thus with high latent heat, thermal power from the hot utilities is adopted only to preheat and vaporize the working fluid (see R245fa and R236fa).

6.8. Sixth configuration: Two Stage ORC System

In Section 6.7, the advantages of the fifth configuration (Figure 6-11) compared with the other four configurations previously studied are explained. Using only the whole air cooler thermal power, the output powers with two working fluids (R227ea and R236fa) are the highest compared to the previous four configurations. But jacket water and oil lubricating sources are still available, so in this section the system proposed (dual stage system) in Section 2.8 is considered (Figure 6-13). Thus thermal power of jacket water and lubricating oil are recovered as well.

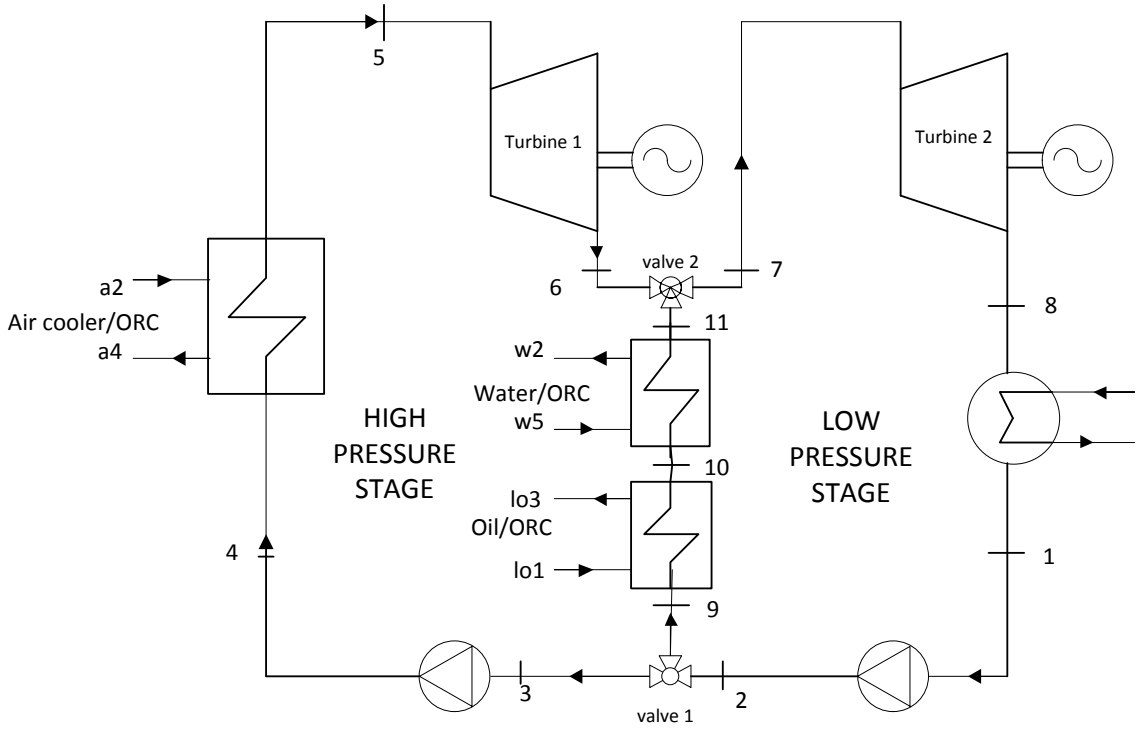

Figure 6-13 Two stage ORC system.

Two stage ORC system comprises two working fluid pump, three heat exchangers, two valves, two expansions and a water cooled condenser.

The working fluid is pumped (1-2) to the valve 1, where it is divided into two mass flow rates. Mass flow rate $\dot{m}_3$ is pumped (3-4) to the evaporator at high pressure (Air cooler/ORC heat exchanger 4-5) where it is heated, vaporized and overheated by air cooler. The generated high pressure vapor flows into Turbine 1 (5-6), and it drives the generator and electric power ($\dot{W}_{net}$) is produced. Then the working fluid mass flow rate $\dot{m}_3$ is mixed to mass flow rate $\dot{m}_9$ in valve 2. At the same time, after valve 1, mass flow

rate $\dot{m}_9$ flows through Lubricating oil/ORC heat exchanger (9-10), and Jacket Water/ORC heat exchanger (10-11) where it is heated, vaporized and overheated by lubricating oil and jacket water. After the valve 2, the vapor working fluid flows into Turbine 2 (7-8) where mechanical power is produced and in the generator it is converted in electric power ($\dot{W}_{net}$). Then the working fluid is condensed in the condenser (8-1). The condensed working fluid is pumped back to valve 1 and a new cycle begins. The condensation heat is transferred to sea water.

The thermodynamic equations and the assumptions for the components are the same as described in Section 5.2. Two more equations are introduced.

Mass balance at valve 1:

$$\dot{m}_9 + \dot{m}_3 = \dot{m}_1 \tag{6.4}$$

Energy balance at valve 2:

$$\dot{m}_3 h_6 + \dot{m}_9 h_{11} = \dot{m}_1 h_7 \tag{6.5}$$

The low pressure stage in Figure 6-14 clearly suggests that it is difficult to have a good match between composite curves, because most of the power from lubricating oil is not recovered. The maximum power for the low pressure loop is obtained only for high pressure (p_2) and low mass flow rate ($\dot{m}_9$). Even if, the cooler temperature is 25°C of sea water, Table 6-11 and Figure 6-14 show the thermal power recovered from lubricating oil is 37, 50, 32, 41 kW for the working fluids: R134a, R227ea, R245fa, R236fa, respectively and their values in proportional of the thermal power recovered from jacket water (There is this comparison because both of them are the sources of the low pressure stage) are 10.5, 8.6, 7.7, 6.5 % for R134a, R227ea, R245fa and R236fa, respectively

The advantages using two stage system is the possibility to recover more thermal power from the three heat sources (jacket water, lubricating oil, air cooler) than the other five configuration studied. Table 6-11 shows that heat recovery efficiencies (ϕ) are about 77% for R236fa, R134a, R227ea and 48.7% for R245fa, the highest ϕ coefficient found between the six configurations studied. Thus, the two stage ORC configuration produces the highest power: 311 kW for R134a, 302.5 kW for R227ea, 260.26 kW for R245fa and 354.13 kW for R236fa. The highest total net efficiency (η_{net}) is about 8.5% when R236fa is adopted. The total efficiencies are 7.5, 7.2, 6.2% corresponding to R134a, R227ea, R245fa, respectively (see Table 6-1). In comparison to the fifth configuration (the best solution of the previous five configurations) the relative improvement in power is 13%, 14%, 16.7% and 11.4% for fluids R134a, R227ea, R245fa and R236fa, respectively. R245fa has the maximal improvement and R236fa has the minimum advantage, but its power is still the highest.

Table 6-11 Main parameters of the sixth configuration (see Figure 6-13).

Parameter		Working fluids			
Symbol	Units	R134a	R227ea	R245fa	R236fa
$\dot{Q}_{av}$	kW	4147	4147	4147	4147
$\dot{Q}_{ca,recovered}$	kW	2677	2687	2020	2690
$\dot{Q}_{jw,recovered}$	kW	477	477	477	477
$\dot{Q}_{lo,recovered}$	kW	37	50	32	41
$\dot{Q}_{IN}$	kW	3191	3214	2529	3208
T_{a2}	°C	154.9	154.9	154.9	154.9
T_{a4}	°C	43	41.97	70	41.9
T_{w5}	°C	72	72	72	72
T_{w2}	°C	68.9	68.9	68.9	68.9
T_{lo1}	°C	49.5	49.5	49.5	49.5
T_{lo3}	°C	49.1	48.9	49.12	49.03
T_1	°C	30	30	30	30
T_2	°C	30.74	30.54	31.16	30.30
T_3	°C	30.74	30.54	31.16	30.30
T_4	°C	32.52	31.97	31.53	31.86
T_5	°C	106	122	92.82	122
T_6	°C	62	93	68	60.8
T_7	°C	62	85.9	66	60.6
T_8	°C	32.1	67	44	39.89
T_9	°C	30.74	30.54	30.54	30.30
T_{10}	°C	39.4	39.5	39.5	39.5
T_{11}	°C	62	59.86	59.6	59.74
p_{cond}	bar	7.66	5.26	1.76	3.19
p_2	bar	16.53	11.59	4.51	7.5
p_3	bar	38	28.5	10.64	30
$\dot{m}_1$	kg/s	16.25	20.18	11.21	18.57
$\dot{m}_9$	kg/s	2.75	4.21	2.44	3.2
$\dot{m}_3$	kg/s	15.97	15.97	8.77	15.37
Δs_{hl}	kJ /kg K	0.11	0.11	0	0.0088
Δs_{ll}	kJ /kg K	0	0	0	0
η_{net}	[-]	0.075	0.072	0.062	0.085
η_R	[-]	0.097	0.094	0.128	0.11
ϕ	[-]	0.77	0.77	0.487	0.77
$\dot{W}_{net}$	kW	311	302.5	260.26	354.13
Sp_1	m	0.20	0.24	0.30	0.27
Sp_2	m	0.33	0.41	0.53	0.50
v_6/v_5	-	2.69	2.93	2.50	6.83
v_8/v_7	-	2.25	2.32	2.54	2.46

High pressure Loop

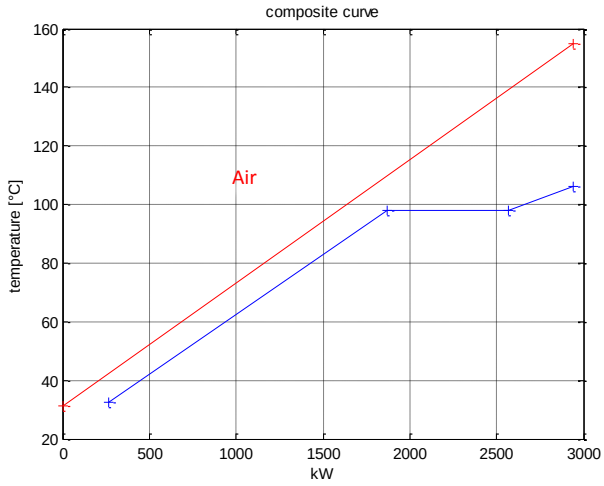

Low pressureloop

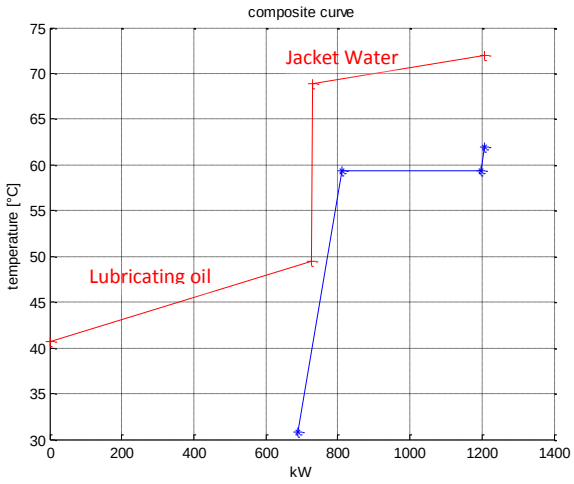

R134a

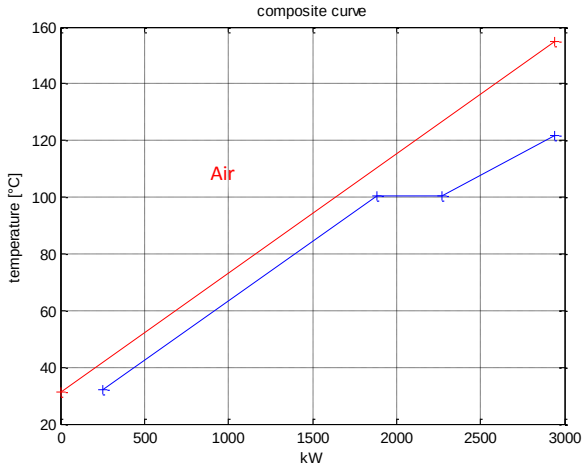

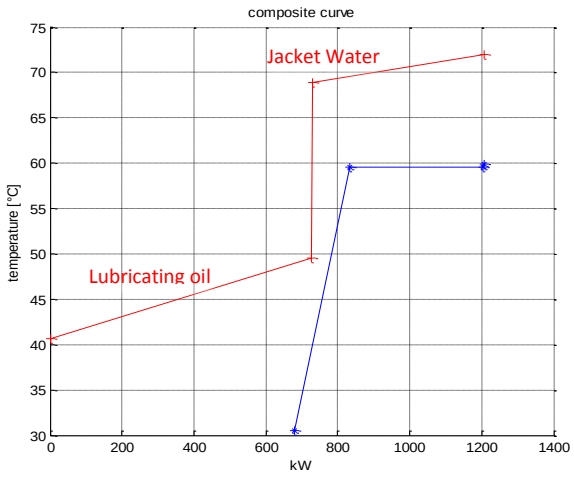

R227ea

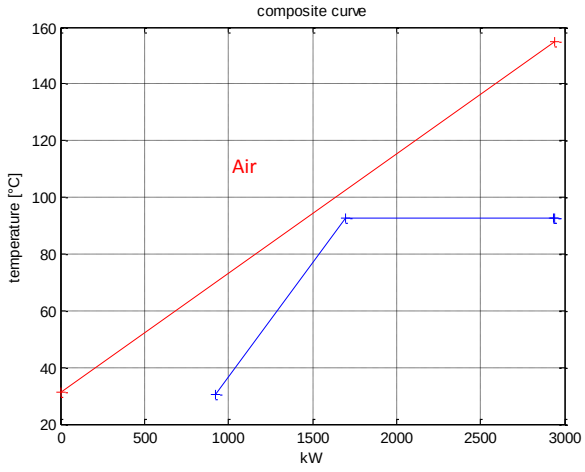

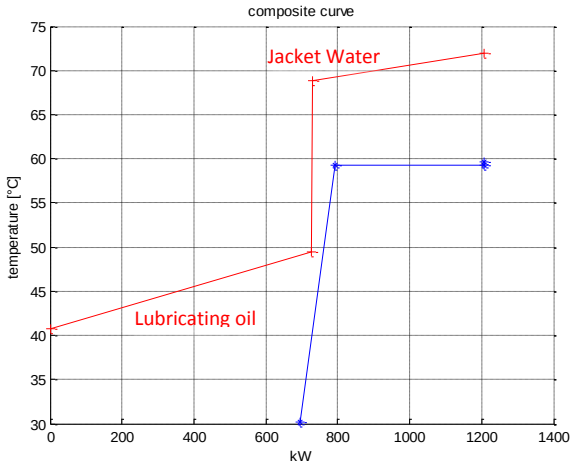

R245fa

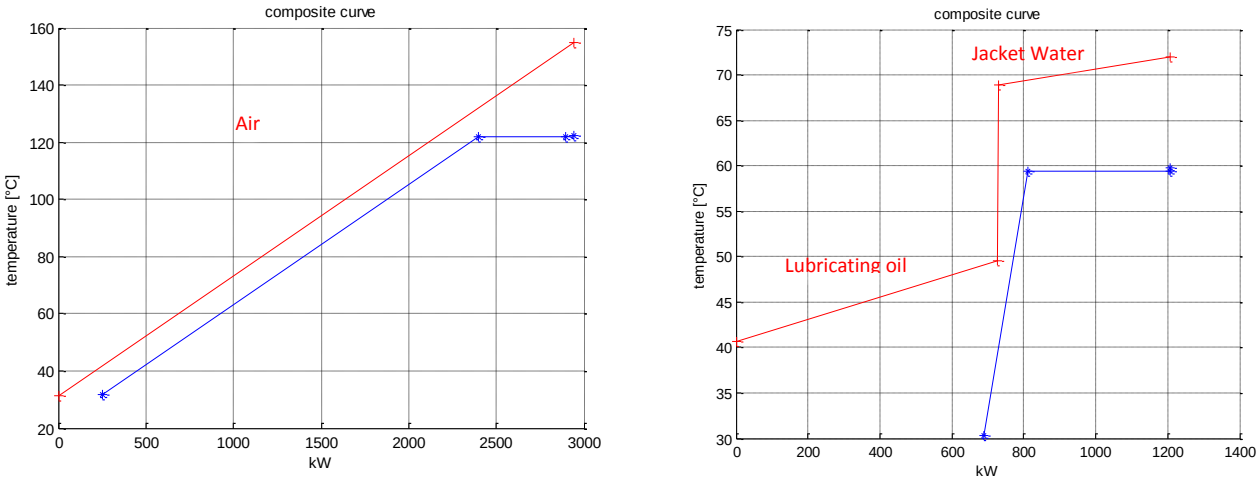

R236fa

Figure 6-14 Composite curve of sixth configuration (see Figure 6-13).

Figure 6-14 is divided in two columns and four rows. The first column represents the high pressure stage, where hot composite curve is supercharging air, and cold composite curve is the working fluid (AIR/ORC heat exchanger). The second column represents low pressure stage where hot composite curve is the combination among lubricating oil and jacket water, cold composite curve is the working fluid (from point 9 to point 11 in Figure 6-11). The four rows are the four working fluids. Each graph shows a red curve that is the HCC, a blue curve which is the cold composite curve shifted horizontally until the smaller vertical distance (pinch point) between the two composite curves is reached.

Figure 6-14 shows that the whole thermal power from jacket water is recovered. Thermal power from air cooler and from lubricating oil is recovered only in part and so they need to be cooled down from the central fresh water cooler. Moreover, Figure 6 14 shows that even if the thermal power recovered from lubricating oil is lower than the thermal powers recovered from air and jacket water, it is enough to warm up the working fluid. For example using R236fa, the temperature improvement in the Oil/ORC heat exchanger is nearly of 9°C, from 30.3°C to 39.5°C (see T_9 and T_{10} in Table 6 11). In fact the value of the mass flow rate which flows in the low pressure stage is 3.2 kg/s, strongly lower than the mass flow rate in high pressure stage (15.37 kg/s). Hence, using a low value of thermal heat in a stream of low mass flow rate, there is a great temperature improvement. In conclusion thermal power from lubricating oil is still taken into consideration because it allows to preheat the working fluid of 9°C.

6.9. Conclusion

In this chapter an evaluation of ORC systems is described. Engine load of 80% was considered as the design point for all ORC systems being considered. Several configurations were investigated: five simple Rankine cycles, a regenerated system, and a two-stages of ORC.

At first an ORC system was evaluated using the Hot Composite Curve at 80% of engine load. This is an “ideal configuration” because the task to define the heat exchanger network is not taken into consideration and the maximum output power is estimated.

The first proposed configuration is similar to the cycle proposed by Yue et al. (2012), with three sources: air cooler, jacket water and lubricating oil and with two different condenser sources, sea water at 25°C and fresh water from the cooling system at 36°C.

The second configuration is a simple ORC with two heat sources (air cooler and jacket water), and the condenser source is fresh water from the cooling system. It was decided to investigate this system, because from the first configuration, when the fresh water was used in the condenser, the maximum output power was obtained without the lubricating oil heat. The second and third configurations have the same hot utility (supercharging air and jacket water) and fresh water in the condenser, but in the third configuration it is studied a regenerative ORC system. A condenser with fresh water at 36°C does not allow energy recovery from vapor outside of the expansion because the difference temperature between the output of turbine and the output of the pump is too low to have an heat exchange (see Table 6-8). On the other hand, a condenser with sea water at 25°C allows to energy recovery from lubricating oil because the oil temperature range is within 49.5°C and 42.7°C and the power obtained from this different temperatures can be used to warm up the working fluid. Thus, the fourth configuration has the three hot utilities (jacket water, lubricating oil, supercharging air), and sea wateris adopted in the condenser. The fourth configuration needs several heat exchangers: three preaheater, one evaporator and one superheater for the simple cycle (see R236fa example in section 6.6). The fifth configuration was proposed to avoid this problem. Air cooler thermal power is considered as the only one hot utility, so that only three heat exchangers are required. The results of fifth configuration are close to the results of the fourth configuration. This configuration suggests the possibility to have more power realizing a dual stage system.

The sixth configuration proposes a two stage ORC system and sea water as a cold utility. Supercharging air is the source of the high pressure stage and jacket water plus lubricating oil are the heat sources of the low pressure stage.

In the first configuration, using fresh water as a cold utility the output powers ($\dot{W}_{net}$) are 140, 136, 134.8, 112 kW for R227ea, R236fa, R134a, R245fa but using sea water as a cold utility, powers output ($\dot{W}_{net}$) are 180, 187.5, 182 for R236fa, R134a,

R245fa, respectively. It appears that a higher pressure ratio leads to a higher output power. Thus, a lower condenser pressure (a lower condenser temperature) is preferred. The power output of the first configuration is lower than the power output of the other configurations (see Table 6-12). The effect of using jacket water as heat transfer medium between air cooler and working fluid introduces further irreversibility that causes a reduction in efficiency and in output power.

In the second configuration the powers output ($\dot{W}_{net}$) are 252, 217.22, 200, 175.84 for R236fa, R134a, R227ea, R245fa, respectively. The powers in second configuration is higher than the first configuration because there is not jacket water as heat transfer medium between air cooler and working fluids.

In the third configuration, the output powers are 246, 217.16, 202, 177 kW for R236fa, R134a, R227ea, R245fa, respectively. If these output powers are compared to the output powers of the second configuration, there are a slight improvements for R227ea (from 200 kW to 202 kW) and for R245fa (from 175.84 kW to 177 kW) but there is a worsening using R236fa (from 252 kW to 246 kW) and using R134a (from 217.22 kW to 217.16 kW). Thus, using a recuperator, there is not a great improvement.

In the fourth configuration the maximal output power is 311 kW with R236fa. Output powers ($\dot{W}_{net}$) are 278.9, 259, 223 kW for R134a, R227ea, R245fa, respectively. The powers are higher than the previous four configurations because the fourth configuration recovers heat from three sources (jacket water, air cooler, lubricating oil) and at the same time it uses sea water in the condenser.

In the fifth configuration, the maximum power output is 317.8 kW when R236fa is adopted. The output powers ($\dot{W}_{net}$) are 273.83, 266, 223 kW for R134a, R227ea, R245fa, respectively. Using only the air cooler heat exchanger the output powers are compared to the results of the fourth configuration. The power output decrease of 2.7% and 1.9% for working fluids R227ea and R236fa, respectively and for the other two working fluids (R245fa, R134a) the output power values are unchanged.

Out of the six configurations, the sixth one generates the maximal powers: 311 kW for R134a, 302.5 kW for R227ea, 260.26 kW for R245fa and 354.13 kW for R236fa. The difference in terms of power if compared to the fifth configuration is 13% with R134a, 14% with R227ea, 16.7% with R245fa, and 11.4% with R236fa. So, R245fa gives the highest improvement compared to the fifth configuration and R236fa gives the lowest, but still the best fluid for the sixth configuration among the working fluids taken into consideration in this work is R236fa.

Table 6-12 shows the output power ($\dot{W}_{net}$) for all the configurations.

Table 6-12 Powers result of the six configuration.

Power	T_{cond}	Working fluids			
[kW]	**[°C]**	**R134a**	**R227ea**	**R245fa**	**R236fa**
First configuration	25	187	193	182	188
	36	134.8	140	112	136
Second configuration	36	217	200	175	252
Third cobnfiguration	36	217	202	177	246
Fourth configuration	25	278	259	223	311
Fifth configuration	25	274	266	223	317
Sixth configuration	25	311	302	260	354

7. Output Power Evaluation of the ORC Systems at 70% and 55% of the Engine Load

7.1. Introduction

In Chapter 6, six configurations and four working fluids are studied. Considering the design point at 80% of the engine load, the best configuration and the best working fluids are determined. The dual stage system and the working fluid R236fa reach the maximum power output (Optimization function of this study). In Section 3.4, three main operating loads are mentioned (80%, 70% and 55% engine load). The task of this chapter is to find the maximum output power for the other two operating loads (70% and 55%) using dual stage system and R236fa as working fluid.

7.2. Model and Results

An approximate evaluation of the maximum output power at 70% and 55% of the engine load is carried out, without using a detailed off-design ORC model. The model (see Figure 7-1) and the assumptions are those described in the Section 6.8 and Section 5.2.

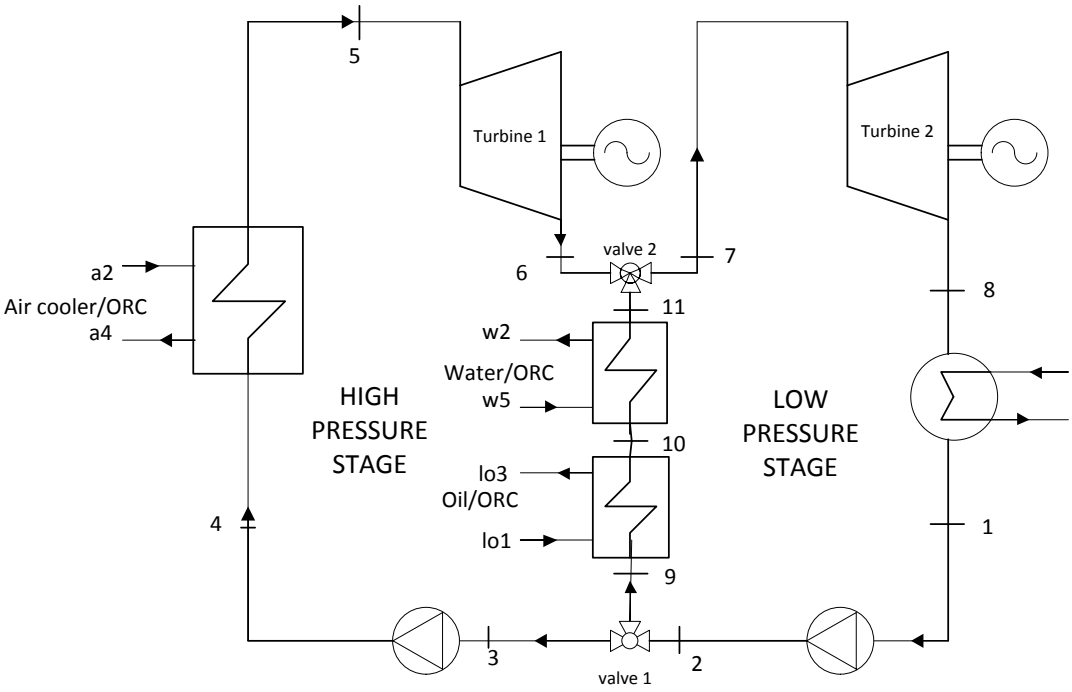

Figure 7-1 Two stage ORC system.

Mass flow rate and pressure are supposed variable and efficiency of pumps and turbines are kept constant. Two more constraints are included in these simulations. Mass flow rate and pressure of both stages cannot reach higher values than those at 80% of the engine load.

The minimum approach temperature is set at 10°C in the evaporator and 5°C in the condenser in accordance with Lakew and Bolland (2010). Seawater at 25°C (ISO condition) is adopted as a cooling medium in the condenser. The values of the three hot utilities are 2402 kW from the air cooler, 693 kW from lubricating oil and 415 kW from jacket water at 70% of the main engine load. At 55% main engine load the thermal powers are 1598 kW, 241 kW, 627 kW from air cooler, jacket water and lubricating oil, respectively. The amount of heat available at 70% of the engine load is 3510 kW, whereas at 55% engine load is 2466 kW.

Table 7-1 summarizes the main parameters described in Figure 6-13. At 70% engine load, output power ($\dot{W}_{net}$) is equal to 182.44 kW and the net efficiency system (η_{net}) is equal to 5.2%. At 55% engine load, output power ($\dot{W}_{net}$) is equal to 75 kW and the net efficiency system (η_{net}) is equal to 3%.

From Table 7-1 and Table 6-11, it is possible to see that in the high pressure stage the evaporation pressure varies in a wide range from 30 bar (80% engine load) to 8.65 bar (55% engine load), while in the low pressure stage the evaporation pressure is lower from 7.5 bar (80% engine load) to 6.53 bar (55% engine load). These two different pressure ranges can be explained with the fact that jacket water and lubricating oil do not vary much in the different engine loads, but the power of the air cooler is reduced by 55% at 55% engine load, decreasing the performance of the high pressure stage and consequently of the ORC.

Figure 7-2 is divided in two rows and two columns. Rows depict engine loads, first row 70% engine load, second row 55% engine load. First column represents high pressure stage where hot composite curve is supercharging air, and cold composite curve is the working fluid (AIR/ORC heat exchanger in Figure 7-1). Second column represents low pressure stage where hot composite curve is the combination among lubricating oil and jacket water, cold composite curve is the working fluid (from point 9 to point 11 in Figure 7-1). Each graph shows a red curve that is the HCC, a blue curve which is the cold composite curve shifted horizontally until the smaller vertical distance (pinch point) between the two composite curves is reached.

Table 7-1 Results of 70% and 55% Engine load.

Parameter		Working fluid R236fa	
Symbol	Units	70 Engine Load	55 Engine Load
$\dot{Q}_{av}$	kW	3510	2466
$\dot{Q}_{ca,recovered}$	kW	1625	879
$\dot{Q}_{jw,recovered}$	kW	415	241
$\dot{Q}_{lo,recovered}$	kW	36	17
$\dot{Q}_{IN}$	kW	2076	1137
T_{a2}	°C	136.3	106.7
T_{a4}	°C	64.47	62
T_{w5}	°C	70	66
T_{w2}	°C	67	64
T_{lo1}	°C	49.5	49.6
T_{lo3}	°C	49.2	49.4
T_1	°C	30.3	30
T_2	°C	30.3	30.2
T_3	°C	30.7	30.2
T_4	°C	30.7	30.4
T_5	°C	84.8	65
T_6	°C	64.3	57
T_7	°C	62	56
T_8	°C	43.8	39.7
T_9	°C	30.3	30.2
T_{10}	°C	39	37.5
T_{11}	°C	57.5	54.2
p_{cond}	bar	3.19	3.19
p_2	bar	7.12	6.53
p_3	bar	13.81	8.65
$\dot{m}_1$	kg/s	12.10	6.96
$\dot{m}_9$	kg/s	2.81	1.63
$\dot{m}_3$	kg/s	9.29	5.33
Δs_{hl}	kJ /kg K	0	0
Δs_{ll}	kJ /kg K	0	0
η_{net}	[-]	0.052	0.03
η_R	[-]	0.087	0.065
ϕ	[-]	0.46	0.46
$\dot{W}_{net}$	kW	182.44	75
Sp_1	m	0.25	0.24
Sp_2	m	0.41	0.32
v_6/v_5	-	2.17	1.36
v_8/v_7	-	2.31	2.11

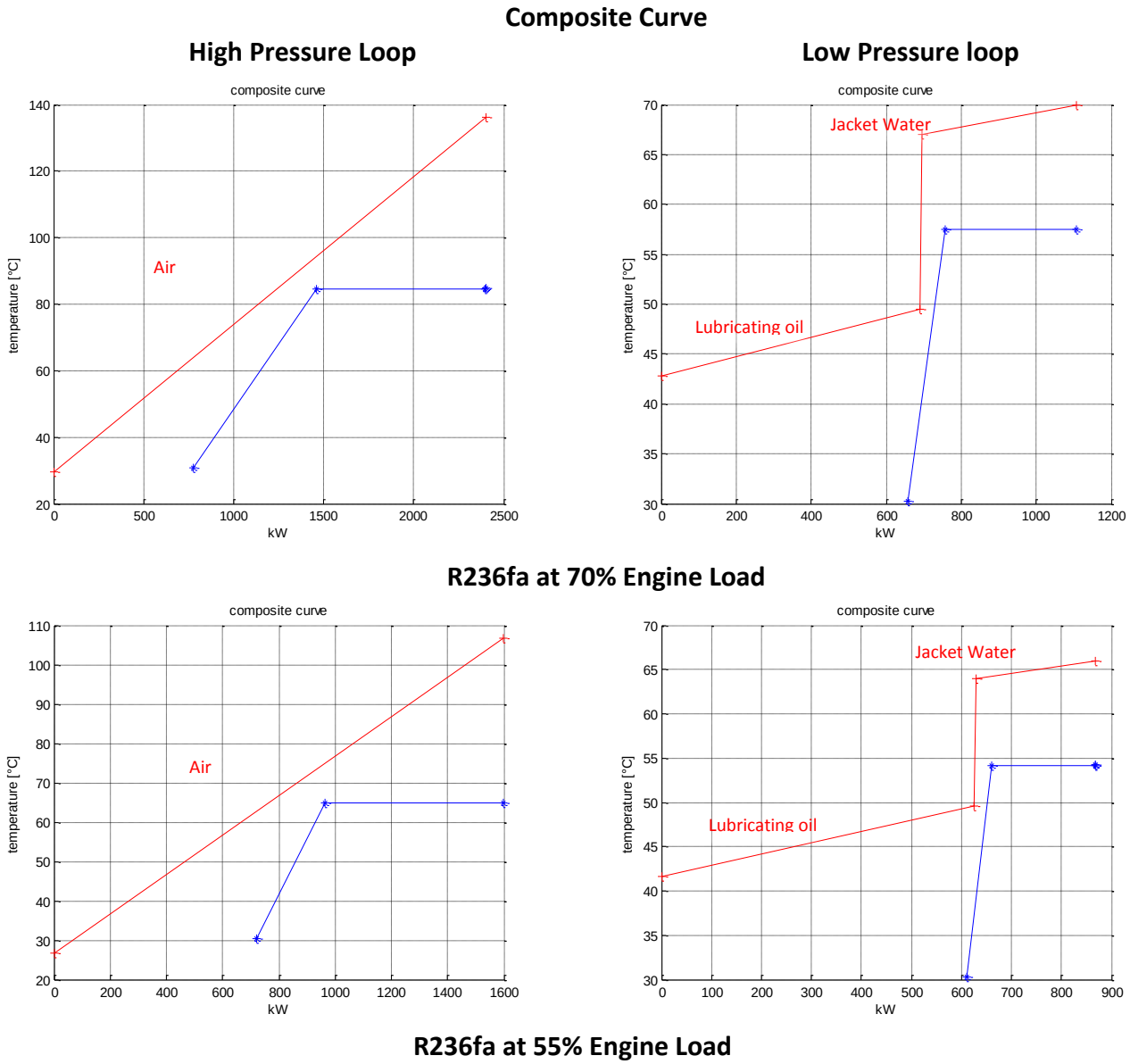

Figure 7-2 Composite Curve of R236fa at 70% and 55% Engine Load.

As previous states, in the high pressure stage, the evaporation pressure varies in a wide range (on varying the engine load) and in the low pressure stage the evaporation pressure is almost constant. This change is shown in Figure 7-2 as well, but it appears in the form of temperature. The value of maximum temperature reached in the high pressure stage is 84.8°C at 70% engine load, and 65°C at 55% engine load. Instead the maximum temperature reached in the low pressure stage is 57.5°C at 70% engine load and 54.2°C at 55% engine load (almost the same).

8. Annual Energy Savings

8.1. Introduction

In Chapter 6, dual stage ORC system and R236fa are found out as the best choices, among the configurations and working fluids taken into consideration. Moreover, the output power ($\dot{W}_{net}$) at design point (80% engine load) is evaluated (354 kW). In chapter 7, the maximum output powers for the other two operating loads (70 and 55% engine load) are evaluated. At 70% engine load, output power is equal to 182.44 kW and at 55% engine load is 75 kW. After that the output power for each operating load is known and the operating profile is given in Section 3.4. Thus the amount of energy recovered could be calculated during one year.

8.2. Calculation of Annual Energy Savings

The total power output that would be produced during one year has been calculated. It has been defined by a dual stage system, with R236fa as working fluid and for three main operating loads (80%, 70% and 55% engine load). To get a preliminary estimate of the annual energy savings, the formula below is used:

$$E_y = \sum_{i=1}^{j} n_{h,i} \dot{W}_{net,i} \tag{8.1}$$

where:

j=3 Number of operating loads (80%, 70%, 55%).
n_h= Number of hours at each operating load.
$\dot{W}_{net}$ Maximal power output at each operating load [kW].
E_y Saved energy during one year with ORC [kWh].

The following Table 8-1 shows the maximal power output for own operating load.

Table 8-1 Duration and Power output for every operating profile.

	Engine Load	n_h	$\dot{W}_{net}$
	%	h	kW
1	80	3039	354.13
2	70	2752	182.44
3	55	482	75

After this information (Table 8-1 and Eq(8.1)), the value of annual energy savings (E_y) is 1614 MWh per year, as given by Eq.(8.2):

$$E_y = 3039 \cdot 354.13 + 2752 \cdot 182.44 + 482 \cdot 75 = 1614\ MWh \tag{8.2}$$

The average power during a year is:

$$\dot{W}_{net,c} = \frac{E_y}{n_T} \tag{8.3}$$

where:

n_T Total hours number of the operating main engine (6273 h).
$\dot{W}_{net,c}$ ORC Power output if ORC operates at constant power.

$\dot{W}_{net,c}$ is equal to 257 kW, that means 72% of the ORC design power. The electricity on board is supplied by three Diesel generator sets. The type of all Diesel generators is L23/30H of the MAN B &W. One of them works during the "voyage", the second works only during the cargo unloading (the ship needs more electric power for the operation) and the third is on reserve. The specific fuel consumption is 191.3 g/kWh in reference condition (ISO 3046) for the diesel generator sets. Under this assumption (the specific fuel consumption) and with the annual energy savings, a saving of 308.7 tons of fuel (Marine Diesel oil) per year is achieved, as derived by the following equation

$$F_s = E_y \cdot b_f = 1614\ [MWh] \cdot 191.3\ \left[\frac{kg}{MWh}\right] = 308.7\ tons \tag{8.4}$$

where:

F_s fuel savings.
E_y annual energy savings.
b_f specific fuel consumption of the engine generator sets (191.3 g/kWh).

9. Economic Feasibility

9.1. Introduction

The two stage ORC system is analyzed from an economic point of view. During one year the energy savings is 1614 MWh (using dual stage system and R236fa as working fluid) and 308.7 tons of fuel (Marine Diesel Oil) are saved, see Chapter 8. The economic feasibility of the two stage ORC system is assessed by three parameters: Net Present Value (NPV), Dynamic Payback Period (DPP) and Internal Rate of Return (IRR). In Chapter 9, at first Economic Feasibility model is explained and then it will be used for the configuration chosen in Chapter 6.

9.2. Parameters of Economic Feasibility

NPV (net present value) is defined as the sum of discounted cash inflows and outflows, in order to compare the present value of an investment to the value of saving that will be obtained in well-defined period. NPV is describe by Eq. (9.1):

$$NPV = \sum_{i=0}^{n_y} \frac{F_i}{(1+a_i)^i} \tag{9.1}$$

where

i	considered year
F_i	net annual cash flow for year i
a	market discount rate
n_y	economic analysis period

The net annual cash flow rate for the year *I (*F_i) is given by Eq. (9.2) and Eq. (9.3):

$$F_i = -C \quad (\text{first year } i=0) \tag{9.2}$$

$$F_i = C_{fs,i} - C_{om,i} \quad (i=1,2\ldots n_y) \tag{9.3}$$

$$C_{om,i} = C_{om,ORC,i} - C_{om,EG,I} \quad (i=1,2\ldots n_y) \tag{9.4}$$

$$C_{fs,i} = E_{y,i} \cdot b_f \cdot c_{f,i} \tag{9.5}$$

where

C	initial investment
$C_{fs,i}$	cost of fuel saved
$C_{om,ORC,i}$	cost of operating and maintenance of the ORC

$C_{om,EG,i}$ savings of operation and maintenance of the diesel-generator sets
C_{om} sum of operating and maintenance cost between the ORC and the Diesel-generator sets
E_y energy saved
b_f specific fuel energy consumption of the engine-generator sets
c_f unit cost of the fuel

The energy annual saving (E_y) and the cost of the fuel (c_f) are considered constant so the Eq. (9.1) can be rewrite:

$$NPV = F_0 + F_1 \cdot \sum_{i=0}^{n_y} \frac{1}{(1+a_i)^i} \tag{9.6}$$

Also the market discount rate (a) is considered constant during the period studied. Based on this, Eq. (9.6) can be reedited in this form:

$$NPV = F_0 + F_1 \cdot \frac{1-(1+a)^{-n_y}}{a} \tag{9.7}$$

Dynamic Payback Period (DPP), which is defined by the Eq. (9.8) evaluates how long a given ORC system will pay for itself.

$$NPV = F_0 + F_1 \cdot \frac{1-(1+a)^{-DPP}}{a} = 0 \tag{9.8}$$

Under the specific assumptions (market discount rate, cost of the fuel, annual saving are considered constant), DPP is evaluated by Eq. (9.9).

$$DPP = \frac{-\ln(1+a\frac{F_0}{F_1})}{\ln(1+a)} \tag{9.9}$$

If it is:

$$1 + a\frac{F_0}{F_1} < 0 \tag{9.10}$$

Eq. (9.9) does not have a solution, and the configuration considered will require an infinitive number of years, in order to recover the initial investment.

The internal rate of return (IRR) is the interest that makes the Net Present Value equal to zero at the end of the period studied:

$$NPV = 0 = F_0 + F_1 \cdot \frac{1-(1+IRR)^{-n_y}}{IRR} \tag{9.11}$$

$$-F_0 = F_1 \cdot \frac{1-(1+IRR)^{-n_y}}{IRR} \quad (9.12)$$

$$C = F_1 \cdot \frac{1-(1+IRR)^{-n_y}}{IRR} \quad (9.13)$$

Thus IRR is given by Eq. (9.13).

9.3. Economic Feasibility of dual Stage ORC

The model described in Section 9.2 is used on the dual stage ORC. The energy annual saving (E_y) and the cost of the fuel (c_f) are considered constant. The initial investment (C) is considered proportional to the maximal net power of the system. The range of the initial investment is chosen from 2000 US$/kW to 8000 US$/kW. The value C_{om} (sum of the operation and maintenance cost of the ORC and diesel-generator sets) is considered proportional to the MWh produced by ORC system in the first year, moreover C_{om} is kept constant during the whole period taken into account (20 years). The specific fuel consumption (b_f) is 191.3 g/kWh in reference condition (ISO 3046) for the diesel generators. The range of the Marine Diesel Oil is chosen between 500 US$/ton and 1000 US$/ton.

These assumptions for the calculations are reported in Table 9-1.

Table 9-1 Values of the parameters for the economic analysis.

Parameter		Value
Symbol	**Units**	**[-]**
n_y	**years**	20
a	**%**	8
b_f	**g/kWh**	191.3
$\dot{W}$	**kW**	354.13
E_y	**kWh**	1614
C_{om}	**US$/MWh**	3
c_f	**US$**	500-1000

The results are summarized in the following table and graphs.

Table 9-2 is divided in two parts: on the top the initial investment is presented, and on the bottom the net present value (NPV) is calculated as a function of the initial investment and of the fuel cost. In the white cells the investment can be economically attractive. In the cells with a pink background the investment is not profitable, because the NPV value is negative and with those two conditions (fuel cost and initial investment), the ORC system will not pay for itself. Table 9-3 shows the dynamic payback period as a function of the initial investment and of the fuel cost. In the white cells the investment can be profitable, and in the pink cells the dynamic payback period is longer than twenty years (period of the economic analysis). In the red boxes, Eq. (9.9) does not have a solution because the argument of the logarithm is not positive number. The meaning is that, if the market discount is considered 0.08 (assumption of this study), the configuration will never recover the initial investment under the specific data. In order to recover the initial investment, the market discount has to be lower than the market discount considered in the study. Table 9-4 reports the internal rate of return (the interest that makes the Net Present Value equal to zero at the end of the period studied) as a function of the fuel cost and initial investment. Under the same specific data of the red boxes in Table 9-3, the internal rate of return is lower than the market discount considered (8%). Moreover, net present value, payback period, internal rate of return are described in Figure 9-1, Figure 9-2 and Figure 9-3, respectively as functions of the fuel cost and of the specific cost of the initial investment. In the graphs, the x-axis are the initial investment, the ordinate represents NPV in Figure 9-1, dynamic Payback period in Figure 9-2, and internal rate of return in Figure 9-3. Moreover in each graph there are five curves, each one considers a different fuel (Marine Diesel Oil) cost from 500 to 1000 US$/ton.

Table 9-2 Initial Investment and Net Present Value.

Initial Investment							
US$/kW	2.000	3.000	4.000	5.000	6.000	7.000	8.000
US$	708.260	1.062.390	1.416.520	1.770.650	2.124.780	2.478.910	2.833.040
Fuel cost [US$/ton]	**Net Present Value (NPV) [US$]**						
500	759.917	405.787	51.657	-302.473	-656.603	-1.010.733	-1.364.863
600	1.063.061	708.931	354.801	671	-353.459	-707.589	-1.061.719
700	1.366.204	1.012.074	657.944	303.814	-50.316	-404.446	-758.576
800	1.669.347	1.315.217	961.087	606.957	252.827	-101.303	-455.433
1000	2.275.634	1.921.504	1.567.374	1.213.244	859.114	504.984	150.854

Table 9-3 Payback period as a function of the fuel cost and of the specific cost of the initial investment.

PayBack Period (PP)	Initial Investment [US$/kW]						
Fuel cost [US$/ton]	**2.000**	**3.000**	**4.000**	**5.000**	**6.000**	**7.000**	**8.000**
500	6	11	18	38	-	-	-
600	5	8	13	19	37	-	-
700	4	7	10	14	21	36	-
800	3	6	8	11	16	22	36
1000	3	4	6	8	11	14	18

Table 9-4 Internal rate of return as a function of the fuel cost and of the specific cost of the initial investment.

Internal rate of return (IRR)	Initial Investment [US$/kW]						
Fuel cost [US$/ton]	**2.000**	**3.000**	**4.000**	**5.000**	**6.000**	**7.000**	**8.000**
500	20,6	12,8	8,5	5,6	3,5	1,8	0
600	25,2	16,5	11,2	8	5,6	3,8	2,4
700	29,7	19,3	13,7	10,2	7,6	5,7	4,1
800	34,1	22,4	16,2	12,3	9,5	7,4	5,7
1000	42,9	28,4	20,9	16,3	13	10,6	8,7

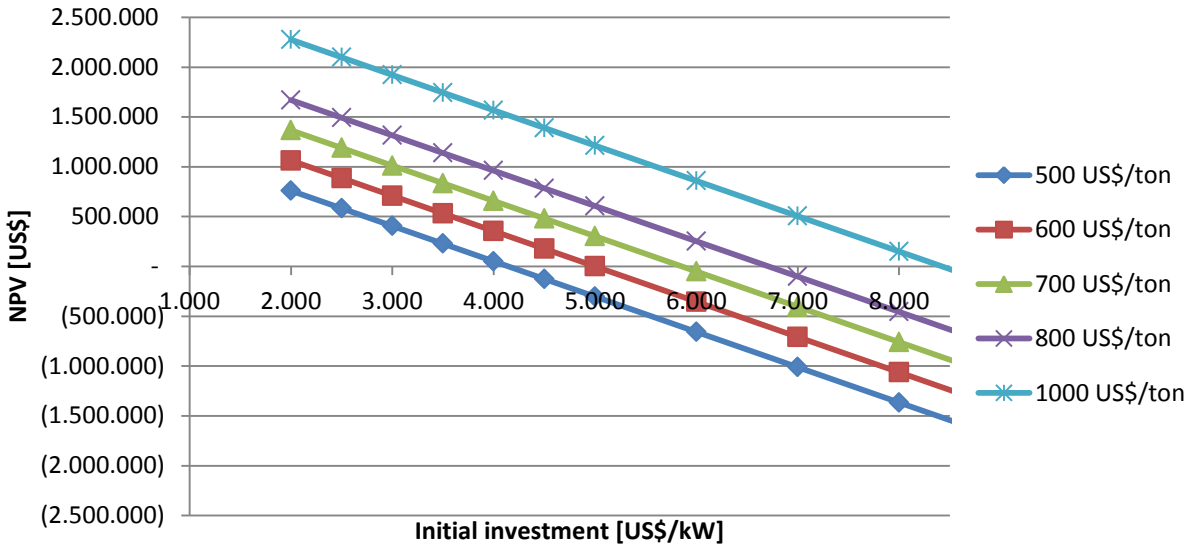

Figure 9-1 Net Present Value as a function of the fuel cost and of the specific cost of the initial investment.

Figure 9-1 shows that the value of NPV is high when low values of the initial investment and high values of the marine diesel oil cost, thus the dual stage system is profitable. On the other hand, high values of initial investment and low values of marine diesel oil cost point out the system is uneconomical.

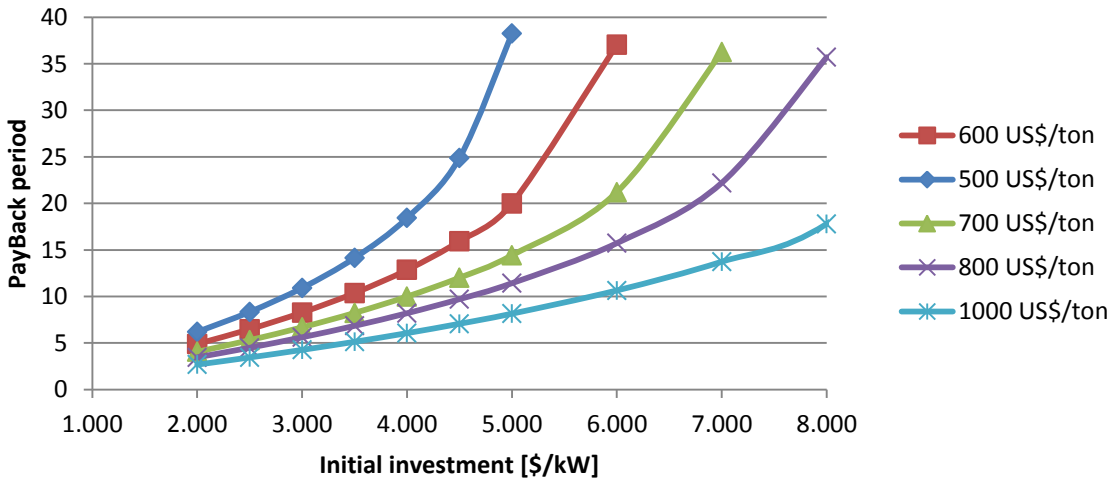

Figure 9-2 Dynamic Payback Period as a function of the fuel cost and of the specific cost of the initial investment.

Figure 9-2 shows if the marine diesel oil cost is considered constant (same curve), the value of Dynamic Payback Period increases when the value of initial investment becomes higher, then the dual stage system will never pay for itself. For example, the dynamic payback period reaches values of 100 years when the value of marine diesel oil is equal to 500 US$/ton, and the value of initial investment is 6000 US$/ton.

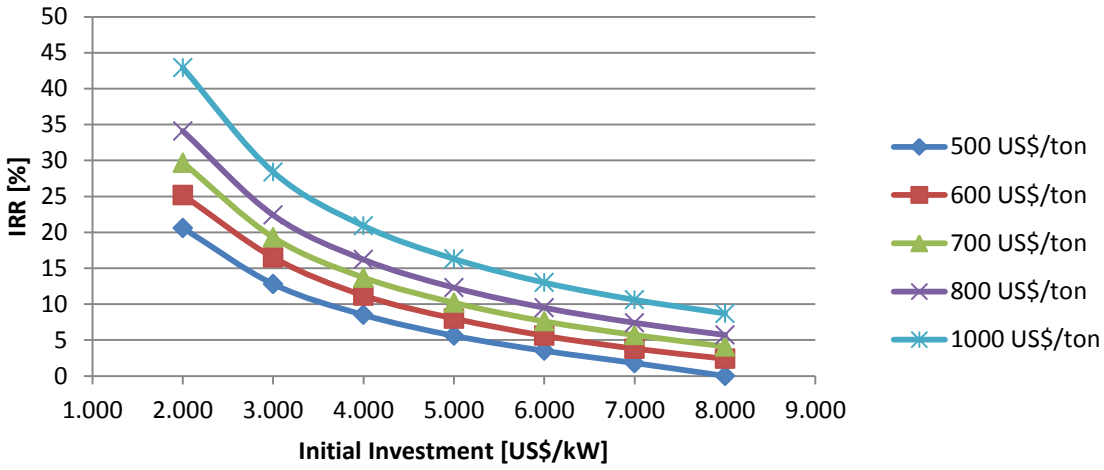

Figure 9-3 Internal rate of the return as a function of the fuel cost and of a specific cost of the initial investment.

In Figure 9-3, the value of internal rate of return (IRR) is nearly zero when the value of initial investment is high. On the other hand, IRR reaches high values when value of fuel cost is high, and initial investment is low.

9.4. Conclusion

In Chapter 7, the maximal power is found out for 70% and 55% of the engine load, using a dual stage ORC system and R236fa as a working fluid. In Chapter 8, using the output power and the duration for each operating load (see Table 8-1), the annual energy saving was calculated (1614 MWh per year).

An economic analysis is performed with three parameters: net present value (NPV), dynamic payback period (DPP) and internal rate return (IRR). They are functions of the initial investment and of the fuel cost (Marine Diesel Oil). The initial investment is considered proportional to the design power of the system (354.13 kW), the range is chosen from 2000 US$/kW to 8000 US$/kW. The fuel cost varies between 500 US$/ton and 1000 US$/ton. The operating and maintained cost of the ORC and the diesel generator sets are constant. The difference of them is proportional to the electric energy produced in the year (3 US$/MWh) see Eq. (9.4).

The results show that a high value of the initial investment and a low value of the fuel cost, lead to a negative value of NPV, to a value of dynamic payback period higher than 20 years (reference period of the analysis investment) and to a low value of IRR. On the other hand, a low initial investment and a high cost of fuel mean high value of NPV, low dynamic payback period and high IRR (see Figure 9-1 to 9-3). For example, if the specific value of the initial investment is 4000 US$/kWh (initial investment is 1.416.520 US$ see Table 9-2) and the fuel cost is 700 US$/ton, the value of NPV is 657.944 US$ (see

Table 9-3Table 9-2), the dynamic payback period is equal to 10 years (see Table 9-3), and the IRR is equal to 13.7% (see Table 9-4).

10. Conclusion

In the present study, heat recovery power generation system applied to the cooling system of the main engine of a tanker ship was investigated. In the literature review, R227ea, R134a, R245fa, R236fa are supposed to be the best working fluids for this project. In chapter 3, the energy balance is evaluated. Air cooler, jacket water, lubricating oil heats are available for ORC cycle. Waste heat from exhaust gas is already recovered by the exhaust gas boiler. The energy balance is evaluated for the three main operating loads: 80%, 70% and 55% of the main engine (see Table 3-8). The hot composite curves for each operating load are built in Chapter 4 (see Figure 4-2). The operating load at 80% of the main engine is chosen as a design point for the ORC system. Several configurations were studied in Chapter 6.

At first a simple ORC system was evaluated, using the HCC at 80% engine load. Note that, according to this approach, the heat exchanger network within the ORC system remains undefined and can be found by applying Pinch Analysis rules. Two cold utilities in the condenser are compared, sea water at 25°C and fresh water from cooling system at 36°C.Using the sea water at 25°C as cooling medium in the condenser, the maximum power output (323 kW) is achieved by R236fa. The Power output values for the remaining fluids are 280.5, 280.13, 225 kW for R134a, R227ea, R245fa, respectively. Using fresh water at 36°C as cooling medium in the condenser, the maximum power output achievable is 255kW using R236fa. The power output values for the remaining fluids are 221, 209, 181 kW for R134a, R227ea, R245fa, respectively. The use of sea water for condenser cooling results in lower condensation temperatures, and consequently lower condensation pressures. The turbine operates with higher pressure ratios and it produces more power for the same mass flow rate .

The first proposed configuration recovers heat from the three heat source: supercharging air, jacket water, lubricating oil but it does not consider heat exchange between air cooler and working fluid. Jacket water is used as heat transfer medium between air cooler and working fluid. Thus working fluid exchanges heat with jacket water and lubricating oil in a simple Rankine cycle. Also in this configuration two cold utilities in the condenser are compared (sea water and fresh water). Using sea water as cooling medium in the condenser, the maximum output power is about 193 kW, achieved by R227ea. The power output for the remaining fluids is 180, 187.5, 182 for R236fa, R134a, R245fa, respectively. Using fresh water at 36°C, the maximum power output is 140kW adopting R227ea and the output powers for the remaining fluids are 136, 134.8, 112 kW for R236fa, R134a, R245fa. These results clearly show that using this

configuration the power output of all working fluids is strongly reduced. This eventuality is described by the fact that input thermal power of the simple ORC system is low, because Jack water is used as heat transfer between air cooler and working fluid, and the temperature of the jacket water is kept low to avoid steam in the pipes.

The second configuration is a simple ORC with two heat sources (from air cooler and jacket water), and fresh water as cooling medium in the condenser. It was decided to investigate this system, because from the first configuration, when the fresh water was used in the condenser, the maximum output power was obtained without the lubricating oil heat. In the second configuration the power output values are 252, 217.22, 200, 175.84 for R236fa, R134a, R227ea, R245fa, respectively. In second configuration the power is higher than in the first configuration because there is not jacket water as heat transfer medium between air cooler and working fluids.

The third configuration is a regenerated ORC system with two heat sources (from air cooler and jacket water) and fresh water (36°C) as cold utility. The output power values are 246, 217.16, 202, 177 kW for R236fa, R134a, R227ea, R245fa, respectively. If these output powers are compared to the output power values of the second configuration, there is a slight improvement for R227ea (from 200 kW to 202 kW) and for R245fa (from 175.84 kW to 177 kW) but there is a worsening using R236fa (from 252 kW to 246 kW) and using R134a (from 217.22 kW to 217.16 kW). Thus, using a recuperator, there is not a great improvement. A condenser with fresh water at 36°C does not allow energy recovery from vapor after the expansion because the difference of temperature between the output of the turbine and the output of the pump is too low to have an heat exchange. On the other hand, a condenser with sea water at 25°C allows energy recovery from lubricating oil because the oil temperature range is within 49.5°C and 42.7°C and the power obtained from this temperature difference can be used to warm up the working fluid.

Thus, the fourth configuration recovers heat from the three hot utilities, and sea water is adopted as cold utility in the condenser. Maximal output power is 311 kW reached by R236fa. Output powers for the remaining fluids are 278.9, 259, 223 kW for R134a, R227ea, R245fa, respectively. The powers are higher than the previous configurations because the fourth configuration recovers heat from the three sources and at the same time it uses sea water in the condenser. The fact that the surface has to be cleaned regularly to avoid deposition of salts and corrosion and the need for a clever selection of materials (no copper alloys can be used) represent two disadvantages of sea water cooling. On the other hand, if the increase of net power output can cover the cleaning cost of the heat exchanger, this solution is convenient.

The fifth configuration explores the possibility to recover energy only from air cooler, and sea water is used as cooling medium in the condenser. The maximum power output is 317.8 kW achieved by R236fa. The output powers for the remaining fluids are 273.83, 266, 223 kW for R134a, R227ea, R245fa, respectively. Using only the thermal

power from supercharging air the output powers are close to the results obtained from the fourth configuration, even if jacket water and lubricating oil sources are still available.

Thus the sixth configuration proposes a two stage ORC system and sea water as a cooling medium in the condenser. Supercharging air is the source of the high pressure stage. Jacket water plus lubricating oil are the heat sources of the low pressure stage. Out of the six configurations, the sixth one generates the maximal powers: 311 kW for R134a, 302.5 kW for R227ea, 260.26 kW for R245fa and 354.13 kW for R236fa. If compared to the fifth configuration, the improvement in terms of power is 13% with R134a, 14% with R227ea, 16.7% with R245fa, and 11.4% with R236fa. So, R245fa gives the highest improvement compared to the fifth configuration and R236fa gives the lowest, but R236fa is still the best fluid for the sixth configuration among the working fluids taken into consideration in this work.

The dual stage ORC system with R236fa as a working fluid leads the maximum net power output (354.13 kW); the thermodynamic properties are listed in (Table 6-11). Using the same configuration and the same working fluid the net power outputs are 182.44 kW and 75 kW for 70% and 55% of the engine load, respectively. These powers are found without a detailed off-design ORC model. The annual energy saving was calculated (1614 MWh per year), and it leads to 308 tons of marine diesel oil saved (Section 8.2) using the output power and the duration for each operating load (see Table 8-1),

An economic analysis is performed with three parameters: net present value (NPV), dynamic payback period (DPP) and internal rate return (IRR). They are functions of the initial investment and of the fuel cost (Marine Diesel Oil). The initial investment is considered proportional to the design power of the system and the range is chosen from 2000 US$/kW to 8000 US$/kW. The fuel cost varies between 500 US$/ton and 1000 US$/ton. The sum of operating and maintenance cost of the ORC and the diesel generator sets are considered constant. The difference of them (see Eq. (9.4)) is proportional to the electric energy produced in the year (3 US$/MWh). The parameters NPV, DPP, IRR are showed in Tables 9.2, 9.3, 9.4 and in Figures 9.1, 9.2, 9.3. The results show that a high value of the initial investment and a low value of the fuel cost, lead to a negative value of NPV, to a value of dynamic payback period higher than 20 years (reference period of the analysis investment) and to a low value of IRR. The dual stage system is not convenient. On the other hand, a low initial investment and an high cost of fuel mean a high value of NPV, low dynamic payback period and high IRR. Therefore the dual stage system could be profitable.

Nowadays, the cost of fuel is around of 600 US$/ton. It means that the dual stage ORC system (using the assumption and the economic model in chapter 8) is profitable, if the cost of the initial investment is below 5000 US$/kW (see section 9.3). In fact, if 5000 US$/kW is taken into consideration, net present value (NPV) is equal to 671 US$, dynamic payback period is nearly to 20 years and the internal rate of return (IRR) is 8% (same value considered in the model in Section 9.3).

11. Suggestions for further work

In order to improve and to continue the present work, I suggest to develop an off-design model. To investigate the exact amount of electrical power produced (therefore the energy saved in one year) at 70% and 55% engine load, it could be used a dual stage system (sixth configuration, which reaches highest value of electric output power), and also simple ORC (fourth and fifth configurations which need less space than the sixth configuration). In this way two objectives could be investigated: the maximal output power produced and the space occupied. After that, the work requires a study of economic feasibility: the cost for each component, the cost for the installation of the ORC system on board, and all the issues which concern marine application must be taken into account.

Bibliography

Andersen W.C., Bruno T.J. (2005), "Rapid screening of fluids for chemical stability in Organic Rankine Cycles applications," *Industrial and Engineering Chemistry Research*, Vol. 44, pp. 5560-5566.

Angelino G., Gaia M., Macchi M. (1984), "A review of Italian activity in the field of Organic rankine cycle,", Proceedings of the international VDI-Seminar held, ZÜrich, 10-12 September.

Bao Junjiang, Zhao Li (2013), "A review of working fluid and expander selections for Organic Rankine cycle,", *Renewable and Sustainable Energy Reviews*, Vol. 24 pp. 325-342.

Bejan A., Tsatsaronis G., Moran M. (1996), "*Thermal Design and Optimization,*" John Wiley & Sons, New York.

Borsukiewicz-Gozdur (2010), "A. Dual-fluid-hybrid power plant co-powered by low temperature geothermal water" *Geothermics*, Vol. 39, pp. 170–6.

Calderazzi L., Di Paliano P.C. (1997), "Thermal stability of R-134, R-141b, R-131, R-7146, R-125 associated with stainless steel as a containing material," *International Journal of Refrigerant,* Vol. 20, pp. 381-389.

Chen H., Yogi Goswami D., Stefanakos E.K, (2010), "A review of thermodynamic cycles and working fluids for the conversion of low-grade heat", *Renewable and Sustainable Energy Reviews,* Vol. 34, pp. 3059-3067.

Chen H., Goswami Y.D., Rahman M.M., Stefanakos E.K. (2011), "Energetic and exergetic analysis of CO_2- and R32-based transcritical Rankine cycles for low-grade heat conversion," *Applied Energy,* Vol. 88, pp. 2802-2808.

Choi C. B., Kim Min Y. (2013), "Thermodynamic analysis of a dual loop heat recovery system with trilateral cycle applied to exhaust gases of internal combustion engine for propulsion of the 6800 TEU container ship", *Energy,* Vol.1 pp. 1-13.

Eide M., Chryssakis C., Alvik S., Endresen Ø, (2012) "Pathways to low carbon shipping-abatement potential towards 2050", Det Norske Veritas, Hoevik, Norway.

He C., Liu C., Gao H., Xie H., Li Y., Wu S., Xu J. (2012), "The optimal evaporation temperature and working fluids for subcritical organic Rankine cycle", *Energy,* Vol. 38, pp 136-143.

Lakew A.A, Bolland O. (2010), "Working fluids for low-temperature heat source", *Applied Thermal Engineering,* Vol. 30, pp. 1262-1258.

Liu B.T., Chen K.H. and Wang C.C (2004), "Effect of working fluids on organic Rankine cycle for waste heat recovery", *Energy* , Vol 29 pp.1207-1217.

MAN B&M (2009), "MAN B&W S60MC6 project guide", 7th Edition, January.

Manente G, (2011), "Analysis and development of innovative binary cycle power plants for geothermal and combined geo-solar thermal resources ", Ph.D. Thesis, *University of Padova,* Italy.

Marindagen S., Haraldson L. (2011), “Potentialer för verkningsgrasförbättringar”, Wartsila, 4 May.

MARPOL (2002) Act, Annex VI, Regulation No. 12, “Ozone depleting substances”.

Marechal F., “Exergy, Energy system analysis and optimization-Vol. I Pinch Analysis”, Ecole Polytechnique Fédérale de Lausanne (EPFL), Switzerland.

Pugh S.J., Hewitt G.F., H. Mülle-Steinhagen (2003), “ Fouling during the use of seawater as coolant the development of a “User Guide””, ESDU International, London, UK.

Roy J.P., Mishra M.K., Misra A. (2010), “Parametric optimization and performance analysis of a waste heat recovery system using Rankine Cycle”, *Energy,* Vol 35, pp.5049-5062.

Schuster A., Karellas S., Aumann R., (2010) “Efficiency optimization potential in supercritical organic rankine cycles”, *Energy,* vol. 35, pp. 1033-1039.

Smolen S. (2011), “Simulation and thermodynamic analysis of a two-stage organic Rankine cycle for utilization of waste heat at medium and Low temperature levels,” *Energy Science and Technology,* Vol. 1, pp. 64-78.

Stine W.B., Harrigan R.W. (1985), *“Solar Energy Fundamentals and Design,”* Wiley.

Tempesti D., Manfrida G., Fiaschi D. (2012), “Thermodinamic analysis of two micro CHP systems operating with geothermal and solar energy”, *Applied Energy,* Vol. 97,pp. 609-617.

Toffolo A., Lazzaretto A., Manente G., Rossi N. (2010), “Synthesis/Design Optimization of Organic Rankine Cycles for Low Temperature Geothermal Sources with HEATSEP Method,”*23rd international Conference on Efficiency, Cost, Optimization, Simulation and Environmental Impact of Energy Systems*, ECOS 2010, Lausanne, Switzerland, 14-17 June.

Vaja I., Gambarotta A. (2010), “Internal combustion engine (ICE) bottoming with organic Rankine cycles (ORCs),” *Energy,* Vol 35, pp. 1084-1093.

Wang E.H., Zhang H.G., Yhao Y., Fan B.Y., Wu Y.T., Mu Q.H. (2012), “Performance analysis of a novel system combining a dual loop organic Rankine cycle (ORC) with a gasoline engine,” *Energy*, Vol. 43, pp. 385-395.

Wang Z.Q., Zhou N.J., Guo J., Wang X.Y. (2011), “Fluid selection and parametric optimization of organic Rankine cycle using low temperature waste heat”, *Energy,* Vol. 40, pp 107-115.

Walter W.F. et al. “ASHRAE (2012) Position Document on Refrigerants and their Responsible Use”, *Atlanta* ASHRAE.

Yu G., Shu G., Tian H., Wei H., Liu L. (2013), “Simulation and thermodynamic analysis of a bottoming Organic Rankine Cycle (ORC) of a diesel engine (DE),” *Energy,* Vol. 51, pp. 281-290.

Yue G., Dong S., Zheng Q. and Li J. (2012), “Design of Marine Diesel Engine Waste Heat Recovery System with Organic Rankine Cycle” *Applied Mechanics and Materials,* Vols. 148-149 pp 1264-1270.